Antibody-mediated initiation and lymphocyte-targeting therapies in CNS demyelinating disease

Doctoral Thesis

In partial fulfilment of the requirements for the degree
"Doctor rerum naturalium (Dr. rer. nat.)"

in the Molecular Medicine Study Program

at the Georg-August University Göttingen

submitted by

Sebastian Torke

born in Dresden

Göttingen, May 2019

MEMBERS OF THE THESIS COMMITTEE:

First member of the thesis committee

Prof. Dr. Martin Sebastian Weber

Department of Neuropathology
University Medical Centre, Georg-August-University Göttingen

Second member of the thesis committee

Prof. Dr. Jürgen Wienands

Department of Cellular and Molecular Immunology
Georg-August-University Göttingen

Third member of the thesis committee

Prof. Dr. Fred Wouters-Bunt

Department of Neuropathology
University Medical Centre, Georg-August-University Göttingen

Date of Disputation: 10.07.2019

AFFIDAVIT

Here I declare that my doctoral thesis entitled “Antibody-mediated initiation and lymphocyte-targeting therapies in CNS demyelinating disease” has been written independently with no other sources and aids than quoted.

_____

Göttingen, May 2019

Datasheet

Title:	Antibody-mediated initiation and lymphocyte-targeting therapies in CNS demyelinating disease
Department:	Neuropathology
Name, Given Name:	Torke, Sebastian
Matriculation Number:	21009450
Address:	Ludwig-Prandtl-Straße 52 37077 Göttingen
Phone:	0178/4082183
E-Mail:	sebastian.torke@online.de
First Evaluator (Supervisor):	Prof. Dr. Martin Sebastian Weber
Contact:	Neuropathology, University of Goettingen
Date of Delivery:	29.05.2019

Für meine ganze Familie.

List of Publications

Original articles

Häusler D*, Torke S*, Peelen E, Bertsch T, Djukic M, Nau R, Larochelle C, Zamvil SS, Brück W, Weber MS (2019). Continuous high dose vitamin D exacerbates central nervous system autoimmune disease by raising T cell excitatory calcium. BRAIN in press

Häusler D, Häusser-Kinzel S, Feldmann L, Torke S, Lepennetier G, Bernard C.C.A, Zamvil S.S, Brück W, Lehmann-Horn K, and Weber M.S. (2018). Functional characterization of reappearing B cells after anti-CD20 treatment of CNS autoimmune disease. Proc. Natl. Acad. Sci. *115*, 9773–9778.

Kinzel S*, Lehmann-Horn K*, Torke S, Häusler D, Winkler A, Stadelmann C, Payne N, Feldmann L, Saiz A, Reindl M, Lalive PH, Bernard CC, Brück W, Weber MS (2016): Myelin-reactive antibodies initiate T cell-mediated CNS autoimmune disease by opsonisation of endogenous antigen. Acta Neuropathol (Berl) 132, 43–58

*these authors contributed equally

Abstracts

13th International Congress of Neuroimmunology, 26th - 29th of September 2016, Jerusalem, Israel, poster presentation:

B cell-derived IL-10 regulates pro-inflammatory activity of myeloid cells in a clinically meaningful manner

Torke S; Kinzel S; Lehmann-Horn K; Brück W; Weber MS.

16th European School of Neuroimmunology, 26th - 30th of July 2017, Venice, Italy, poster presentation:

Exploring the role of BTK inhibition in induced and spontaneous EAE models

Torke S; Weber MS.

33th Congress of the European Committee for Treatment and Research in Multiple Sclerosis, 25th to 28th of October 2017, Paris, France, oral presentation:

B cell-mediated experimental CNS autoimmunity is modulated by inhibition of Bruton's tyrosine kinase

Torke S; Grenningloh R; Boschert U; Weber MS.

34th Congress of the European Committee for Treatment and Research in Multiple Sclerosis, 10th to 12th of October 2018, Berlin, Germany, poster presentation:

Inhibition of Bruton's tyrosine kinase selectively prevents antigen-activation of B cells and ameliorates B cell-mediated experimental autoimmune encephalomyelitis

Torke S; Grenningloh R; Boschert U; Weber MS.

71st Annual meeting of the American Academy of Neurology,
4th to 10th of May 2019, Philadelphia, USA, poster presentation:

Inhibition of Bruton's Tyrosine Kinase Selectively Prevents Antigen-Activation of B cells and Ameliorates B-Cell-Mediated Experimental Autoimmune Encephalomyelitis ´

Torke S; Grenningloh R; Boschert U; Weber MS.

Table of contents

Danksagung

An erster Stelle möchte ich mich bei **Prof. Dr. Martin S. Weber** dafür bedanken, dass er mich in diesem Projekt betreut hat. Die Arbeit hat mir immer viel Spaß gemacht und mich sowohl in professioneller als auch in persönlicher Hinsicht sehr vorangebracht.

Des Weiteren bedanke ich mich auch bei **Prof. Dr. Jürgen Wienands** und **Prof. Dr. Fred Wouters-Bunt** für Ihr Interesse, Ihre Ideen und die Unterstützung während der jährlichen Thesis committee Treffen.

Außerdem möchte ich mich bei **Prof. Dr. Wolfgang Brück** bedanken, für die Gelegenheit meine Doktorarbeit in dem Institut für Neuropathologie anzufertigen.

Ein riesiger Dank geht an **Julian Koch** und **Katja Grondey**, die mir bei allen Experimenten tatkräftig geholfen haben. Ihr habt dafür gesorgt, dass jedes noch so große Experiment machbar wurde und die Tage im Labor trotzdem unterhaltsam waren.

Außerdem möchte ich **Darius** sehr für seine Zusammenarbeit danken. Unser gemeinsames Projekt hat mir sehr viel Spaß gemacht. Außerdem konnte ich mich immer mit jeder Frage an dich wenden und immer auf deine Hilfe zählen. Vielen Dank dafür.

Ich möchte mich außerdem bei allen bedanken, mit denen ich ein Büro geteilt habe und die mir die Arbeit mit Kaffeepausen und Gesprächen angenehm gemacht haben, vor allem aber bei **Kim, Anastasia** und **Christin**.

Außerdem danke ich allen anderen **Kollegen** für Ihre Unterstützung, egal ob groß oder klein. Besonders danke ich **Susi**, der ich einige freie Wochenenden zu verdanken habe.

Ich bedanke mich bei **Cynthia** und **Heidi** für Ihre Hilfe sowie den Mitarbeitern des Promotionsprogrammes Molekulare Medizin, vor allem **Dr. Erik Meskauskas**.

Außerdem bedanke ich mich bei **Fabian**, **Sebi** und **Robin** für die Spieleabende, bei **Irina** und **Cathrin** für die Geburtstagsfeiern, bei **Malle** für die Kaffeefahrten, bei **Maike**, **Caro**, **Sarina** und **Matze** für MMoT und bei allen zusammen für die lange Freundschaft.

Der größte Dank geht an meine Familie.

Meine **Großeltern**, die mir immer vorgelebt haben, welche Art Mensch ich sein möchte.

Meine **Eltern**, die immer stolz auf mich sind und mich bei allem unterstützen.

Stephan und **Sunny**, die mir das Beste Beispiel setzen wie eine perfekte Familie aussehen sollte.

Meine **Schwiegerfamilie**, die mich sehr herzlich aufgenommen hat und bei der ich mich so wohl fühle wie Zuhause.

Und am wichtigsten von allen bei **Sarah**, die mich jeden Tag zum Lachen bringt und mich unendlich glücklich macht.

Abstract

Multiple sclerosis is inflammatory central nervous system disease, characterised by areas of demyelination and axonal loss. The pathogenic mechanism behind the disease still remains unknown, however it is thought to be mainly T cell-mediated. Notwithstanding this, B cells have increasingly been recognized as key mediators of disease. This work focuses on three distinct characteristics of MS pathology in the animal model experimental autoimmune encephalomyelitis (EAE).

The first project focused on establishing inhibition of Bruton´s tyrosine kinase (BTK) as a novel therapeutic approach. BTK is centrally placed in B cell receptor (BCR) signalling. In a B cell-mediated EAE model, induced by injection of MOG protein, we observed that evobrutinib, a novel BTK inhibitor, dose-dependently reduced clinical disease. Evobrutinib inhibited BCR-mediated phenotypic maturation of B cells from follicular (FO) II to FO I and reduced activation of B cells and T cells. It diminished calcium mobilization and cytokine production after BCR stimulation in murine and human B cells. Investigating MS patients, we did not observe a difference in B cell frequency, BTK expression or phosphorylation of BTK after BCR stimulation. Taken together, we demonstrated that BTK inhibition (BTKi) is a promising new strategy to control pathogenic B cell activity in a model of CNS autoimmunity.

The second project investigated the effects of long-term high dose vitamin D supplementation on the peripheral immune system and EAE severity. We observed clinical and histological deterioration of EAE after long-term high dose supplementation of vitamin D. Further investigations traced this effect to a secondary hypercalcemia, which in contrast to vitamin D, increased the activation and differentiation of T cells both in vitro and in vivo. Since MS patients are often continuously supplemented with vitamin D over long periods of time, our work cautions patients and clinicians to be attentive of potential side effects by hypercalcemia.

The third project focused on antibodies in the initiation of disease. We investigated the capacity of myelin-reactive antibodies to facilitate encephalitogenic responses via opsonisation of CNS antigen. We observed that antibody production in the absence of B cells was sufficient to induce EAE in a transgenic mouse model. Additionally, adoptive transfer of antibodies in mice containing MOG-specific T cells induced disease via otherwise

unresponsive myeloid antigen-presenting cells (APCs). MOG-targeting antibodies enabled Fc-receptor (FcR) mediated recognition and phagocytosis in in vitro differentiated macrophages. Additionally, antibody preparations from neuromyelitis optica patients positive for MOG antibodies similarly facilitated recognition by myeloid APCs. These results establish opsonisation of CNS antigen by specific antibodies as a novel mechanism to trigger CNS demyelination.

Abbreviations

Ab	Antibody
APC	Antigen-Presenting Cell
AQP	Aquaporin
BBB	Blood-Brain Barrier
BCR	B Cell Receptor
BTK	Bruton´s Tyrosine Kinase
CAM	Cell Adhesion Molecules
CD	Cluster of Differentiation
CIS	Clinically Isolated Syndrome
CNS	Central Nervous System
DMD	Disease Modifying Drug
DMF	Dimethyl Fumarate
DNA	Deoxyribonucleic Acid
DPI	Days Post Immunization
EAE	Experimental Autoimmune Encephalomyelitis
EDSS	Expanded Disability Status Scale
FcR	Fc-Receptor
FO	Follicular
GA	Glatiramer Acetate
GM-CSF	Granulocyte-Macrophage Colony-Stimulating Factor
HC	Healthy Control
IFN	Interferon

Ig	Immunoglobulin
IL	Interleukin
IU	International Unit
mAb	Monoclonal Antibody
MAG	Myelin-Associated Glycoprotein
MHC	Major Histocompatibility Complex
MOG	Myelin Oligodendrocyte Glycoprotein
MRI	Magnetic Resonance Imaging
MS	Multiple Sclerosis
NAWM	Normal-Appearing White Matter
NMO	Neuromyelitis Optica
NMSS	National Multiple Sclerosis Society
OCB	Oligoclonal Band
OVA	Ovalbumin
PCR	Polymerase Chain Reaction
PML	Progressive Multifocal Leukoencephalopathy
PPMS	Primary Progressive Multiple Sclerosis
q	Quantitative
RA	Rheumatoid Arthritis
RIS	Radiologically Isolated Syndrome
ROS	Reactive Oxygen Species
RRMS	Relapsing-Remitting Multiple Sclerosis
S1P	Sphingosine-1-Phosphate

SLE	Systemic Lupus Erythematodes
SPMS	Secondary Progressive Multiple Sclerosis
TCR	T Cell Receptor
TNF	Tumor-Necrosis Factor
UV	Ultraviolet
WT	Wildtype

1. Introduction

1.1. Multiple Sclerosis

Multiple sclerosis (MS) is the most common autoimmune disorder of the central nervous system (CNS). It affects more than 2.3 million people worldwide, has a two to three times higher incidence in women when compared to men and is commonly diagnosed in young adults between 25 and 50 years of age (nationalmssociety.org/What-is-MS/Who-Gets-MS). The first to describe the clinical characteristics of MS was Robert Carswell in 1838, illustrating the appearance of lesions within the spinal cord (Compston, 1988). Hallmarks of MS pathology are inflammation, demyelination as well as glial and axonal loss in the CNS. The inflammation is characterised by microglial activation and the infiltration of macrophages and lymphocytes (Kuhlmann et al., 2017).

1.1.1. History

The fact that symptoms of MS can emerge and subside, taken together with the variety of symptoms that can occur, has made this disease difficult to diagnose. Therefore it is not surprising that a distinct description of the disease was only first made by Jean-Martin Charcot in 1868. Although typical details of the disease were previously described by Robert Carswell and Jean Cruveilhier, Charcot was the first to characterise MS as an independent disease and named it *sclerose en plaques* (Compston, 1988). Three of the key symptoms—intention tremor, nystagmus and scanning speech—became known as Charcot´s triad.

1.1.2. Symptoms and diagnosis

The large variety of MS symptoms often includes partial or complete loss of vision, changes in the sensation in the extremities as well as fatigue. However, it can further extend to an impairment of balance, muscle spasms, problems with speech, and bladder and bowel difficulties (Smith and McDonald, 1999).

Patients often present with isolated events of the typical symptoms mentioned above for which CNS disease cannot be clearly excluded. For the diagnosis of MS, the McDonald criteria are used, which were first described in 2001 and revised in 2010 and 2017. Using the number of relapses, magnet resonance imaging (MRI) data, cerebrospinal parameters such

as the presence of oligoclonal bands (OCB), and clinical symptoms, MS can be diagnosed with a sensibility of 82% (Gaetani et al., 2018). Important information about a dissemination in time as well as space can be concluded from MRI data and thereby assists in the differentiation to clinically similar diseases (Thompson et al., 2018).

1.1.3. Clinical course

The US National Multiple Sclerosis Society (NMSS) Advisory Committee on clinical trials in MS has described 4 separate clinical courses of MS in 1996: relapsing-remitting (RRMS), secondary-progressive (SPMS), primary-progressive (PPMS) and progressive-relapsing (PRMS) MS. Their definition has been revised in 2013 and 2 entities have been added that not yet fulfil the diagnostic criteria of MS: clinical isolated syndrome (CIS) and radiologically isolated syndrome (RIS, https://www.nationalmssociety.org/What-is-MS/Types-of-MS). Furthermore, the PRMS phenotype was included into the PPMS subgroup.

The most common type of disease is RRMS with about 85% of patients. RRMS is a defined by relapses— the occurrence of worsening of symptoms—which is followed by full remission or only minor remaining deficits with longer periods of stability between the relapses (Goldenberg, 2012). Approximately 70% of patients will develop a SPMS about 20 years after onset of disease (Weinshenker, 1998). SPMS is characterised by steady progression of disability after an initial RRMS course and only rarely shows relapses. A continuous disease progression from the diagnosis on points towards PPMS, which has a later onset compared to RRMS. About 10-15% of patients show this disease course, in which disease plateaus or minor improvements can occur. A continuous increase in disability over months or years distinguishes this subgroup from RRMS, in which symptoms can quickly occur but resolve over time (Lublin et al., 2014).

1.1.4. Pathogenesis

Studies in experimental autoimmune encephalomyelitis (EAE), an animal model of MS, have shown that the inflammatory response within the CNS is likely caused by infiltration of peripheral immune cells after initial activation. The key mediators of disease in EAE are $CD4^+$ T cells, whereas in contrast MS is most strongly associated with $CD8^+$ T cells (Lassmann and Bradl, 2017). These auto-reactive T cells, after infiltration into the CNS, release pro-inflammatory cytokines such as Tumor-necrosis factor (TNF)-α and Interferon (IFN)-γ,

causing the production of other cytokines (e.g. CXC3L1, CCL3, CCL5). Their presence activates endothelial cells in the blood-brain barrier (BBB), loosening their tight adhesion by cell adhesion molecules (CAM) and easing the transmigration of peripheral immune cells through the BBB (Larochelle et al., 2011). The inflammation caused by infiltrating B cells, T cells, plasma cells and dendritic cells disrupts the astroglial and oligodendroglial homeostasis. Furthermore, intrathecal production of antibodies by plasma cells might contribute to the damage of glial cells and the myelin sheath (Wekerle, 2017). Activated microglia and infiltrating macrophages can injure the myelin sheath further and cause axonal damage by the production and release of reactive oxygen species (ROS) (Ohl et al., 2016). This interplay of microglia/macrophages and lymphocytes and the damage they mediate leads to the formation of inflammatory phagocytic lesions.

1.1.5. Pathology

Inflammation and gliosis resulting in demyelination and axonal damage are the pathological hallmarks of MS. Although white matter lesions can occur all over the CNS, they are most often seen in the spinal cord, optic nerve, periventricular areas or brain stem (Pan et al., 2013). In the early disease stages, most lesions detected are called active lesions, which arise quickly and vanish after a while (Lassmann et al., 2007). In contrast, smouldering lesions, which are present over a longer period of time and slowly expand, are more prominent in chronically diseased patients (Popescu et al., 2017). However, active lesions can still arise in SPMS patients. In PPMS patients, smouldering lesions predominate and active lesions contribute only to a small amount of plaques. In addition, in PPMS or SPMS patients a higher frequency of cortical lesions and a higher chance of injury to the normal-appearing white matter (NAWM) are observed. Changes in the NAWM are characterised by diffuse inflammation and potential axonal injury in non-demyelinated areas (Popescu et al., 2017). Pathological differences between early and chronic MS lesions can be described by their amount of infiltrating inflammatory cells, overall demyelination and axonal damage. In early lesions, macrophages containing myelin fragments are dominant, whereas the density of T cells, B cells and plasma cells can vary and incomplete demyelination and acute axonal damage can be observed. Remyelination is often more pronounced in early lesions compared to chronic lesions (Lassmann et al., 1997). Lymphocytes and macrophages are not as dominant in chronic lesions and oligodendrocyte precursor cells are present, whereas

mature oligodendrocyte numbers are reduced. Additionally, the axonal density is often decreased in areas of chronic MS lesions (Popescu et al., 2017).

For early active lesions, four distinct patterns can be characterised by the extent of demyelination, oligodendrocyte loss, size and localization of plaques, infiltration of immune cells as well as immunoglobulin (Ig) and complement deposition. Pattern I lesions show predominantly T cell and macrophage-associated inflammation and active demyelination with sharply demarcated edges. Although pattern II lesions appear similar to pattern I, additional depositions of Ig and complement C9neo differentiate the patterns and suggest the involvement of a humoral component. Pattern III lesions show a preferential loss of myelin-associated glycoprotein (MAG) compared to other myelin proteins and a pronounced apoptosis of oligodendrocytes. Pattern IV lesions have only been described in single autopsy cases and are associated with DNA fragmentation in oligodendrocytes without morphological characteristics of apoptosis (Lassmann et al., 2001).

1.1.6. Treatment of MS

The therapeutic options for MS patients differ between treating acute relapses and the long-term control of disease activity. Currently, there are more than ten different disease-modifying drugs (DMDs) available and the choice depends on benefit-risk evaluation and the state of disease.

Acute relapses are most often treated with intravenous injections of high-dose corticosteroids for multiple consecutive days. If symptoms persist, a second curse of steroids can be given. Alternatively, immunoadsorption or plasma exchange can be helpful to enhance recovery from a relapse (Berkovich, 2016).

First-line treatments for patients with mild to moderate disease activity are IFNβ, glatiramer acetate (GA), dimethyl fumarate (DMF) and teriflunomide. These drugs show a moderate immunomodulatory action by reducing relapse rate, expanded disability status scale (EDSS) worsening and the development of new MRI lesions. They furthermore have a high safety profile, which is why they are often given initially to patients after the first diagnosis. IFNβ is known to stabilize the ratio of pro- to anti-inflammatory cytokines and reducing the number of immune cells that invade the CNS (Zafranskaya et al., 2007). GA is a random polymer of four amino acids and is thought to act as a decoy to myelin proteins as well as shifting the

T cell population towards anti-inflammatory or regulatory subsets (La Mantia et al., 2016). DMF has shown several immunomodulatory effects but its mechanism of action is not fully understood (Diebold et al., 2018). Teriflunomide inhibits the pyrimidine de-novo synthesis and thereby affects rapidly dividing cells, such as activated T cells (Chan et al., 2016).

Patients with a higher disease activity or those in which first-line treatments have failed to control disease are often treated with monoclonal antibodies (mAbs) such as natalizumab, alemtuzumab or the oral agent fingolimod. These drugs show a higher effectiveness in reducing relapse rate, MRI activity and EDSS progression in comparison to IFNβ. Natalizumab targets the cell-adhesion molecule α4-integrin and thereby prevents immune cells from crossing the blood barrier to invade the CNS. One mayor safety issue with natalizumab is the development of progressive multifocal leukoencephalopathy (PML) in patients positive for the JC-virus, which should therefore be tested before starting the treatment (Brandstadter and Katz Sand, 2017). Alemtuzumab is a mAb against CD52 and thereby marks mature lymphocytes for destruction (Trebst et al., 2010). Fingolimod is a sphingosine-1-phosphate receptor (S1PR) modulator, sequestering lymphocytes in the lymph nodes (Chaudhry et al., 2017).

If disease activity can still not be controlled accordingly, the highly effective drugs mitoxantrone or ocrelizumab are given. Mitoxantrone is a topoisomerase inhibitor which disrupts both DNA synthesis and repair, affecting rapidly dividing cells (Ramkumar et al., 2008). Ocrelizumab is an anti-CD20 targeting antibody, binding B cells and leading to their destruction. It is a highly effective therapy, reducing the number of new lesions and the annual relapse rate drastically (Rahmanzadeh et al., 2018).

DMDs have largely been tested for effectiveness in progressive MS, with mostly disappointing results. Immunomodulation and –suppression have failed to show strong benefits for patients, suggesting that promoting myelin repair and remyelination as well as neuroprotection might be more successful approaches. However, understanding the pathology of progression in MS is essential and needs to be studied in more detail to promote the development of novel therapeutics in progressive MS (Ontaneda et al., 2017).

It has been observed, that MS incidence correlates with geographical latitude and that the serum levels of vitamin D are often reduced in MS patients (Häusler and Weber, 2019).

Therefore, it is clinical practice to supplement vitamin D in patients, although its efficacy in reduced disease activity is questionable.

Besides the aim to reduce relapses and disease progression, MS patients are often given medication to treat comorbidities, e.g. muscle relaxants and drugs against fatigue, bladder/bowel control problems, depression and visual impairment (Moss et al., 2017). Furthermore, physical therapy can be helpful to improve mobility and slow EDSS progression (Kalron et al., 2017).

1.2. Experimental autoimmune encephalomyelitis

EAE is the most commonly used animal model of MS and was first described in 1933 by Rivers and colleagues (Constantinescu et al., 2011). The characteristic immune-cell mediated inflammation and resulting demyelination can be induced by either injection of myelin components emulsified in adjuvant (active immunization) or adoptive transfer of activated, myelin-specific T cells (passive immunization). Several subtypes of the model were developed over the years, representing distinct characteristics of disease. The most commonly used active immunization model is myelin-oligodendrocyte glycoprotein (MOG) 35-55 peptide EAE. Depending on the mouse-strain which is immunised, the animals display a relapsing-remitting (SJL or Biozzi mice) or chronic-progressive (C57Bl/6) disease course (Glatigny and Bettelli, 2018). The immunization leads to the unspecific binding of MOG_{35-55} to mayor histocompatibility complex (MHC) class II molecules on antigen-presenting cells (APCs), such as dendritic cells, macrophages and B cells, resulting in the activation and proliferation of encephalitogenic T cells (Molnarfi et al., 2013). In contrast to MS, in which $CD8^+$ T cells are the most relevant, in this model $CD4^+$ T cells are the key mediators of disease (Sinha et al., 2015). The autoreactive T cells migrate over the BBB into the CNS, become reactivated by resident APCs presenting myelin fragments and subsequently facilitate the infiltration of other immune cells and further inflammatory processes. This ultimately leads to demyelination and axonal injury. Since in this model, B cell depletion by anti-CD20 targeting therapy leads to a worsening of disease, it can be considered B cell-independent. Another approach, involving B cells in the disease initiation and progression, utilizes recombinant MOG 1-117 protein. The native MOG_{1-117} needs to be recognized by APCs, internalized and processed in order to be presented on MHCII molecules on the surface.

Specifically B cells can recognize MOG_{1-117} via their B cell receptor (BCR), facilitating B cell activation and pathogenic differentiation in addition to the generation of encephalitogenic T cells. In this approach, B cell depletion considerably reduces clinical severity of EAE (Weber et al., 2010). Both active immunization models are characterised by ascending paralysis, caused by spinal cord demyelination, with an onset of approximately twelve days post immunization (dpi). Although these models represent distinct features of MS pathology and immunology, a more suitable model utilizes spontaneous onset EAE. Therefore, double-transgenic mice are generated by cross-breeding mice inhabiting transgenic, MOG-specific T cells with mice transgenic for MOG-specific B cells. Approximately 50% of the double-transgenic mice develop spontaneous symptoms of ascending paralysis, usually 5-10 weeks after birth (Glatigny and Bettelli, 2018).

1.3. Aim of this work

This thesis consists of three original publications, including one first authorship, currently being prepared for submission, and one co-first authorship.

1.3.1. Aim of project 1: Inhibition of Bruton´s tyrosine kinase ameliorates CNS autoimmune disease by preventing B cell activation

The first study aimed to test a novel therapeutic approach of MS, the inhibition of Bruton´s tyrosine kinase (BTK) in the mouse model EAE. Therefore, mice were immunized with MOG protein and treated with evobrutinib, a newly developed BTK inhibitor. We then analysed the clinical and histological outcome as well as the direct and indirect effects on the peripheral immune system. We focused on changes in the B-cell phenotype and the activation of B and T cells. Furthermore, we conducted mechanism-of-action studies *in vitro* by examining BCR signalling effects on calcium mobilization, cytokine production and the ability of B cells to act as APCs and stimulate T cells in a co-culture setting.

1.3.2. Aim of project 2: Continuous high dose vitamin D exacerbates central nervous system autoimmune disease by raising T cell excitatory calcium

The second project focused on vitamin D supplementation, a common practice for MS patients. We compared long-term effects of low-dose, standard and high-dose vitamin D diet and the clinical and histological outcome. Additionally, we investigated effects of long-term supplementation on the peripheral immune system by analysing the activation status of

immune cells and their proliferation response to restimulation. We specifically targeted hypercalcemia, a secondary effect of long-term high dose vitamin D, analysing the influence of elevated calcium on T cells in terms of calcium mobilization, cytokine release and migration ability.

1.3.3. Aim of project 3: Myelin-reactive antibodies initiate T cell-mediated CNS autoimmune disease by opsonization of endogenous antigen.

The third project analysed the effect of CNS-reactive B cells and specifically the pathogenic role of MOG-specific antibodies (Abs). Therefore, clinical, histological and immunological features were analysed in mice containing MOG-specific T cells when MOG antibodies were administrated. Furthermore, the reactivity of innate immune cells, specifically macrophages and dendritic cells, towards antibody-targeted MOG was assessed. Lastly, the phagocytosis-inducing capacity of MOG Abs and MOG-reactive patient serum was analysed in the context of Fc-receptor recognition of opsonized MOG.

2. Inhibition of Bruton´s tyrosine kinase ameliorates CNS autoimmune disease by preventing B cell activation

2.1. Background

B cells have been intensely studied over the recent years as mediators of MS pathology (Rahmanzadeh et al., 2018). The most striking notion of their involvement is likely the tremendous success of B cell depletion therapies. However, this not only targets pathogenic B cells but will also affect regulatory B cell functions, such as the production of anti-inflammatory cytokines (Häusler et al., 2018). An alternative approach might be the specific inhibition of pro-inflammatory B cell responses by interfering with BCR signalling. One promising target is BTK. BTK is a member of the TEC family of kinases and is centrally involved in BCR signalling und the subsequent activation and differentiation of B cells (Corneth et al., 2016). BTK inhibition is thereby a promising new target to control pathogenic B cell function in disease such as antigen presentation and cytokine production, while potentially leaving anti-inflammatory properties unaffected.

2.2. Approach

In this work we evaluated the novel BTK inhibitor evobrutinib for its effectiveness as a monotherapy in MOG protein-induced EAE. Prophylactic treatment with evobrutinib led to a dose-dependent reduction of disease severity over a 60-day observation period. These clinical findings were substantiated by histological analysis at the end of the study. We observed reduced infiltration of immune cells into the spinal cord and reduced demyelination. Looking into closer detail, we specifically identified diminished numbers of infiltrating B cells. Likely as a secondary effect, we observed a reduction in infiltrating T cells and macrophages. Next, we focused on the effect on B cells and observed an inhibition of maturation. The B cells accumulated in a more naïve phenotype and less in an antigen-activated phenotype. Dissecting the B cell phenotype, we observed that specifically the transition from follicular II B cells to follicular I B cells was affected. This step is known to be mediated by a strong BCR antigen and is BTK dependent. Additionally, the expression of the key activation markers CD86, MHC class II and CD69 was reduced. Furthermore, we detected reduced expression of the activation markers CD25 and CD69 on T cells, as well as a reduced number of memory T cells, identified by a high expression of CD44. Co-culturing B cells from

evobrutinib treated animals together with MOG-specific T cells, we observed that the proliferation of T cells was diminished by evobrutinib. Furthermore, T cell differentiation into Th1 and Th17 cells, characterised by the production of IFNγ and IL-17 respectively, was reduced while FoxP3 expressing regulatory T cell numbers were slightly increased. Investigating the direct down-stream effects of evobrutinib on BCR signalling, we observed reduced calcium mobilization upon anti-IgM stimulation *in vitro* as well as *ex vivo* on murine and human B cells. Additionally, B cells were inhibited in their production of IFNγ, analysed by quantitative PCR. Analysing B cells from healthy individuals and MS patients for their B cell frequency, BTK expression and BTK phosphorylation response to BCR stimulation, we did not detect any differences. However, evobrutinib diminished the production of cytokines by human B cells. Taken together, we here demonstrated that BTK inhibition is a promising new therapeutic approach to target pathogenic B cells in EAE.

2.3. Contribution

I was majorly involved in the design of the study. I planned and conducted all experiments, collected and analysed the data. I supervised the human experiments, performed and analysed by Roxanne Pretzsch. I performed the statistical analysis and prepared the figures. I drafted and revised the manuscript.

2.4. Original publication

The manuscript is currently being prepared for submission to a scientific journal.

Inhibition of Bruton´s tyrosine kinase selectively diminishes pathogenic B cell development in inflammatory CNS demyelinating disease

Sebastian Torke[1], Darius Häusler[1], Roxanne Pretzsch[1], Philipp Haselmayer[2], Roland Grenningloh[3], Ursula Boschert[4], Wolfgang Brück[1] and Martin S. Weber[1,5]

[1]Institute of Neuropathology, University Medical Center, Göttingen, Germany; [2]Translational Innovation Platform Immunology, Merck KGaA, Darmstadt 64293, Germany; [3]EMD Serono Research and Development Institute, Inc.*, Billerica, MA, USA; [4]Ares Trading S.A., an affiliate of Merck Serono S.A., Eysins, Switzerland; [5]Department of Neurology, University Medical Center, Göttingen, Germany

*A business of Merck KGaA, Darmstadt, Germany

Address correspondence to: Martin S. Weber, MD

Department of Neuropathology

Department of Neurology

University Medical Center, Georg August University

Robert-Koch-Str. 40, 37099 Göttingen, Germany

Phone +49-551 39-7706

Fax +49-551-39-10800

E-mail: martin.weber@med.uni-goettingen.de

Key words: multiple sclerosis, experimental autoimmune encephalomyelitis, Bruton´s tyrosine kinase, BTKi, evobrutinib

Total

1500 words

4 Figures

Introductory paragraph

B cells are increasingly recognized in multiple sclerosis (MS), which was substantiated by the success of their anti-CD20 mediated removal. A potentially superior strategy may be the selective abrogation of pathogenic B cell properties by targeting B cell differentiation. In this regard, inhibition of Bruton's tyrosine kinase (BTK), an enzyme centrally involved B cell receptor-mediated activation showed promising results in a recent phase II trial. Here, we dissected how the respective BTK inhibitor evobrutinib is achieving this clinical benefit mechanistically. We observed that in a B cell-accentuated experimental autoimmune encephalomyelitis (EAE) model, oral evobrutinib in a dose equivalent to the range tested in MS substantially ameliorated disease severity by a diminishing B cell activation and pro-inflammatory differentiation. This resulted in an impaired capacity of B cells to act as antigen-presenting cells for developing encephalitogenic T cells. These data suggest that evobrutinib is fully capable of controlling pathogenic B cell properties without the requirement to unselectively remove this cell lineage.

Main text

Multiple Sclerosis (MS) is a demyelinating autoimmune disease of the central nervous system (CNS), affecting approximately 2.5 million people worldwide[1]. Although it is thought to be mainly T cell-mediated, an increasing effort has gone into deciphering the involvement of B cells[2]. Next to the hallmark diagnostic criterion of antibody production in the cerebrospinal fluid (CSF), the striking success of B cell depleting therapies proves their contribution to the disease[3,4]. However, complete depletion of B cells may not be the optimal strategy, since it also affects anti-inflammatory properties, such as the production of immune system controlling cytokines[5]. Furthermore, after cessation of the therapy, repopulation of the relevant immune organs can take up to several months[6]. Therefore, specifically controlling pathogenic B cell function might be an alternative approach, for example by inhibiting BCR function. One centrally placed signaling protein within the BCR cascade is BTK[7]. Since BTK mutation is a known cause of B cell malignancies, it has been extensively studied[8]. However, up to date BTK inhibition (BTKi) has not been tested in models of MS. Here we investigated a novel BTK inhibitor, evobrutinib, in B cell-mediated experimental autoimmune encephalomyelitis (EAE), an animal model of MS. Evobrutinib is an orally-available, highly-specific BTK inhibitor that has shown efficacy in other animal models of autoimmune disease[9]. Here, for the first time, we report the effectiveness of a BTK inhibitor in reducing clinical severity of an animal model of MS.

Immunization of C57BL6 mice with conformational MOG1-117 protein leads to its recognition by B cells with subsequent internal processing and presentation to T cells. Therefore, this model is considered B cell-mediated and shows a strong clinical effect of B cell depletion by anti-CD20 antibody treatment (**suppl. Figure 1**). As indicated in **Figure 1a**, evobrutinib treatment with 1, 3, or 10 mg/kg led to groups of animals with BTK blood exposure levels of 36 nM, 159 nM, or 719 nM 1 hour after oral gavage. Prophylactic treatment with evobrutinib, starting 7 days prior to immunization, in this model led to a significantly reduced clinical severity of EAE over a 60 day observation period and a reduction of overall mortality from 30% in control treated to 0% in animals treated with an intermediate dose (**Figure 1b**). Further histological analysis at the end of the study revealed reduced spinal cord immune cell infiltration from 302 cells/10^6px to 62.7 cells/10^6px (p=0.008, **Figure 1c**). Immunhistological stainings for B cells, macrophages and T cells showed that specifically the infiltration of B cells and T cells were dose-dependently reduced by evobrutinib treatment (**Figure 1d-f**). In addition, there was a trend towards a reduction of infiltrating macrophages. Furthermore, white matter demyelination was reduced from 19.4% in control treated to 9.1% in animals treated with

3mg/kg evobrutinib (p=0.001, **Figure 1g**). Since these findings most likely are based on a direct effect on B cells, we next investigated the phenotype and activation status of B cells after immunization.

WT mice were prophylactically treated with evobrutinib, immunized with conformational MOG_{1-117} protein and sacrificed at day 12 before the onset of clinical signs of EAE. We were specifically investigating the B cell subsets present in the secondary lymphoid organs after evobrutinib treatment according to their maturation as shown in **Figure 2a** and **suppl. Figure 2a.** We could observe a dose-dependent accumulation of follicular (FO) II B cells from 27.26% to 42.79% (p<0.0001), and a corresponding reduction of FO I B cells from 37.44% to 26.24% (p<0.0001) when comparing vehicle to 10 mg/kg evobrutinib treatment (**Figure 2b-c**). Similar changes in the frequency of FO II and FO I B cells were observed in the blood, inguinal and cervical lymph node (**suppl. Figure 2b-d**).

Additionally, the expression of MHCII which is essential for antigen-presentation, was reduced by 9.65% (p<0.0338, **Figure 2d**). Furthermore, the B cell activation markers CD86 and CD69 were reduced by 14.72% (p=0.0028, **Figure 2e**) and 9.01% (p<0.0958, **Figure 2f**), respectively, when comparing control to evobrutinib treated animals. The expression of CD80 was unchanged (**suppl. Figure 3a**). On $CD4^+$ T cells, the main effector cells in this model, the expression of CD25 and CD69 was reduced by 12.23% (p=0.0052, **Figure 2g**) and 14.04% (p=0.0092, **Figure 2h**), respectively. Although not significant, the frequency of $CD44^{hi}$ expressing memory T cells was reduced by 3.38% (p=0.17, **Figure 2i**). Similar, but less pronounced, tendencies for reduced expression were observed on $CD8^+$ T cells (**suppl. Figure 3b-d**). On $CD11b^+$ myeloid cells we observed a reduction of the expression of CD80 by 13.4% (p=0.0051) and CD86 by 9.53% (p=0.0246) when comparing vehicle control and 10 mg/kg evobrutinib. There was no change in the expression of MHCII or CD69 (**suppl. Figure 3e**). These findings, together with the reduced clinical severity and infiltration into the spinal cord, point towards diminished pathogenicity of B cells after evobrutinib treatment. Next we were interested in the ability of these B cells to stimulate T cell proliferation and differentiation.

Using a co-culture system with B cells isolated from evobrutinib treated, immunized animals together with naïve MOG-specific T cells from 2D2 mice, we investigated the ability of these B cells to act as antigen-presenting cells (APCs). Analyzing the proliferation of T cells by CFSE dilution, we observed an inhibition of proliferation by evobrutinib (**Figure 3a**). Additionally, the differentiation of T cells into IFN-γ producing Th1 and IL-17 producing Th17 cells was diminished from 4.02% to 1.72% (p< 0.0001, **Figure 3b**) and 3.87% to 2.04% (p= 0.0004,

Figure 3c), respectively. Interestingly, the frequency of regulatory, $FoxP3^+$ T cells was increased from 0.11% to 0.18% (p= 0.0452, **Figure 3d**). Next we were interested in dissecting the mechanism of action of the inhibitor by investigating its effects on induced BCR signaling. We therefore analyzed the mobilization of calcium and the production of cytokines after anti-IgM stimulation.

Purified murine or human B cells were pre-incubated with the indicated doses of evobrutinib for at least 30 minutes prior to measurement for in vitro assays, or isolated from healthy animals after 3 days of oral treatment. Using the calcium-sensitive dyes Fluo-3 and Fura Red, we analyzed the intra-cellular mobilization of excitatory calcium upon BCR and TCR stimulation (**suppl. Figure 3f**). Evobrutinib showed a dose-dependent inhibition of BCR induced calcium flux by up to 89.7% (p= 0.0002), comparing 1 µM evobrutinib to control with a stimulation of 5µg/ml αIgM. Interestingly, this effect could be partially overwritten by increasing the strength of the stimulus. A four-fold increase in stimulation lead to an overall stronger calcium release which 1 µM evobrutinib could then only reduce by 69.5% (p < 0.0001, **Figure 3e**). Investigating off-target effects by analyzing a potential inhibition of ITK, the BTK homologue in T cells, we stimulated the TCR after evobrutinib pre-treatment. There we again observed a reduction of BCR induced calcium, but no inhibition could be detected on either $CD4^+$ or $CD8^+$ T cells after CD3/CD28-mediated calcium mobilization (**Figure 3f**). Stimulating isolated B cells from healthy animals treated with evobrutinib for 3 days, we observed a reduction of BCR-mediated calcium mobilization by 53.2% (p=0.0005, **Figure 3g).**

We next investigated the effect of evobrutinib on cytokine production following BCR stimulation. Therefore, isolated murine B cells were pre-incubated with the indicated concentrations of evobrutinib and stimulated via the BCR for 3h. An evobrutinib concentration of 1 µM showed no clear effect on the expression of IL-6 or IL-10. However, the production of IFN-γ was reduced by dose-dependently reduced by up to 81.66% (p<0.0001, **Figure 3h**).

In light of the recent successful phase II clinical trial of evobrutinib in RRMS, we were interested in evaluating BTK expression and activity on human cells. Therefore, we analyzed peripheral blood mononuclear cells (PBMCs) from healthy individuals and MS patients (**suppl. Table 1**) for the B cell frequency, the levels of BTK expression and the inducibility of BTK phosphorylation. We categorized B cells into naïve (IgD^+CD27^-), activated but not class-switched (IgD^+CD27^+, IgM^+CD27^+) and fully class switched ($IgD^-IgM^-CD27^+$) subsets. We observed no effect on the B cell frequency (**Figure 4a**) or the overall expression of BTK (**Figure 4b**). BTK phosphorylation via the BCR could be induced on all subsets. Interestingly,

pBTK inducibility was increased in fully class-switched as well as activated B cells compared to naïve B cells. Comparing healthy controls and MS patients we did not observe a difference in pBTK inducibility within each subset (**Figure 4c**).

Next we analyzed the cytokine production and calcium mobilization of B cells from healthy individuals. Calcium mobilization was reduced by 75.48% ($p<0.0001$, **Figure 4d**). We furthermore observed a dose-dependent reduction in the production of IL-6 ($p=0.0005$, **Figure 4e**) and IL-10 ($p< 0.0001$, **Figure 4f**). Taken together this indicates that BTK is expressed on all subsets but is functionally increased in activated and class-switched B cells. Additionally, evobrutinib has the potential to diminish excitatory calcium and cytokine production in human B cells.

The therapeutic approach of targeting B cells in MS has proven to be a highly efficient strategy to reduce disease burden, making B cells an attractive target[10]. However, available therapies aim at the long-term absence of B cells[11]. Long-term studies with B cell-depleting therapies have so far not shown severe side effects[12,13]. However after several years, long-lived plasma cell frequencies decline, possibly leading to an increased risk of infections and reduced protection by vaccines[14]. Additionally, after cessation of depleting therapies, reconstitution of the B cell pool takes several month. Furthermore, if the disease is still ongoing, animal experiments have shown that B cells repopulate in a more activated and pathogenic manner[6]. This hints that there might be a demand for alternative treatment options. In this manuscript, we investigated the potential of BTK inhibition in EAE and its effects on B cells. Up to date, BTKi has not been tested in a model of CNS autoimmune disease. Our results showed that evobrutinib, a novel BTK inhibitor, reduces disease severity of mice in a B cell-mediated model of MS, in its strength comparable to pan B cell depletion by anti-CD20 treatment. This was supplemented by diminished spinal cord infiltration and demyelination.

In a recently finished phase II clinical trial, evobrutinib has shown effectiveness as a monotherapy in RRMS patients by reducing the total number of gadolinium-enhanced lesions and the annual relapse rate[15]. Our mechanistic data in the murine model of MS supports these findings and can at least partially explain the mechanism of action of this inhibitor. Additionally, our human data demonstrates that, although MS patients do not differ in BTK expression, BTK becomes more involved in BCR signaling with increasing activation and maturation. Therefore, a therapeutic intervention would especially target these mature cells, highlighting BTK as a promising novel therapeutic target.

Isolated B cells from treated animals showed an arrest in the B cell maturation and decreased expression of activation markers. Specifically, the conversion of FO II towards FO I, an event that requires a strong BCR antigen and has been reported to be BTK dependent[16], was impaired in the spleen, lymph nodes and the blood. Furthermore, these cells had a weakened response to BCR stimulation, determined by calcium mobilization and the production of cytokines. This could potentially explain the mechanism of action of evobrutinib and possibly explain the disease controlling activity. Additionally, if the same conversion from FO II to FO I is impaired in human B cells, this would be a reliably biomarker to monitor efficacy of treatment in patients.

In vitro we observed an impaired production of IFNγ in evobrutinib treated B cells. IFNγ is a strong regulator of MHCII expression which is essential for antigen presentation[17]. Therefore, we could link reduced cytokine production and impaired APC function of B cells with the diminished T cell proliferation and differentiation into Th1 and Th17 cells. Interestingly, IFNγ producing B cells are furthermore known to suppress Treg differentiation[18]. Therefore, the inhibition of pro-inflammatory B cell functions directly led to a reduction in pathogenic T cells and an increase in regulatory T cells.

Additionally, evobrutinib has shown efficacy in other models of autoimmune disease by successfully diminishing BTK phosphorylation upon BCR stimulation. Furthermore, evobrutinib inhibited Fc receptor (FcR) signaling and the activation of basophils. This translated into a near complete inhibition of disease in both RA and SLE models[9]. Fc receptor-mediated recognition of antibody opsonized myelin components has been demonstrated to be another mode of initiation of autoimmune CNS disease in mice. This lead to the presentation of endogenous antigen on myeloid cells, subsequently activating encephalitogenic T cells[19]. Blocking antigen presentation on myeloid cells by BTKi could potentially inhibit CNS disease in this model. Additionally, BTK is involved in toll-like receptor (TLR) signaling[20,21]. Since evobrutinib has been shown to penetrate the CNS in relevant doses, it thereby could also act on TLR signaling in microglia.

Taken together this proves that BTKi has the potential to control pathogenic B cell activity in a B cell-mediated animal model of CNS autoimmunity.

References

1. Huang, W.-J., Chen, W.-W. & Zhang, X. Multiple sclerosis: Pathology, diagnosis and treatments. *Exp. Ther. Med.* **13**, 3163–3166 (2017).
2. Weber, M. S. & Hemmer, B. Cooperation of B cells and T cells in the pathogenesis of multiple sclerosis. *Results Probl. Cell Differ.* **51**, 115–126 (2010).
3. Winger, R. C. & Zamvil, S. S. Antibodies in multiple sclerosis oligoclonal bands target debris. *Proc. Natl. Acad. Sci. U. S. A.* **113**, 7696–7698 (2016).
4. Myhr, K.-M., Torkildsen, Ø., Lossius, A., Bø, L. & Holmøy, T. B cell depletion in the treatment of multiple sclerosis. *Expert Opin. Biol. Ther.* **19**, 261–271 (2019).
5. Häusser-Kinzel, S. & Weber, M. S. The Role of B Cells and Antibodies in Multiple Sclerosis, Neuromyelitis Optica, and Related Disorders. *Front. Immunol.* **10**, (2019).
6. Häusler, D. *et al.* Functional characterization of reappearing B cells after anti-CD20 treatment of CNS autoimmune disease. *Proc. Natl. Acad. Sci.* **115**, 9773–9778 (2018).
7. Sharma, S., Orlowski, G. & Song, W. Btk regulates B cell receptor-mediated antigen processing and presentation by controlling actin cytoskeleton dynamics in B cells. *J. Immunol. Baltim. Md 1950* **182**, 329–339 (2009).
8. Pal Singh, S., Dammeijer, F. & Hendriks, R. W. Role of Bruton's tyrosine kinase in B cells and malignancies. *Mol. Cancer* **17**, (2018).
9. Haselmayer, P. *et al.* Efficacy and Pharmacodynamic Modeling of the BTK Inhibitor Evobrutinib in Autoimmune Disease Models. *J. Immunol. Baltim. Md 1950* **202**, 2888–2906 (2019).
10. Hauser, S. L. *et al.* B-cell depletion with rituximab in relapsing-remitting multiple sclerosis. *N. Engl. J. Med.* **358**, 676–688 (2008).
11. Sabatino, J. J., Zamvil, S. S. & Hauser, S. L. B-Cell Therapies in Multiple Sclerosis. *Cold Spring Harb. Perspect. Med.* **9**, (2019).

12. Memon, A. B. *et al.* Long-term safety of rituximab induced peripheral B-cell depletion in autoimmune neurological diseases. *PloS One* **13**, e0190425 (2018).

13. Chen, D. R. & Cohen, P. L. Living life without B cells: is repeated B-cell depletion a safe and effective long-term treatment plan for rheumatoid arthritis? *Int. J. Clin. Rheumatol.* **7**, 159–166 (2012).

14. Brynjolfsson, S. F. *et al.* Long-Lived Plasma Cells in Mice and Men. *Front. Immunol.* **9**, (2018).

15. Montalban, X. *et al.* Placebo-Controlled Trial of an Oral BTK Inhibitor in Multiple Sclerosis. *N. Engl. J. Med.* (2019). doi:10.1056/NEJMoa1901981

16. Cariappa, A. *et al.* The recirculating B cell pool contains two functionally distinct, long-lived, posttransitional, follicular B cell populations. *J. Immunol. Baltim. Md 1950* **179**, 2270–2281 (2007).

17. Steimle, V., Siegrist, C. A., Mottet, A., Lisowska-Grospierre, B. & Mach, B. Regulation of MHC class II expression by interferon-gamma mediated by the transactivator gene CIITA. *Science* **265**, 106–109 (1994).

18. Olalekan, S. A., Cao, Y., Hamel, K. M. & Finnegan, A. B cells expressing IFN-γ suppress Treg-cell differentiation and promote autoimmune experimental arthritis. *Eur. J. Immunol.* **45**, 988–998 (2015).

19. Kinzel, S. *et al.* Myelin-reactive antibodies initiate T cell-mediated CNS autoimmune disease by opsonization of endogenous antigen. *Acta Neuropathol. (Berl.)* **132**, 43–58 (2016).

20. Horwood, N. J. *et al.* Bruton's tyrosine kinase is required for TLR2 and TLR4-induced TNF, but not IL-6, production. *J. Immunol. Baltim. Md 1950* **176**, 3635–3641 (2006).

21. Taneichi, H. *et al.* Toll-like receptor signaling is impaired in dendritic cells from patients with X-linked agammaglobulinemia. *Clin. Immunol. Orlando Fla* **126**, 148–154 (2008).

Online Materials and Methods

Approval of human sampling

Human peripheral blood mononuclear cells (PBMCs) were obtained after informed consent. The protocol was approved by the Ethics committee of the University Medicine of Göttingen, approval number 3/4/14.

Mice

Wild type (WT) C57BL/6 mice were bred in-house. MOG p35-55 TCR transgenic 2D2 mice were kindly provided by Dr. Kuchroo (Boston, USA). All animal experiments were carried out in accordance with the guidelines of the Central Department for Animal Experiments, University Medical Center, Göttingen and approved by the Office for Consumer Protection and Food Safety of the State of Lower Saxony (protocol number 33.9-42502-04-16/2267).

Evobrutinib dosing and BTK exposure

Evobrutinib was formulated in 20% Kleptose HPB (Roquette) in 50 mM Na-Citrate buffer pH 3.0. The compound was administered by oral gavage, and 1 hour after dosing blood was collected via the vena facialis into serum tubes. The tubes were centrifuged, serum was collected and used for measurement of the compound concentrations by LC–MS.

EAE induction and scoring

Female WT mice were immunized subcutaneously with 75 µg MOG protein 1-117 emulsified in Complete Freund's Adjuvant (CFA; Sigma-Aldrich, St. Louis, USA) containing 250 µg killed *Mycobacterium tuberculosis* H37 Ra (BD Bioscience, Heidelberg, Germany) followed by intraperitoneal injections of 300 ng of *Bordetella pertussis* toxin (Sigma-Aldrich) at the day of immunization and 2 days thereafter. EAE severity was assessed daily on a scale from 0 to 5 scale as follows: 0 = no clinical signs; 1.0 = tail paralysis; 2.0 = loss of righting reflex; 3.0 = beginning hind limb paresis; 4.0 = paralysis of both hind limbs; 4.5 = beginning forelimb paresis 5.0 = moribund / death.

Histology and immunohistochemistry

Mice were transcardially perfused with PBS followed by 4% paraformaldehyde (PFA) and tissue was paraffin embedded. One µm-thick sections were stained with hematoxylin and eosin (H&E) and luxol fast blue / periodic acid shift (LFB/PAS). T cells, B cells and macrophages were detected by immunohistochemistry with an avidin-biotin technique using antibodies

specific for CD3 (SP7; DCS Innovative Diagnostik-Systeme, Hamburg, Germany), CD45R/B220 (RA3-6B2; BD Biosciences) and Mac-3 (M3/84; BD Biosciences). Histological sections were captured using a digital camera (DP71; Olympus Europa GmbH, Hamburg, Germany) mounted on a light microscope (BX51; Olympus Europa GmbH) or a VS120 slide scanner (Olympus Europa GmbH). The percentage of demyelinated white matter was calculated using ImageJ. Overall immune cell infiltration was assessed on HE stained slides using an automated counting macro. Inflammatory cells were quantified at 400x magnification using an ocular counting grid and are shown as cells/mm². At least 4 spinal cord cross sections were taken for each analysis.

Isolation of human and murine leucocytes

PBMCs from healthy donors were isolated after Ficoll gradient centrifugation (Biochrom GmbH, Berlin, Germany). Human B cells were purified from PBMCs by positive MACS separation using a human CD19 isolation kit (Miltenyi, Bergisch Gladbach, Germany). Single cell suspensions of murine lymphoid tissues were generated by gentle dissection and passing through a 70 µm cell strainer (Greiner bio-one, Kremsmuenster, Austria). Murine blood was collected in PBS containing 1 mM EDTA followed by erythrocyte lysis using BD Pharm Lysing Buffer. Murine B and T cells were isolated by negative MACS separation using a mouse pan T cell isolation kit II (Miltenyi, Bergisch Gladbach, Germany) or positive MACS separation using a MojoSort mouse B cell isolation (BioLegend, San Diego, USA).

Flow cytometry

Murine immune cells was analyzed using the following antibodies: CD3 (145-2C11, BioLegend), CD4 (GK1.5, BioLegend), CD8 (53-6.7, BioLegend), CD11b (M1/70, BioLegend), CD19 (6D5, BioLegend; 1D3, BioLegend), CD21 (7G6, BD Biosciences), CD23 (B3B4, BioLegend), CD25 (PC61.5; eBioScience), CD27 (LG.3A10, BioLegend), CD44 (IM7; BioLegend), CD45R/B220 (RA3-6B2, BioLegend), CD69 (H1.2F3; BioLegend), CD80 (GL1; BD BioSciences), CD86 (GL-1; BD BioScience), CD93 (AA4.1, BioLegend), IgD (11-26c.2a, BioLegend), IgM (AF6-78, BD Biosciences) and MHCII (AF6-120.1; BioLegend).

Human immune cells was analyzed using the following antibodies: BTK (53/BTK, BD PhosFlow), pBTK (N35-88, BD PhosFlow), CD19 (HIB19, BioLegend), CD27 (L128, BD BioScience), CD38 (HIT-2, BioLegend), IgD (IA6-2, BD BioScience), IgM (MHM-88, BioLegend).

For the analysis of T cell proliferation, T cells were stained with carboxyfluorescein succinimidyl ester (CFSE). T regulatory cell differentiation was evaluated by intracellular staining for FoxP3 (FJK-16s; eBioScience) after fixation and permeabilization using the fixation/permeabilization kit (eBioScience). To investigate Th1 and Th17 cell differentiation cells were stimulated with 50 ng/ml phorbol 12-myristate 13-acetate (PMA; Sigma-Aldrich) and 0.5 µg/ml ionomycin (Sigma-Aldrich) for 3h with subsequent addition of 1 µl/ml brefeldin A (BD Bioscience) for 2h. Cytokine production was analyzed by intracellular staining for IFN-γ (XMG1.2; BioLegend) and IL-17A (TC11-18H10; BD Bioscience) after fixation/permeabilization (BD Bioscience). Dead cells were stained with LIVE/DEAD™ Fixable Aqua Dead Cell Stain Kit (Thermo Fisher Scientific, Waltham, USA). Samples were acquired on a BD LSR Fortessa (BD Bioscience). All data evaluation was performed using FlowJo software (FlowJo LLC, Ashland, USA).

Calcium flux

Purified B or T cells were stained in complete HBSS medium (HBSS medium containing 1.3 mM CaCl2, 0.5 mM MgCl2 and 1% FCS) containing 0.02% Pluronic F-68 (Life Technologies, Waltham, USA) at 37°C for 30 minutes in the presence of 4 mg/ml Fluo-3 AM and 10 mg/ml Fura Red AM (Biomol GmbH, Hamburg, Germany). Cells were kept on ice, pre-incubated with the indicated concentrations of evobrutinib for at least 30 min and directly before flow cytometry acquisition pre-heated to 37°C for 5 minutes. After 25 s baseline recording, human or mouse B cells were stimulated with 20 or 40 µg/ml anti-IgM / IgG $F(ab')_2$ fragment (Dianova), respectively. T cells were marked using antibodies against CD3 (145-2C11, BioLegend) and CD28 (37.51, BioLegend) which, after baseline recording, were crosslinked using 5 µg/ml anti-hamster secondary antibody.

Quantitative PCR

Isolated B cells were incubated with the evobrutinib for 60 minutes at 37°C followed by stimulation with 10 µg/ml anti-IgM / IgG $F(ab')_2$ fragment (Dianova) at 37°C for 3h. RNA was isolated using the RNeasy mini kit (Qiagen, Hilden, Germany) and transcribed into cDNA using the QuantiNova Reverse Transcription kit (Qiagen). Quantitative (q)PCR was performed using 500 nM Primer and qPCRBIO SyGreen (Nippon Genetics Europe GmbH, Dueren, Germany) in a total volume of 10 µl on a QuantStudio 7 (Applied Biosystems, Waltham, USA). Primers specific for IL-6, IL-10, IFNγ, B2M and GAPDH were purchased from Eurofins Genomics. qPCR was performed at 95°C denaturating and 70°C annealing temperature for 30s and 40

cycles with subsequent melt-curve analysis. Primer specificity was validated by product size using a 2% Agarose gel containing GelRed (Biotium) and UV-light illumination. Detailed primer information is listed in the **suppl. table 2**. Samples were analyzed in duplicates or triplicates and considered valid when cycle threshold (Ct) <35 and standard deviation of Ct<0.5. Analyzed cytokine expression was normalized to B2M and GAPDH (delta-Ct). The relative expression was determined in comparison to the control treated group.

Stimulation human B cells

Isolated human B cells were left to rest for 1 hour and pre-incubated with the indicated concentrations of evobrutinib for at least 30 min before stimulation with 4 µg/ml CpG for 24h. Supernatants were collected after centrifugation and stored at -20°C before ELISA detection of IL-6 (BioLegend) and IL-10 (BioLegend) according to the manufacturers' instructions.

Statistical analysis

Statistics were calculated using the software GraphPad Prism 6.01. The clinical score, maturation, qPCR were analyzed by 2-way ANOVA; histology, calcium flux, T cell proliferation, T cell differentiation, cytokine production were analyzed by ordinary 1-way ANOVA; expression of activation markers was analyzed by Kruskal-Wallis. Human data was analyzed by student´s t-test. All groups were compared to control treatment and corrected for multiple comparisons.

Acknowledgements

We thank Katja Grondey and Julian Koch for excellent technical support. M.S. Weber is serving as an editor for PLoS One. He receives research support from the National Multiple Sclerosis Society (NMSS; PP 1660), the Deutsche Forschungsgemeinschaft (DFG; WE 3547/5-1), from Novartis, TEVA, Biogen-Idec, Roche, Merck and the ProFutura Programm of the Universitätsmedizin Göttingen.

Author contributions

S.T. carried out the experiments and analyzed the data. R.P. and S.T. planned and carried out the experiments with human samples. P.H. performed the BTK exposure measurement. S.T. and D.H. prepared the figures. M.S.W. supervised the research. S.T. and M.S.W. drafted the manuscript. S.T., D.H., R.G., U.B., W.B. and M.S.W participated in reviewing and editing the manuscript.

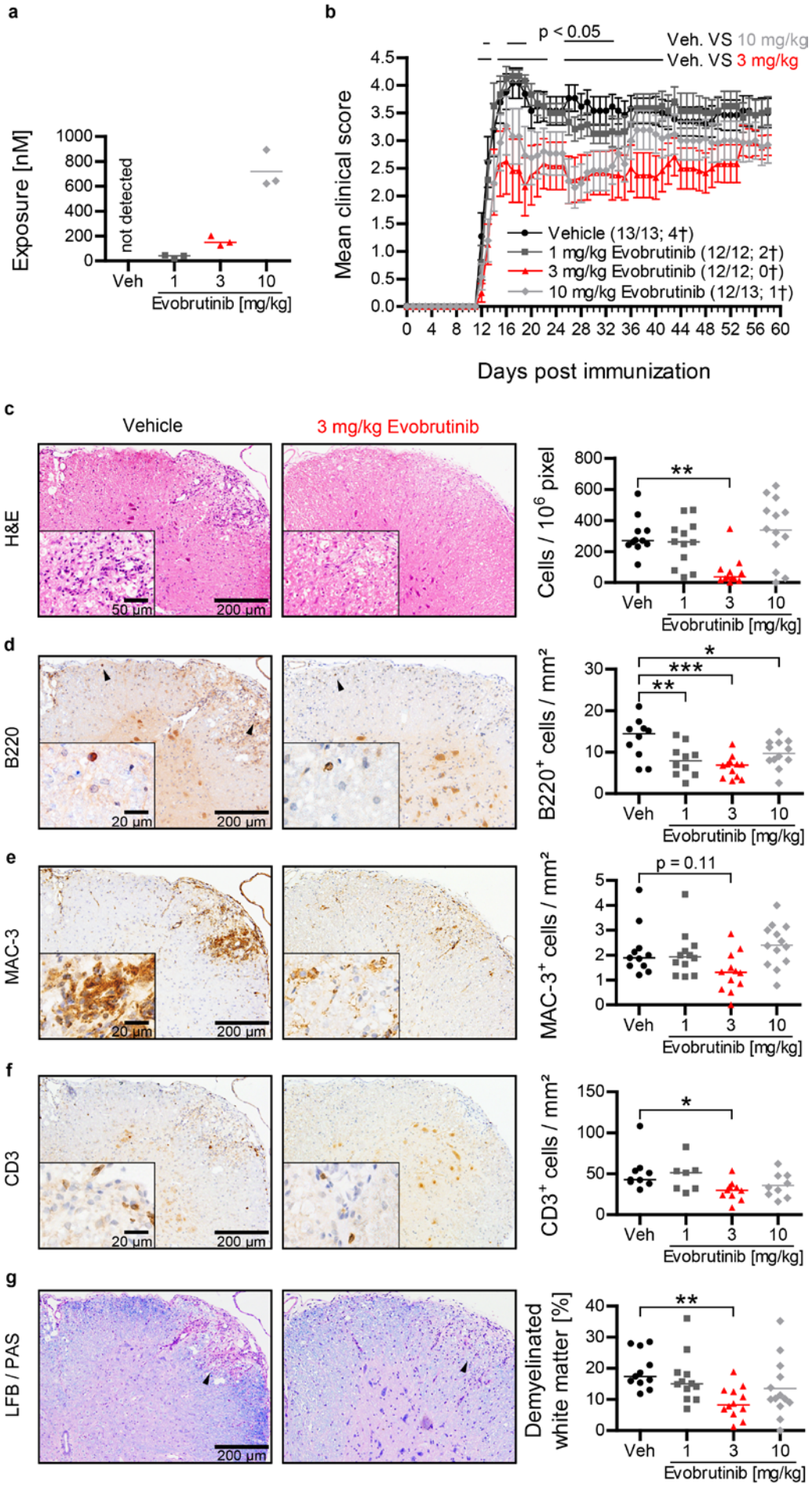
a
Exposure [nM]
1000
800
600
400
200
0
not detected
Veh
1
3
10
Evobrutinib [mg/kg]
b
p < 0.05
Veh. VS 10 mg/kg
Veh. VS 3 mg/kg
Mean clinical score
4.5
4.0
3.5
3.0
2.5
2.0
1.5
1.0
0.5
0.0
Vehicle (13/13; 4†)
1 mg/kg Evobrutinib (12/12; 2†)
3 mg/kg Evobrutinib (12/12; 0†)
10 mg/kg Evobrutinib (12/13; 1†)
0 4 8 12 16 20 24 28 32 36 40 44 48 52 56 60
Days post immunization
c
Vehicle
3 mg/kg Evobrutinib
H&E
50 µm
200 µm
Cells / 10^6 pixel
800
600
400
200
0
**
Veh
1
3
10
Evobrutinib [mg/kg]
d
B220
20 µm
200 µm
B220+ cells / mm²
30
20
10
0
*
***
**
Veh
1
3
10
Evobrutinib [mg/kg]
e
MAC-3
20 µm
200 µm
MAC-3+ cells / mm²
5
4
3
2
1
0
p = 0.11
Veh
1
3
10
Evobrutinib [mg/kg]
f
CD3
20 µm
200 µm
CD3+ cells / mm²
150
100
50
0
*
Veh
1
3
10
Evobrutinib [mg/kg]
g
LFB / PAS
200 µm
Demyelinated white matter [%]
40
30
20
10
0
**
Veh
1
3
10
Evobrutinib [mg/kg]

Figure 1 Evobrutinib reduces clinical and histological EAE

Oral treatment of C57/Bl6 with control or 1, 3 or 10 mg/kg Evobrutinib started 7 days prior to immunization with 75 µg conformational MOG1-117 protein along with 300ng PTX on days 0 and 2. **a** BTK exposure was measured in the serum 1h after oral dosing by LC-MS. **b** Clinical severity was assessed on a standard 0-5 scale. Spinal cords were isolated 60 days after EAE induction and stained for **c** overall immune cell infiltration (HE), infiltration of **d** B cells ($B220^+$), **e** macrophages (Mac3), **f** T cells ($CD3^+$) and **g** overall demyelination (LFB/PAS). Mean±SEM or median, n=9-13, * $p<0.05$, ** $p<0.01$, *** $p<0.001$.

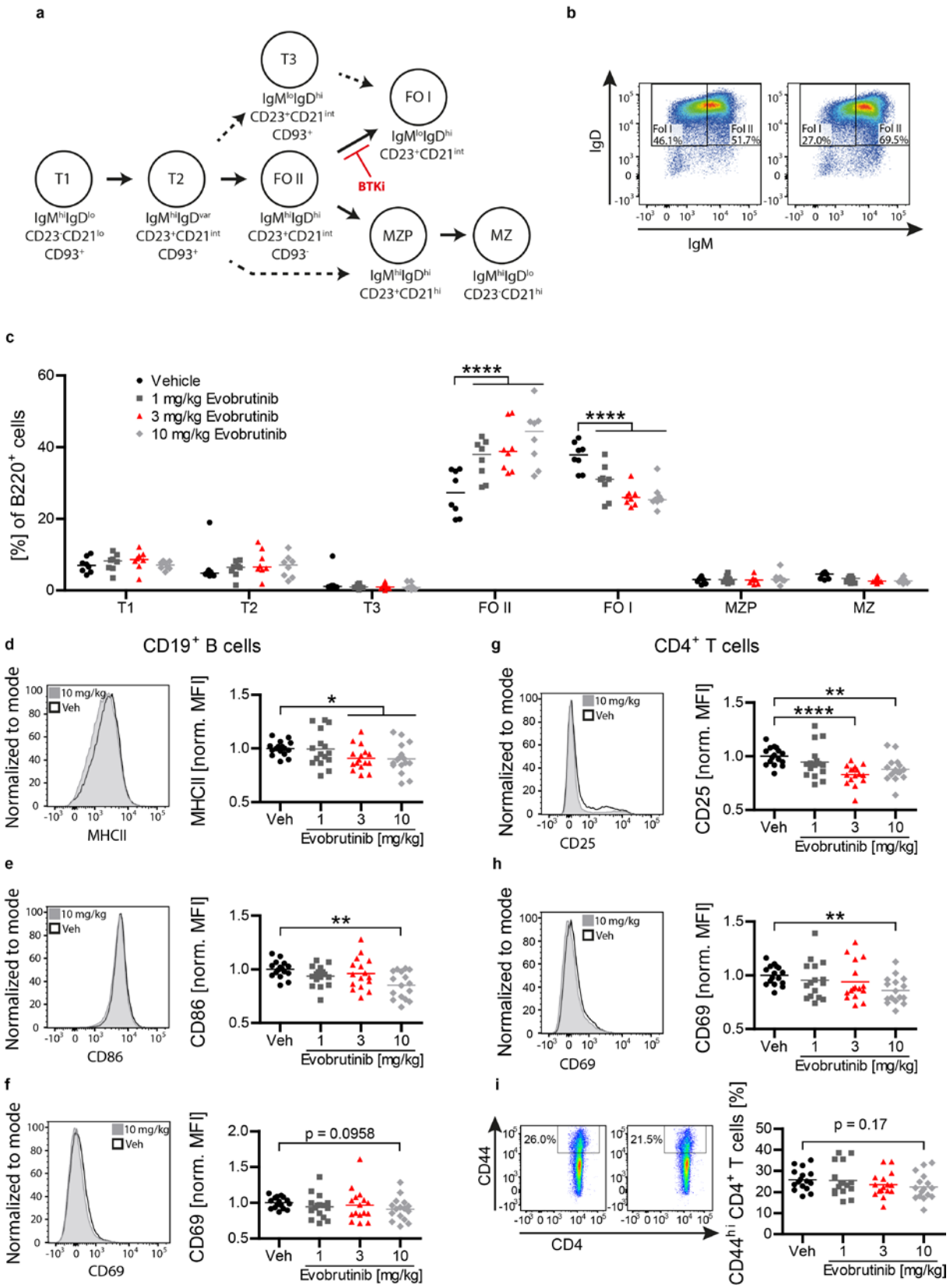
a
T1
IgM^hiIgD^lo
CD23^-CD21^lo
CD93^+
T2
IgM^hiIgD^var
CD23^+CD21^int
CD93^+
T3
IgM^loIgD^hi
CD23^+CD21^int
CD93^+
FO II
IgM^hiIgD^hi
CD23^+CD21^int
CD93^-
FO I
IgM^loIgD^hi
CD23^+CD21^int
BTKi
MZP
IgM^hiIgD^hi
CD23^+CD21^hi
MZ
IgM^hiIgD^lo
CD23^-CD21^hi
b
IgD
IgM
FoI I 46.1%
FoI II 51.7%
FoI I 27.0%
FoI II 69.5%
c
[%] of B220^+ cells
Vehicle
1 mg/kg Evobrutinib
3 mg/kg Evobrutinib
10 mg/kg Evobrutinib
****
****
T1
T2
T3
FO II
FO I
MZP
MZ
d
CD19^+ B cells
Normalized to mode
10 mg/kg
Veh
MHCII
MHCII [norm. MFI]
*
Veh
1
3
10
Evobrutinib [mg/kg]
e
CD86
CD86 [norm. MFI]
**
f
CD69
CD69 [norm. MFI]
p = 0.0958
g
CD4^+ T cells
CD25
CD25 [norm. MFI]
**
****
h
CD69
CD69 [norm. MFI]
**
i
CD44
CD4
26.0%
21.5%
CD44^hi CD4^+ T cells [%]
p = 0.17

Figure 2 Evobrutinib inhibits the maturation of B cells and reduces expression of activation markers on B and T cells

Oral treatment of C57/Bl6 with control or 1, 3 or 10 mg/kg Evobrutinib started 7 days prior to immunization with 75 µg conformational MOG1-117 protein. Splenic cells were analyzed 12 days after immunization by flow cytometry. B cell subsets were categorized into transitional (T), follicular (FO), marginal zone precursor (MZP) and marginal zone (MZ) cells according to **a** and **b**. **c** Frequency of $B220^{+}$ and expression of **d** MHCII, **e** CD86 and **f** CD69 on B cells. Expression of **g** CD25, **h** CD69 and **j** CD44 on T cells. Median, n=8-16 pooled from 4-8 experiments, * $p<0.05$, ** $p<0.01$, **** $p<0.0001$.

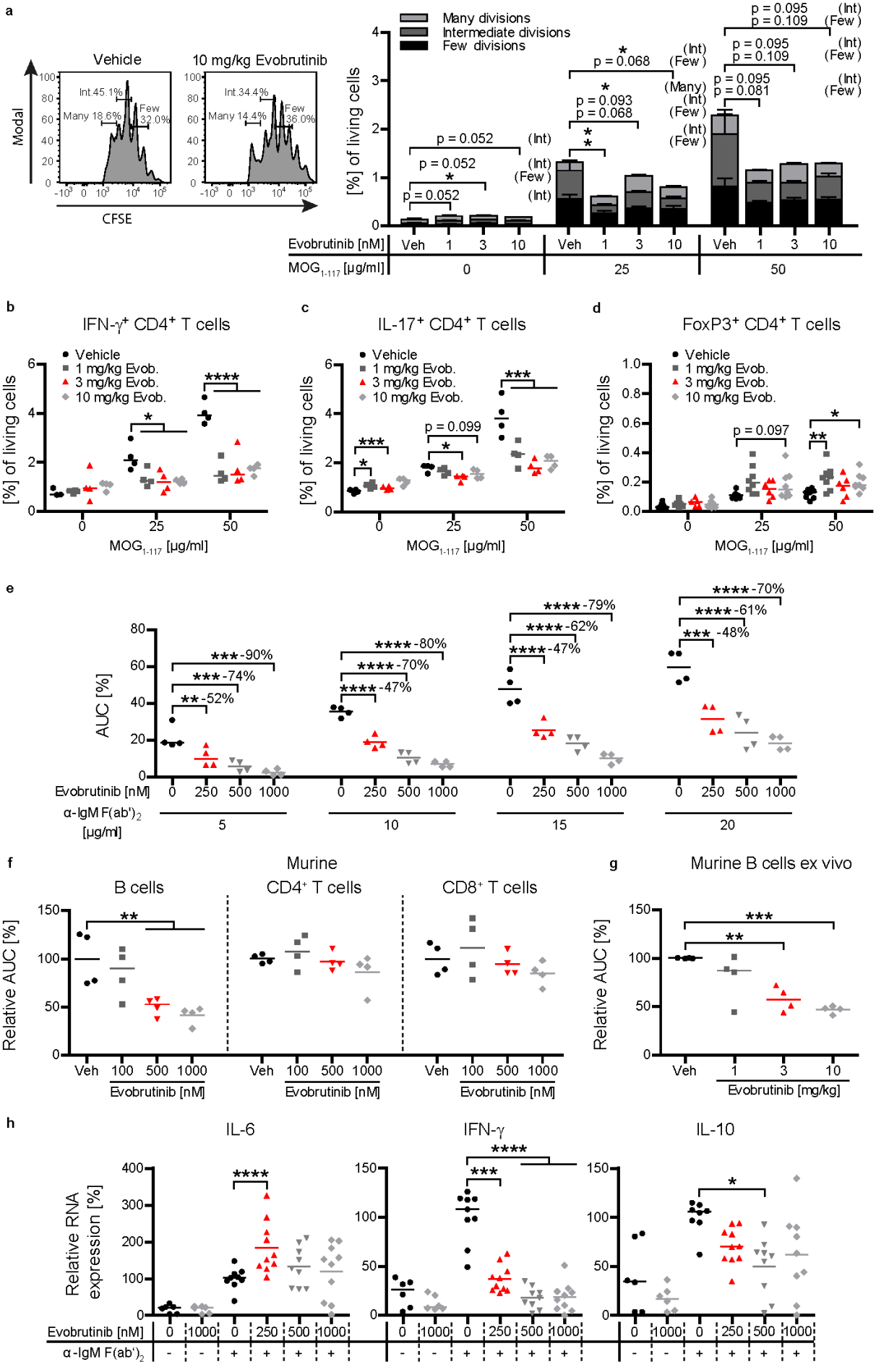
a
Vehicle
10 mg/kg Evobrutinib
Modal
CFSE
Int.45.1%
Many 18.6%
Few 32.0%
Int.34.4%
Many 14.4%
Few 36.0%
Many divisions
Intermediate divisions
Few divisions
[%] of living cells
Evobrutinib [nM]
MOG1-117 [µg/ml]
b
IFN-γ+ CD4+ T cells
c
IL-17+ CD4+ T cells
d
FoxP3+ CD4+ T cells
Vehicle
1 mg/kg Evob.
3 mg/kg Evob.
10 mg/kg Evob.
e
AUC [%]
α-IgM F(ab')2 [µg/ml]
f
Murine
B cells
CD4+ T cells
CD8+ T cells
Relative AUC [%]
g
Murine B cells ex vivo
Evobrutinib [mg/kg]
h
IL-6
IFN-γ
IL-10
Relative RNA expression [%]

Figure 3 Evobrutinib inhibits B cell APC function and excitatory calcium mobilization and cytokine production

Oral treatment of C57/Bl6 with control or 1, 3 or 10 mg/kg Evobrutinib started 7 days prior to immunization with 75 µg conformational MOG1-117 protein. Splenic B cells from mice 12 days after immunization and WT T cells from 2D2 mice were isolated by magnetic separation and co-cultured with B cells for 72h. **a** T cell proliferation was analyzed by CFSE dilution. T cell differentiation was analyzed by intra-cellular flow cytometry for the production of **b** IFN-γ, **c** IL-17 and **d** FoxP3. Calcium mobilization was analyzed using Fluo-3 and Fura Red after at least 30 min pre-incubation with the indicated concentrations evobrutinib. **e** Stimulation with the indicated concentrations anti-IgM. **f** Stimulation with a-IgM (B cells) or a-CD3 / a-CD28 crosslinking. **g** B cells were isolated after 3 days of evobrutinib treatment. **h** Cytokine production was analyzed after 3h a-IgM stimulation via qPCR. Mean±SEM or median, n=4-10 representative data or pooled from at least 2 independent experiments, * $p<0.05$, ** $p<0.01$, *** $p<0.001$, **** $p<0.0001$.

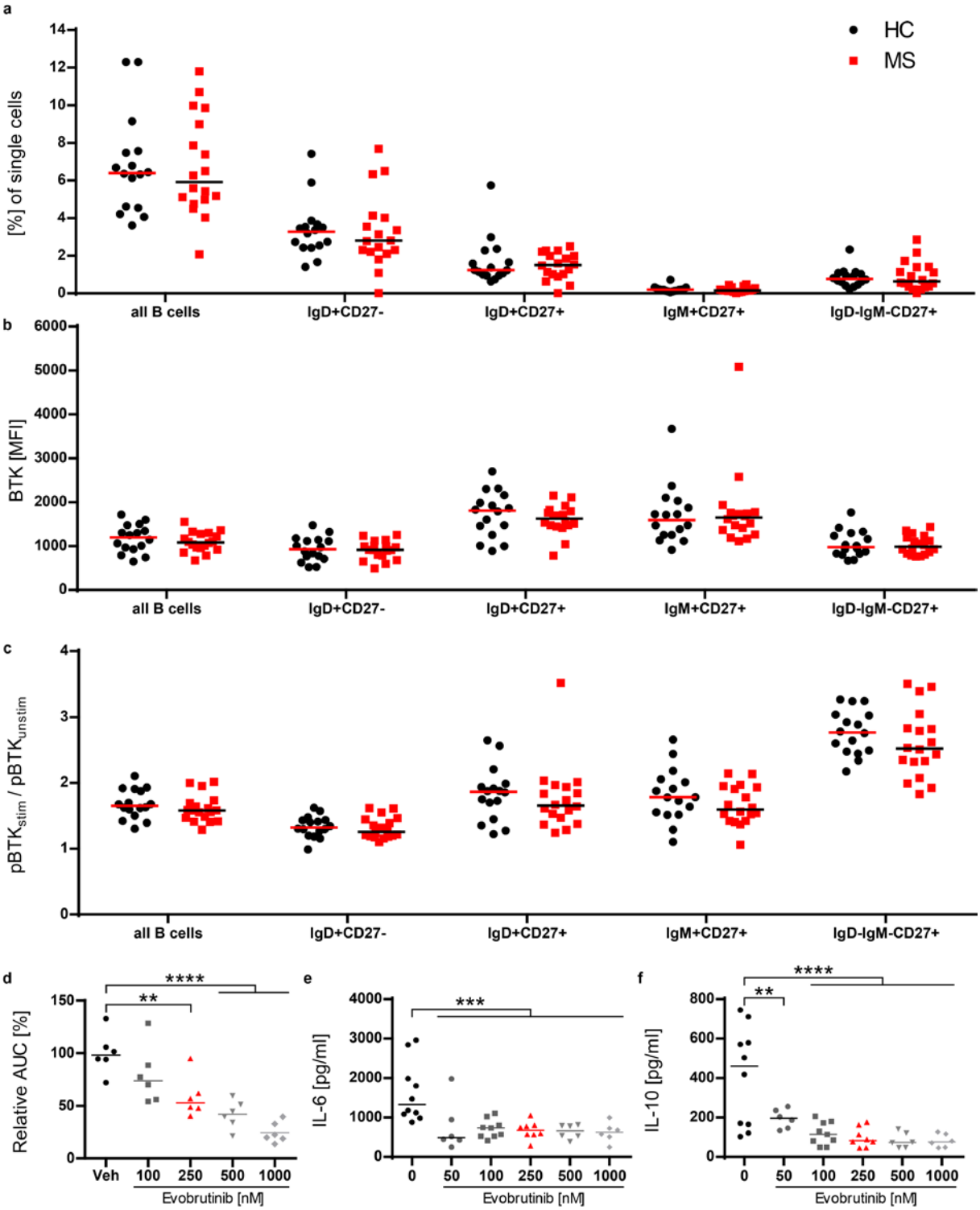
a
HC
MS
[%] of single cells
all B cells
IgD+CD27-
IgD+CD27+
IgM+CD27+
IgD-IgM-CD27+
b
BTK [MFI]
c
pBTKstim / pBTKunstim
d
Relative AUC [%]
Veh
Evobrutinib [nM]
e
IL-6 [pg/ml]
f
IL-10 [pg/ml]

Figure 4 BTK inducibility depends on B cell maturation and activation, evobrutinib reduces cytokine production and calcium mobilization

PBMCs from healthy controls (HC) or MS patients were thawed from -80°C storage, stained for surface markers and stimulated for 30s using a-IgM. After immediate fixation and permeabilization, intra-cellular antibodies for BTK and pBTK were incubated for 1h. **a** Frequency of B cells / B cell subsets on single cells. **b** BTK expression by MFI **c** BTK phosphorylation. **d** Calcium mobilization was analyzed using Fluo-3 and Fura Red after at least 30 min pre-incubation with the indicated concentrations evobrutinib. Isolated human B cells were stimulated using 4 µg/ml CpG for 22h. Cytokine production of **e** IL-6 and **f** IL-10 was analyzed by ELISA. **r**

Supplementary material

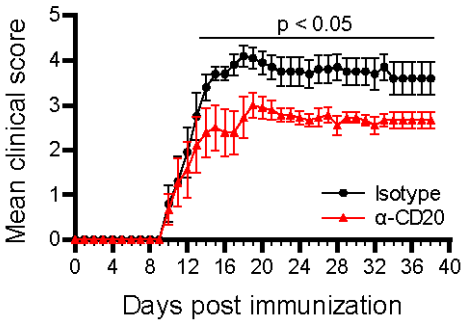

Suppl. Figure 1 Anti-CD20 mediated B cell depletion ameliorates EAE

Prophylactic treatment of C57/Bl6 with control or anti-CD20 antibody started 3 weeks prior to immunization with 75 µg conformational MOG1-117 protein along with 300ng PTX on days 0 and 2. Clinical severity was assessed on a standard 0-5 scale. Mean±SEM, n=10

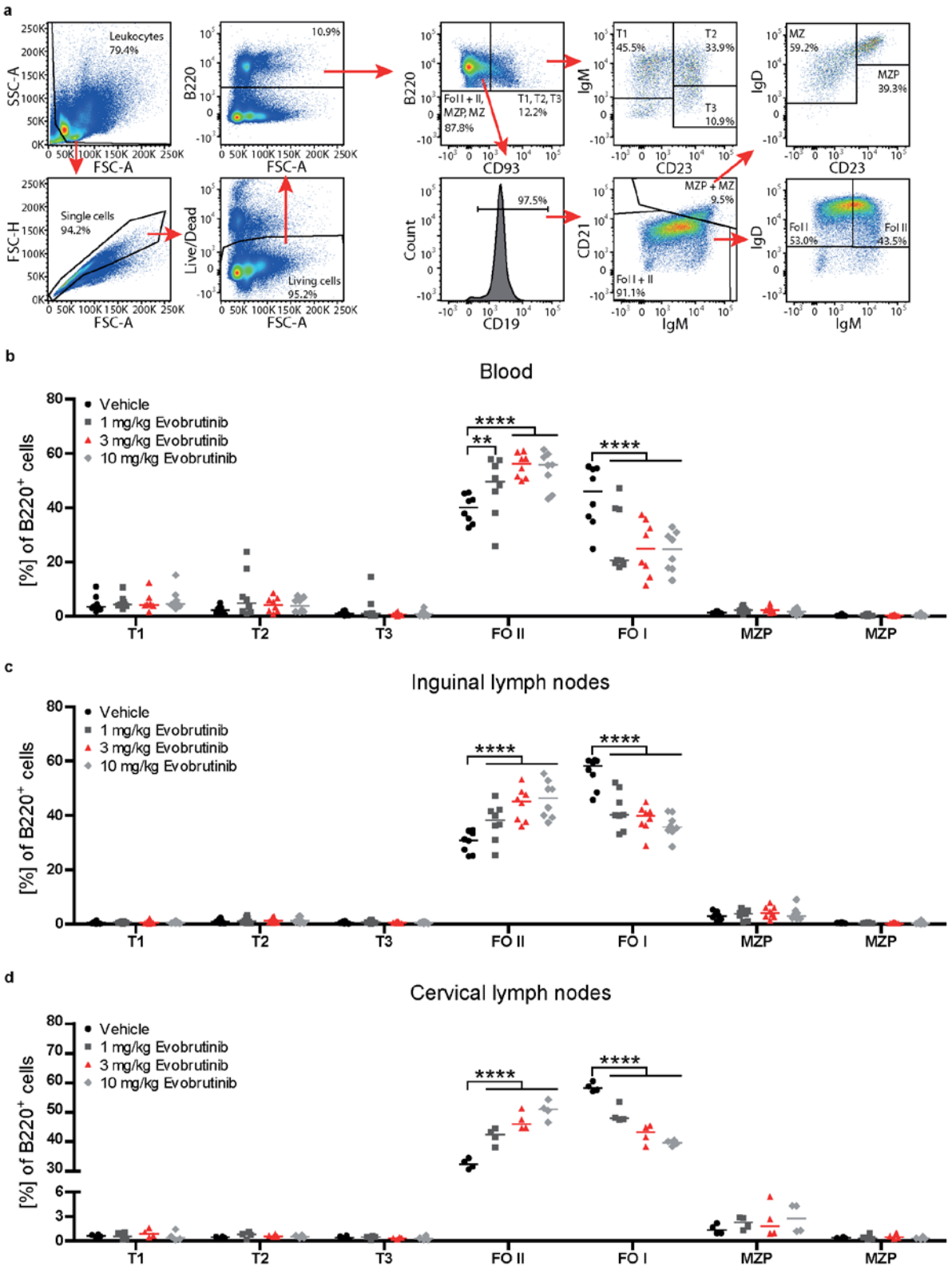
a
Leukocytes
79.4%
SSC-A
FSC-A
10.9%
B220
Single cells
94.2%
FSC-H
Live/Dead
Living cells
95.2%
FoI + II,
MZP, MZ
87.8%
T1, T2, T3
12.2%
CD93
T1
45.5%
T2
33.9%
T3
10.9%
IgM
CD23
MZ
59.2%
MZP
39.3%
IgD
97.5%
Count
CD19
MZP + MZ
9.5%
CD21
FoI + II
91.1%
FoI
53.0%
FoII
43.5%
b
Blood
c
Inguinal lymph nodes
d
Cervical lymph nodes
[%] of B220+ cells
Vehicle
1 mg/kg Evobrutinib
3 mg/kg Evobrutinib
10 mg/kg Evobrutinib
****
**
T1
T2
T3
FO II
FO I
MZP
MZP

Suppl. Figure 2

Oral treatment of C57/Bl6 with control or 1, 3 or 10 mg/kg Evobrutinib started 7 days prior to immunization with 75 µg conformational MOG1-117 protein. Cells isolated from the various organs were analyzed 12 days after immunization by flow cytometry. B cell subsets were categorized into transitional (T), follicular (FO), marginal zone precursor (MZP) and marginal zone (MZ) cells. Frequency of $B220^{+}$ in the **b** blood, **c** inguinal lymph node and **d** cervical lymph node. Median, n=4-8 pooled from 2-4 experiments, ** $p<0.01$, **** $p<0.0001$.

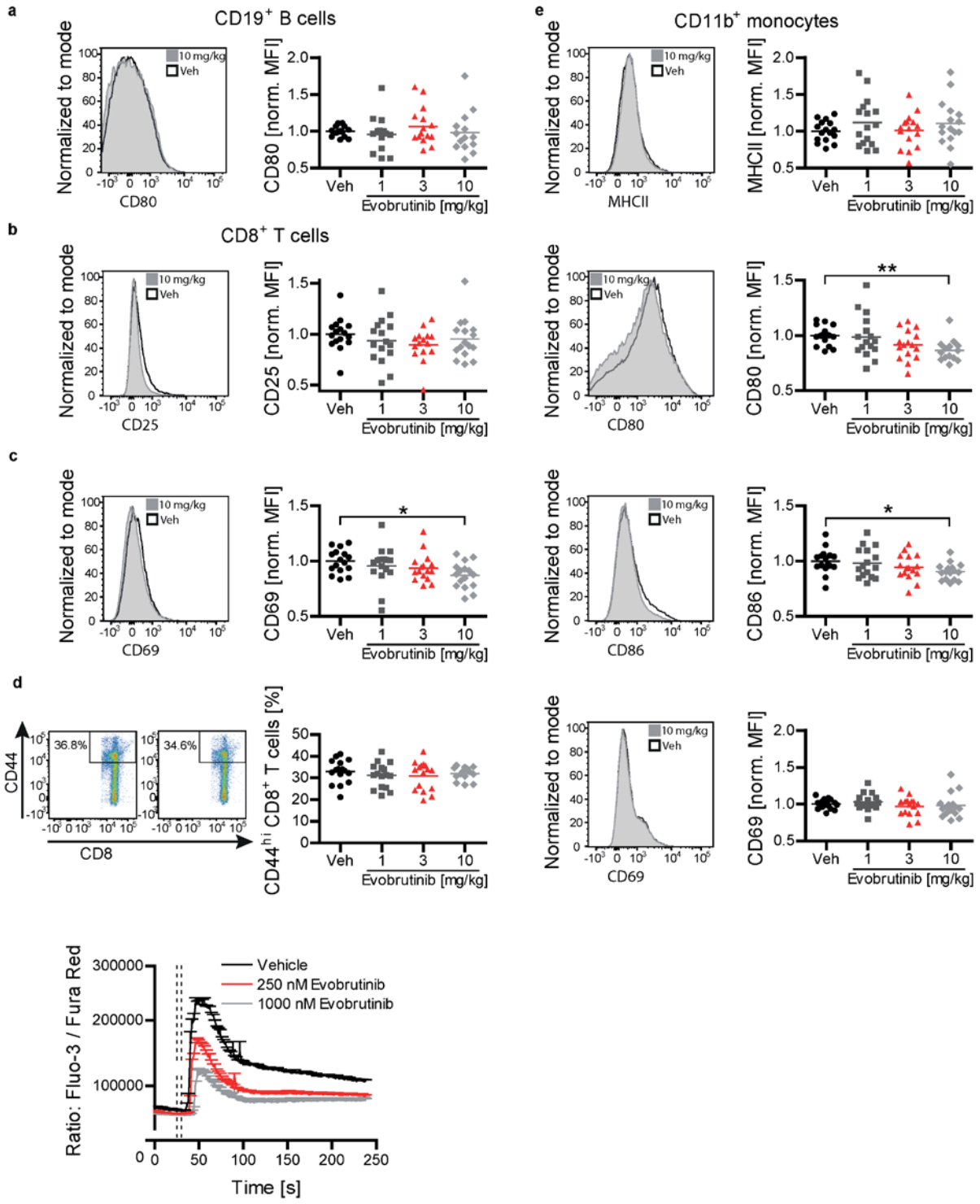
a
CD19+ B cells
Normalized to mode
10 mg/kg
Veh
CD80
CD80 [norm. MFI]
Veh
1
3
10
Evobrutinib [mg/kg]
e
CD11b+ monocytes
MHCII
MHCII [norm. MFI]
b
CD8+ T cells
CD25
CD25 [norm. MFI]
CD80
**
c
CD69
CD69 [norm. MFI]
*
CD86
CD86 [norm. MFI]
d
CD44
CD8
36.8%
34.6%
CD44hi CD8+ T cells [%]
Vehicle
250 nM Evobrutinib
1000 nM Evobrutinib
Ratio: Fluo-3 / Fura Red
Time [s]

Suppl. Figure 3

Oral treatment of C57/Bl6 with control or 1, 3 or 10 mg/kg Evobrutinib started 7 days prior to immunization with 75 µg conformational MOG1-117 protein. Splenic cells were analyzed 12 days after immunization by flow cytometry. Expression of **a** MHCII on $CD19^+$ B cells, **b** CD25 **c** CD69 and **d** $CD44^{hi}$ on $CD8^+$ T cells, and **e** MHCII, CD80, CD86 and CD69 on $CD11b^+$ monocytes. **f** Exemplary plot for calcium flux analysis. Median, n=16 pooled from 8 experiments, * $p<0.05$, ** $p<0.01$.

Suppl. Table 1 Patient characteristics

	HC	**MS**	**p-value**
Age Mean ± SD	37.75 ± 12.12	37.93 ± 13.39	0.9669
Female, n (%)	9 (56.25%)	11 (61.11%)	0.7738
Time since diagnosis [years], mean ± SD	n.a.	4.81 ± 5.83	
EDSS, mean ± SD	n.a.	3.35 ±2.37	
Clinical course of MS, n (%)			
CIS / RIS	n.a.	3 (16.67%)	
RRMS	n.a.	10 (55.55%)	
SPMS / PPMS	n.a.	5 (27.78)	
Treatment			
Corticosteroids (within last 2m)	n.a.	4 (22.22%)	
DMD (>7d, within last 2m)	n.a.	1 (5.55% Copaxone)	
untreated	n.a.	14 (77.77%)	

Suppl. Table 2 Primer Information

Target	Amplicon length	Fw primer	Rv primer
IL-6	152	CCTCTGGTCTTCTGGAGTACC	ACTCCTTCTGTGACTCCAGC
IL-10	206	ATAACTGCACCCACTTCCCA	GGGCATCACTTCTACCAGGT
IFNγ	165	TTCTTCAGCAACAGCAAGGC	TCAGCAGCGACTCCTTTTCC
B2M	227	CGGCCTGTATGCTATCCAGA	GGGTGAATTCAGTGTGAGCC
GAPDH	83	CATGGCCTTCCGTGTTCCTA	TGTCATCATACTTGGCAGGTTTCT

3. Continuous high dose vitamin D exacerbates central nervous system autoimmune disease by raising T cell excitatory calcium

3.1. Background

Although the precise cause of MS is still unknown, several risk factors have been identified such as infection with Epstein Barr virus, smoking or lack of sun light exposure (Häusler and Weber, 2019). The latter correlates with latitude and could be linked to low levels of vitamin D, as it is generated upon ultraviolet (UV) light exposure. Vitamin D can also be ingested with food and although this a minor source compared to UV-radiation depended synthesis, it gains interest when being supplemented as a therapeutic approach. In MS, low serum levels of vitamin D are associated with increased relapse rate and disability progression (Simpson et al., 2018). Although a therapeutic benefit is still unclear, its supplementation is currently widely practised based on its harmlessness. Here we tested long-term high dose supplementation in EAE and its effect on immune cells.

3.2. Approach

In this work we fed mice with low-dose, standard and high-dose vitamin D diet and analysed the effects on EAE severity and the peripheral immune system. After inducing EAE, we observed a worsening of the clinical disease severity both in low-dose and high-dose vitamin D diet in comparison to standard diet. This was substantiated by histological analysis of demyelination and immune cell infiltration, specifically infiltrating T cells and macrophages. In the periphery we observed an increase in the frequency of inflammatory Th1 and Th17 cells, by expression of IFNγ and IL-17 respectively, and a slight reduction of regulatory T cells. Peripheral macrophages showed enhanced expression of MHCII, CD40, CD80 and CD86 as well as increased phagocytic capacity. Additionally, the activation markers CD69 and CD25 were upregulated on T cells, the frequency of memory T cells was increased and T cells showed enhanced proliferation upon *ex vivo* restimulation. By directly exposing T cells to vitamin D and its metabolites, we observed a dose-dependent inhibitory effect of the active variants 25-(OH)-vitamin D and 1,25-$(OH)_2$-vitamin D. However, since long-term high-dose vitamin D led to the development of secondary hypercalcemia in our study, we focused on the direct effects of elevated calcium levels. We observed a dose-dependent stimulatory effect of increased calcium concentrations on T cell proliferation, which we

connected to an increased calcium mobilization after TCR stimulation and increased cytokine production, both in murine and human T cells. Exposing T cells to elevated calcium furthermore facilitated an increase in migration ability, determined in an *in vitro* blood-brain barrier model. Elevating calcium independent from vitamin D in mice led to an increase of the T cell activation markers. In conclusion, we showed that long-term high dose supplementation of vitamin D in mice led to a hypercalcemia which in turn activated T cells facilitating their proliferation and pathogenic differentiation.

3.3. Contribution

I conducted the experiments for figures 2, 3, 5, and 7, and carried out the experiments demanded in the review of the manuscript. I collected, analysed and interpreted the resulting data and was implicated in statistical analysis. I partially prepared the resulting figures and wrote the respective parts of the manuscript.

3.4. Original publication

Häusler D*, Torke S*, Peelen E, Bertsch T, Djukic M, Nau R, Larochelle C, Zamvil SS, Brück W, Weber MS (2019): Continuous high dose vitamin D exacerbates central nervous system autoimmune disease by raising T cell excitatory calcium. BRAIN in press

*these authors contributed equally

High dose vitamin D exacerbates central nervous system autoimmunity by raising T cell-excitatory calcium

Darius Häusler[1*], Sebastian Torke[1*], Evelyn Peelen[2], Thomas Bertsch[3], Marija Djukic[1,4], Roland Nau[1,4], Catherine Larochelle[2], Scott S. Zamvil[5], Wolfgang Brück[1], Martin S. Weber[1,6]

[1]Institute of Neuropathology, University Medical Center, Göttingen, Germany; [2]Department of Neurosciences, Centre de recherche de l'Université de Montréal (CRCHUM), Montréal, Québec, Canada; [3]Institute of Clinical Chemistry, Laboratory Medicine and Transfusion Medicine, General Hospital Nuremberg, Paracelsus Medical University, Nuremberg, Germany; [4]Department of Geriatrics, Evangelisches Krankenhaus Göttingen-Weende, Göttingen, Germany; [5]Department of Neurology, University of California, San Francisco, CA USA; [6]Department of Neurology, University Medical Center, Göttingen, Germany

*These authors contributed equally.

Address correspondence to: Martin S. Weber, MD

Department of Neuropathology

Department of Neurology

University Medical Center, Georg August University

Robert-Koch-Str. 40, 37099 Göttingen, Germany

Phone +49-551 39-7706

Fax +49-551-39-10800

E-mail: martin.weber@med.uni-goettingen.de

Running title: Hypercalcemia by vitamin D exacerbates EAE

Key words: multiple sclerosis, experimental autoimmune encephalomyelitis, vitamin D, T cells, calcium

Abstract

Poor vitamin D status is associated with a higher relapse rate and earlier disability in multiple sclerosis. Based on these associations, MS patients are frequently supplemented with the vitamin D precursor cholecalciferol, although it is unclear whether this regimen is of therapeutic benefit. To model consequences of this common practice, mice were fed for more than three months with a low, medium or high dose of cholecalciferol, representative of vitamin D deficiency, modest and disproportionally high supplementation, respectively, in MS patients. Compared to vitamin D-deprived mice, its moderate supplementation reduced the severity of subsequent experimental autoimmune encephalomyelitis, which was associated with an expansion of regulatory T cells. Direct exposure of murine or human T cells to vitamin D metabolites inhibited their activation. In contrast, mice with 25-(OH) vitamin D levels above 200 nmol/L developed fulminant experimental autoimmune encephalomyelitis with massive CNS infiltration of activated myeloid cells, Th1 and Th17 cells. When dissecting this unexpected outcome, we observed that high, but not medium dose vitamin D had caused mild hypercalcemia which rendered T cells more prone to pro-inflammatory activation. Exposing murine or human T cells to equivalent calcium concentrations in vitro enhanced its influx, triggering activation, upregulation of pro-inflammatory gene products and enhanced transmigration across a blood-brain barrier model. These findings suggest that vitamin D at moderate levels may exert a direct regulatory effect, while continuous high dose vitamin D treatment could trigger MS disease activity by raising mean levels of T cell-excitatory calcium.

Introduction

Although the precise cause of multiple sclerosis (MS) remains unknown, various factors have been discovered, which determine an individual's risk to develop this chronic demyelinating disease of the central nervous system (CNS). A majority of risk alleles identified by genome-wide association studies relate to immune functions (Baranzini and Oksenberg, 2017), supporting an autoimmune etiology for the CNS inflammation, demyelination and neurodegeneration that is characteristic of MS. Environmental factors, such as a symptomatic Epstein Barr virus (EBV) infection at a vulnerable age (Ascherio and Munger, 2010), smoking (Wingerchuk, 2012) as well as lack of sun light exposure (Bjornevik *et al.*, 2014) and low levels of vitamin D (Munger *et al.*, 2006, Ascherio *et al.*, 2010) may also enhance the risk to develop MS. The latter two factors could be interdependent, as the primary form of vitamin D, cholecalciferol (vitamin D3) is generated in the skin upon ultraviolet (UV) radiation; alternatively, vitamin D can be ingested with food. While diet is generally considered the minor source of vitamin D (Holick, 2004), it may become essential when UVB exposure is limited (Holick, 1987). Based on the fact that vitamin D levels can be effectively and rapidly raised by diet, vitamin D supplementation has gained interest over the recent years in MS as well as other chronic conditions.

In general, MS patients have relatively low levels of vitamin D, which may refer to genetic and metabolic alterations associated with MS itself (Nieves *et al.*, 1994, Laursen *et al.*, 2015, Mokry *et al.*, 2015, Bhargava *et al.*, 2017). Lower serum concentrations of vitamin D increase the likelihood of both relapses and early onset of disability progression (Runia *et al.*, 2012), whereas levels above 70 nmol/L are associated with a decreased risk for attacks (Smolders *et al.*, 2008). While these findings clearly highlight low vitamin D levels as a negative predictor in MS, it is currently unclear whether this association is causal and accordingly, whether therapeutically raising the level of vitamin D in patients with MS is of clinical benefit (Stein *et al.*, 2011, Dorr *et al.*, 2012, Bhargava *et al.*, 2014). Primarily based on the perception of its harmlessness it is nevertheless current practice to broadly supplement vitamin D in patients with MS, often at excessively high doses. In light of the current lack of evidence for a clear therapeutic benefit in MS we revisited this concept and investigated the clinical and immunological effect of chronic vitamin D exposure in the preclinical MS model, murine experimental autoimmune encephalomyelitis (EAE).

Materials and Methods

Approval of human sampling

PBMCs were obtained after informed consent. The protocol was approved by the Ethics committee of the University Medicine of Göttingen, approval number 3/4/14.

Mice

Wild type (WT) C57BL/6 mice were purchased from Charles River (Sulzfeld, Germany). MOG p35-55 TCR transgenic 2D2 mice were kindly provided by Dr. Kuchroo (Boston, USA). All animal experiments were carried out in accordance with the guidelines of the Central Department for Animal Experiments, University Medical Center, Göttingen and approved by the Office for Consumer Protection and Food Safety of the State of Lower Saxony (protocol number 33.9-42502-04-13/1201, 33.9-42502-04-15/1804 and 33.9-42502-04-17/2615).

EAE induction and scoring

Female WT mice were immunized subcutaneously with 50 µg MOG peptide (p)35-55 MEVGWYRSPFSRVVHLYRNGK (Auspep, Parkville, Australia) emulsified in Complete Freund's Adjuvant (CFA; Sigma-Aldrich, St. Louis, USA) containing 250 µg killed *Mycobacterium tuberculosis* H37 Ra (BD Bioscience, Heidelberg, Germany) followed by intraperitoneal injections of 200 ng of *Bordetella pertussis* toxin (Sigma-Aldrich) at the day of immunization and 2 days thereafter. EAE severity was assessed daily and scored on a scale from 0 to 5 scale as follows: 0 = no clinical signs; 1.0 = tail paralysis; 2.0 = hindlimb paresis; 3.0 = severe hindlimb paresis; 4.0 = paralysis of both hindlimbs; 4.5 = hindlimb paralysis and beginning forelimb paresis 5.0 = moribund / death.

Vitamin D supplementation and calcium treatment

Mice were fed with a diet containing either low (< 5 IU/kg food), standard (1.500 IU/kg food) or high (75.000 IU/kg food) vitamin D3 concentrations (ssniff Spezialdiaeten GmbH, Soest, Germany) for at least 8 weeks. These doses were chosen after a dose titration, as they generated serum vitamin D levels reflective of vitamin D deficiency (< 30 nmol/l), physiological vitamin D levels (100 nmol/l) and continuous high-dose supplementation (250 nmol/l) in patients

(Vieth, 1999, Burton *et al.*, 2010, Smolders *et al.*, 2010). All three diets contained identical calcium (1%) and phosphate (0.7%) concentrations (**suppl. figure 1**). Hypercalcemia in mice was induced by daily intraperitoneal injection of calcium gluconate (2000 mg/kg/day; Sigma-Aldrich) starting three days before immunization.

Determination of 25-OH-vitamin D3, calcium, phosphate, sodium and chloride

Blood was collected by vein facialis puncture and serum was isolated by centrifugation using gel columns (Sarstedt, Nuembrecht, Germany). 25-hydroxyvitamin D3 concentrations in serum were measured with liquid chromatography-tandem mass spectrometry using a MassChrom® 25-OH-vitamin D3/D2 LC-MS/MS kit (Chromsystems, Munich, Germany) on an AB Sciex API 4000 LC/MS/MS system (AB Sciex, Darmstadt, Germany). Total calcium in serum and culture medium was determined using the Arsenazo III dye binding method on an ARCHITECT c 16000 analyzer (Abbott Diagnostics, Lake Forest, USA). Ionized calcium in culture medium was measured on a blood gas analyzer GEM Premier 4000 (Instrumentation Laboratory, Orangeburg, USA). Total inorganic phosphate in serum was quantified based on Molybdenum blue colorimetric method on an ARCHITECT c 16000 analyzer (Abbott Diagnostics). Total sodium in serum and total chloride in culture medium were measured using ion-selective electrodes on an ARCHITECT c 16000 analyzer (Abbott Diagnostics).

Isolation of human and murine leucocytes

Human peripheral blood mononuclear cells (PBMCs) from healthy donors were isolated after Ficoll gradient centrifugation (Biochrom GmbH, Berlin, Germany). Human T cells were purified from PBMCs by negative MACS separation using MojoSort human T cell isolation kit (BioLegend, San Diego, USA). Single cell suspensions of murine lymphoid tissues were generated by gentle dissection and passing through 70 µm cell strainer (Greiner bio-one, Kremsmuenster, Austria). Murine CNS mononuclear cells were isolated by digestion of perfused CNS tissue using collagenase D (Roche, Mannheim, Germany) and DNase I (Roche) at 37°C for 45 min. Mononuclear cells were passed through a 70 µm cell strainer (Greiner bio-one) and lymphocytes were collected by discontinuous density Percoll gradient (GE Healthcare, Little Chalfont, UK). Murine blood was collected in PBS containing 1 mM EDTA followed by erythrocytes lysis using BD Pharm Lysing Buffer. Murine splenic $CD11b^+$ cells were purified by negative MACS separation using a mouse lineage panel (BD Bioscience). Murine T cells were isolated by negative MACS separation using a mouse pan T cell isolation kit II (Miltenyi,

Bergisch Gladbach, Germany). For separate stimulation of $CD4^+$ and $CD8^+$ T cells murine T cells were isolated by positive MACS separation using CD4 (L3T4) and CD8a (Ly-2) MicroBeads (Miltenyi), respectively.

Histology and immunohistochemistry

Mice were transcardially perfused with PBS followed by 4% paraformaldehyde (PFA) and tissue was paraffin embedded. One µm-thick slices were stained with hematoxylin and eosin (H&E) and luxol fast blue / periodic acid shiff (LFB/PAS). T cells, B cells and macrophages were detected by immunohistochemistry with an avidin-biotin technique using antibodies specific for CD3 (SP7; DCS Innovative Diagnostik-Systeme, Hamburg, Germany), CD45R/B220 (RA3-6B2; BD Biosciences) and Mac-3 (M3/84; BD Biosciences). Histological sections were captured using a digital camera (DP71; Olympus Europa GmbH, Hamburg, Germany) mounted on a light microscope (BX51; Olympus Europa GmbH). The percentage of demyelinated white matter was calculated using cellSens Dimension software (Olympus Europa GmbH). Inflammatory cells were quantified at 400x magnification using an ocular counting grid and are shown as cells/mm^2. At least 8 spinal cord cross sections were taken for each analysis.

Flow cytometry

Composition of murine immune cells was analyzed using the following antibodies: CD3 (145-2C11; BioLegend), CD4 (RM4-5; BioLegend), CD8 (53-6.7; BioLegend), CD45R/B220 (RA3-6B2; BioLegend), CD11b (M1/70; BioLegend), CD11c (N418; BioLegend), F4/80 (BM8; BioLegend) and CD45 (30-F11; BioLegend). Splenic monocyte activation / differentiation was determined using: CD40 (3/23; BD Bioscience), CD80 (16-10A1; BioLegend), CD86 (GL-1; BioLegend), MHCII (AF6-120.1; BioLegend), PD-L1 (MIH5; eBioscience, Waltham, USA) and LAP (TW7-16B4; BioLegend). T cell activation was investigated using: CD25 (PC61; BioLegend), CD69 (H1.2F3; BioLegend), CD95 (Jo2; BD Bioscience) and CD44 (IM7; BioLegend). T regulatory cell differentiation was evaluated by intracellular staining for FoxP3 (FJK-16s; eBioscience) after fixation and permeabilization using the fixation / permeabilization kit (eBioscience). To investigate Th1 and Th17 cell differentiation cell suspensions were stimulated with 50 ng/ml phorbol 12-myristate 13-acetate (PMA; Sigma-Aldrich) and 0.5 µg/ml ionomycin (Sigma-Aldrich) in the presence of 1 µl/ml brefeldin A (BD Bioscience) for 6 h. Cytokine production was analyzed by intracellular staining for IFN-γ (XMG1.2; BioLegend)

and IL-17A (TC11-18H10; BD Bioscience) after fixation and permeabilization (BD Bioscience). Fc receptors were blocked using monoclonal antibody specific for CD16/CD32 (93; BioLegend). Dead cells were stained with a fixable viability kit (BioLegend). Samples were acquired on a BD LSR Fortessa (BD Bioscience). To investigate the cytokine profile of human T cells in migration assays, cells from lower and upper chamber were stimulated with 20 ng/ml PMA and 1 µg/ml ionomycin in the presence of 1µl/ml brefeldin A (BD Bioscience). Dead cells were stained with LIVE/DEAD™ Fixable Aqua Dead Cell Stain Kit (Thermo Fisher Scientific, Waltham, USA). CD3 (OKT3, Biolegend), CD8 (RPA-T8, BD Bioscience) and CD4 (SK3, BD Bioscience) were used for surface staining. To assess cytokine production IL-17 (eBio64CAP17, eBioscience), IFN-γ (B27, BD Bioscience), GM-CSF (BVD2-21C11, BD Bioscience) and IL-4 (8D4-8, BD Bioscience) were used. Samples were acquired on a BD™ LSRII cytometer (BD Bioscience). All data evaluation was performed using FlowJo software (FlowJo LLC, Ashland, USA).

ELISA

Production of IFN-γ, IL-17 and GM-CSF was measured using ELISA MAX Standard Set kits (BioLegend). Absorbance was measured at 450 nm with subtraction of a 540 nm reference wavelength on iMark microplate reader (Bio-Rad laboratories Inc., Hercules, USA).

Phagocytosis assay

Thymocytes were gently dissected from WT mice and passed through a 70 µm cell strainer (Greiner bio-one) and apoptosis was induced by 1 µM dexamethasone (Sigma-Aldrich) incubation overnight. Apoptotic thymocytes were labelled with pHrodo Red, succinimidyl ester (pHrodo Red, SE; Thermo Fisher Scientific) and added to LPS pre-stimulated (50 ng/ml; overnight) splenic $CD11b^+$ cells. After incubation of splenic $CD11b^+$ cells with apoptotic thymocytes at 37°C or on ice for 1 h phagocytosis was assessed by flow cytometry.

a-CD3 / a-CD28 stimulation

For the analysis of T cell proliferation, T cells were stained with carboxyfluorescein succinimidyl ester (CFSE), for evaluation of differentiation or migration across the BBB model, T cells remained unstained. T cells were incubated in anti-CD3 (clone 145-2C11 for murine T cells / clone OKT3 for human T cells) / anti-CD28 (clone 37.51 for murine T cells / clone

CD28.2 for human T cells) (BioLegend) pre-coated wells for 48-72 h (for murine T cells) or 96-120 h (for human T cells). To study the effects of calcium, cholecalciferol, 25-(OH)-vitamin D and 1,25-$(OH)_2$-vitamin D on T cell proliferation and differentiation, T cells were pre-incubated with the respective components at 37°C for 1 h. Calcium chloride was dissolved in complete medium, cholecalciferol, 25-(OH)-vitamin D as well as 1,25-$(OH)_2$-vitamin D were dissolved in absolute ethanol and adjusted to contain equal ethanol concentrations after dilution. Monitoring of pH occurred with inoLab pH Level 1 (WTW GmbH & Co. KG, Weilheim, Germany).

Calcium flux

T cells were pre-incubated in complete HBSS medium (HBSS medium containing 1.3 mM CaCl2, 0.5 mM MgCl2 and 1% FCS) with increasing calcium concentrations at 37°C for 1h followed by staining with 4 mg/ml Fluo-3 AM and 10 mg/ml Fura Red AM (Biomol GmbH, Hamburg, Germany) in complete HBSS (Thermo Fisher Scientific) containing 0.02% Pluronic F-68 (Life Technologies, Waltham, USA) at 37°C for 30 minutes. T cells were kept on ice and directly before flow cytometry acquisition pre-heated to 37°C for 5 minutes. After 25 s baseline recording, human or mouse T cells were stimulated using 10 or 20 ng/ml ionomycin (Sigma-Aldrich), respectively.

Quantitative PCR

T cells were pre-incubated at the indicated calcium concentrations for 1 hour at 37°C followed by stimulation in anti-CD3/anti-CD28 pre-coated 6 well plates for 1-6 hrs (murine T cells) or for 3-20 hrs (human T cells) at 37°C. Total RNA was isolated using the RNeasy mini kit (Qiagen, Hilden, Germany) and transcribed into cDNA using the QuantiNova Reverse Transcription kit (Qiagen) according to the manufacturer´s instructions. Quantitative (q)PCR was performed using 500 nM per Primer and qPCRBIO SyGreen (Nippon Genetics Europe GmbH, Dueren, Germany) in a total volume of 10 µl on a QuantStudio 7 (Applied Biosystems, Waltham, USA). Primers specific for IL-2, GM-CSF, IFN-γ and beta-actin were purchased from Bio-Rad (for mouse) and Thermo Fisher Scientific (for human). qPCR runs were performed at 95°C denaturating and 66°C or 68°C annealing temperature for mouse and human T cells, respectively. Elongation was performed for 30 s and 40 cycles with subsequent melt-curve analysis. Primer specificity was validated by product size analysis using a 2% Agarose gel containing GelRed (Biotium) and UV-light illumination. Detailed primer informations are

listed in the supplementary material (**suppl. table 1**). Samples were analyzed in duplicates or triplicates and considered valid when Ct<35 and SD Ct<0.5. Analyzed cytokine expression was normalized to beta-actin expression loading control (delta-Ct) in mice or human T cells, respectively. Delta-delta-Ct values were calculated in comparison to the 1.0 mM Ca^{2+}-condition and relative gene expression was calculated by 2^(-ddCt).

Blood-brain-barrier transmigration assay

BBB-ECs were isolated and cultured from non-epileptic surgical human CNS material as previously published (Ifergan *et al.*, 2006). Written informed consent was obtained from every donor prior to surgery (CHUM research ethics committee; approval number BH07.001 and HD04.046). In vitro transmigration assays were performed using a modified Boyden chamber as previously published (Ifergan *et al.*, 2006, Larochelle *et al.*, 2012, Larochelle *et al.*, 2015). In brief, human BBB-ECs were grown to confluence on gelatin-coated 3 μm pore size Boyden chambers (Collaborative Biomedical Products, Bedford, USA) in culture medium supplemented with 40% astrocyte-conditioned medium. For the inflamed condition, TNF/IFN-gamma (100 U/ml) was added in the upper chamber 24 h before the assay. Boyden chambers were washed, and fresh medium was used for the transmigration assay. $1X10^6$ anti-CD3 / anti-CD28 stimulated human T lymphocytes which had been pre-incubated with the respective calcium concentrations were added to the upper chamber. After 16 h, cells that had transmigrated across the BBB-ECs layer to the lower chamber were harvested, counted and analyzed by flow cytometry. Migration experiments were performed in triplicates for each donor, in all conditions.

Statistical analysis

Statistics were calculated using the software GraphPad Prism 5.01. All in vivo and ex vivo comparisons were made to the standard vitamin D diet. Serum concentrations of vitamin D3, serum and urine concentrations of calcium, phosphate and sodium as well as body weight, macrophage phagocytosis, ex vivo T cell proliferation, cytokine concentrations are shown as mean ± SEM and were analyzed by the two-tailed t test. qPCR results, in vitro T cell viability, pH / calcium- / chloride concentrations in medium are shown as mean ± SEM and were analyzed by one-way analysis of variance (ANOVA) followed by Bonferroni's multiple comparison test. Clinical scores are depicted as mean ± SEM, composition of immune cells,

WM demyelination / infiltration, monocyte- / T cell activation and differentiation are shown as median and were analyzed using the Mann-Whitney U test. Calcium flux results are presented as mean ± SEM and were analyzed by Kruskal-Wallis test followed by Dunn's test for multiple comparisons. T cell migration results are shown as mean ± SEM and were analyzed by Friedman test followed by Dunn's test for multiple comparisons. Statistical analysis of the in vitro T cell proliferation at increasing calcium, vitamin D or one of the vitamin D metabolite concentrations were performed by linear regression on a logarithmic scale. Outlier detection was performed using ROUT analysis. A value of $p < 0.05$ was considered significant and is shown by one asterisk. Two asterisks and three asterisks indicate significances of $p < 0.01$ and $p < 0.001$, respectively.

Data availability

The data that support the findings of this study are available from the corresponding author, upon reasonable request.

Results

Long-term high-dose oral vitamin D administration is associated with hypercalcemia

Mice received a diet either containing a low concentration of vitamin D3 (<5 IU vitamin D3/kg), representing vitamin D deficiency, a standard (1,500 IU/kg) or a high (75,000 IU/kg) dose of vitamin D3 for 15 weeks. As indicated in **suppl. figure 2a**, the respective diet did not influence mean body weight. In vivo, vitamin D is hydroxylated in the liver and the kidney to its biologically active form 1,25-dihydroxy (1,25-$(OH)_2$) vitamin D3. The half-life of 1,25-$(OH)_2$ vitamin D is relatively short though, so that the vitamin D status is commonly assessed by measuring 25-(OH) vitamin D (Holick, 2009). As shown in **figure 1a**, mice in the low vitamin D group showed an average serum level below 30 nmol/L, which reflects a commonly accepted definition of vitamin D deficiency in humans (Holick, 2007). The standard group contained serum levels around 100 nmol/L, which is considered an upper normal vitamin D level in humans (Holick, 2007) and facility-housed mice (Bolton *et al.*, 2013). The high vitamin D diet led to serum 25-(OH) vitamin D concentrations of approximately 250 nmol/L, a level that is commonly achieved in patients by its continuous supplementation at high doses (Vieth, 1999, Burton *et al.*, 2010, Smolders *et al.*, 2010). Mice that received the high vitamin D diet showed elevated concentrations of both total as well as ionized calcium in their serum. Urine calcium concentrations were also substantially increased, indicating that long-term treatment with high vitamin D doses regularly caused hypercalcemia in a predictable manner **(figure 1b-h)**

High dose vitamin D promotes severe, persistent disability in EAE

Vitamin D exerts immunomodulatory effects on cells within the innate and adaptive immune system, which widely express cell surface vitamin D receptors (VDRs) (Cantorna *et al.*, 2004). Therefore, we examined whether the respective vitamin D diet may have affected the frequency of T cells, B cells and myeloid antigen-presenting cells (APC) in blood, lymph node and spleen. As indicated in **suppl. figure 3**, high vitamin D was associated with an increase in frequency of T cells and fewer B cells in the blood. Moreover, in the spleen, these mice contained an elevated frequency of $CD11c^+$ dendritic cells and $F4/80^+$ macrophages.

EAE was induced after chronic vitamin D supplementation. All three treatment groups developed EAE around day 12 (**figure 2a**). Mice that received the standard dose of vitamin D developed the lowest scores, as expected based on earlier EAE studies showing that short-term oral vitamin D administration ameliorated EAE and impaired activation and CNS migration of

monocytes (Nashold *et al.*, 2000) and T cells (Mayne *et al.*, 2011). Surprisingly, mice supplemented with high vitamin D dose manifested a more severe EAE course. Mice were maintained on their respective diet throughout the entire disease course. Recognizing nutrition as a potential confounder, we monitored weights daily. While low and high vitamin D groups had modestly higher mean body weights within days after immunization, there were no significant differences in body weights in any groups throughout the disease course (**suppl. figure 2b**).

High vitamin D3 diet is associated with increased inflammatory CNS infiltration and demyelination

The unexpected clinical observation of an EAE exacerbation in the group of mice containing high vitamin D serum levels was further corroborated by histologic analyses, revealing a significantly increased inflammatory infiltration of the CNS (**figure 2b**). An abundance of activated CNS infiltrating myeloid cells as well as an elevated number of CNS T cells was observed in the high dose vitamin D group (**figure 2c-e**). Enhanced cellular infiltration was associated with an increase in the extent of CNS demyelination (**figure 2f**). CNS T cells were isolated and evaluated for their differentiation. As indicated in **figure 2g**, CNS T cells from mice with high vitamin D levels contained a significantly higher frequency of IFN-gamma or IL-17 producing Th1- and Th17 cells, respectively. In contrast, the frequency of $FoxP3^+$ regulatory T cells (Treg) within the CNS was slightly lower in the high vitamin D group (**figure 2h**). Taken together, the high dose vitamin D diet was associated with higher absolute numbers of myeloid cells and T cells and pro-inflammatory differentiation of these cells.

High dose vitamin D3 supplementation enhances activation, differentiation and phagocytic activity of peripheral myeloid APC

In light of the increased inflammatory CNS infiltration we analyzed whether continuously high levels of vitamin D had promoted peripheral immune cell activation and differentiation prior to CNS transmigration. As shown in **figure 3a**, myeloid APC from mice in the vitamin D high group indeed showed an enhanced surface expression of MHC class II and co-stimulatory CD40, CD80 and CD86. In contrast, expression of PD-L1, an inhibitory costimulatory molecule (Salama *et al.*, 2003), or latency-associated peptide (LAP), a surface molecule indicative of a

Treg-fostering TGF-beta production (Miyazono *et al.*, 1991), was unaffected by the high vitamin D diet.

As a pre-requirement for presentation to T cells, larger antigens must first be phagocytosed and processed by the APC. As indicated in **figure 3b**, in vivo vitamin D treatment dose-dependently increased the phagocytic capacity of myeloid macrophages. While this is likely of benefit in clearance of infections (Djukic *et al.*, 2015), enhanced uptake of auto-antigen in contrast enlarges the basis to generate an auto-reactive adaptive immune response (Kinzel *et al.*, 2016). In conjunction with the elevated frequency of $CD11c^+$ dendritic cells and highly differentiated $F4/80^+$ macrophages in vitamin D treated naïve mice (**suppl. figure 3**) these data thus suggest that high dose vitamin D supplementation is associated with maturation of myeloid APC, an increased surface expression of the molecular machinery participating in phagocytosis and antigen presentation.

Vitamin D3 high dose diet fosters activation and pro-inflammatory differentiation of peripheral T cells

Standard and high vitamin D3 treatments were associated with a significant increase in expression of the early activation marker CD69 on T cells. There were also dose-dependent increases in the frequencies of activated $CD25^+$ and antigen-experienced $CD44^{hi}$ memory T cells (Baaten *et al.*, 2012) (**figure 4a**). Of interest, standard and high vitamin D supplementation was associated by an increase in Treg (**figure 4b**). When T cells were re-stimulated in vitro by anti-CD3/anti-CD28 however, in vivo high dose vitamin D-exposed T cells proliferated at a significantly higher rate as assessed by dilution of an intracellular dye (**figure 4c**) and preferentially differentiated into IFN-gamma producing Th1 and IL-17 releasing Th17 cells (**figure 4d+e**).

Development of pathogenic T cells in high dose vitamin D-treated mice is driven by a direct in vivo effect on T cells

The possibility that pro-inflammatory Th1 and Th17 differentiation of high vitamin D was due to a direct effect on T cells, or was a secondary effect resulting from enhanced APC maturation was investigated. Here, we utilized a co-culture system, in which naïve T cells were activated by myeloid APC. Either cell type was isolated from mice fed with low, standard or high vitamin D doses. Based on the substantial phenotypic alterations of $CD11b^+$ myeloid cells, we first

focused on a possible APC-driven effect. As indicated in **figure 5a**, myeloid APC continuously exposed to high vitamin D levels triggered a slightly higher proliferation of myelin-specific T cells. Yet, in vivo exposure of T cells to vitamin D exerted the greater contribution to enhanced T cell proliferation; T cells isolated from mice treated with low or high vitamin D doses always proliferated at a significantly higher rate independent of whether the activating myeloid APC had been treated with low, standard or high vitamin D (**figure 5b**). Most strikingly, naïve myelin-specific T cells, which had been exposed to high vitamin D levels in vivo consistently differentiated into Th1 and Th17 cells, largely independent of the respective APC origin (**figure 5c+d**); conversely, low, but even more so high vitamin D effectively prevented development of Treg ex vivo (**figure 5e**). Of note, the standard vitamin D diet generated T cells with the greatest propensity to differentiate into Treg cells when activated ex vivo, which is in line with a reported fostering effect of moderate vitamin D levels on the frequency and function Treg in mice (Korf *et al.*, 2012) and humans (Barrat *et al.*, 2002). To confirm that high 25-(OH) vitamin D levels directly influenced T cell activation and differentiation in an antigen- and APC-independent manner, we next directly stimulated $CD4^+$ or $CD8^+$ T cells purified from naïve mice fed with the low, medium and high vitamin D diet by anti-CD3/anti-CD28. Paralleling our findings in EAE-diseased mice, high-dose vitamin D treatment accelerated proliferation of both $CD4^+$ and $CD8^+$ T cells (**figure 5f+g)**. In addition, T cells from high dose vitamin D-treated mice differentiated in a pro-inflammatory manner, when activated ex vivo **(suppl. figure 4**).

In vitro, vitamin D and its metabolites inhibit proliferation of human and murine T cells

Based on these findings, we next assessed the direct effect of vitamin D and its metabolites on both human and murine T cells in vitro. Purified T cells were pre-incubated with cholecalciferol, 25-(OH)-vitamin D or 1,25-$(OH)_2$-vitamin D at increasing concentrations. Most importantly, these concentrations reflected both the serum ranges measured in our EAE study as well as low, physiological, and supra-physiological levels in humans. None of the vitamin D concentrations affected viability of human or murine T cells in culture (**suppl. figure 5a-f**). As indicated in **figure 6a-f**, 25-(OH)-vitamin D or 1,25-$(OH)_2$-vitamin D clearly inhibited proliferation of both human and murine $CD4^+$ and $CD8^+$ T cells in a dose-dependent manner, while non-hydroxylated cholecalciferol only exerted this effect on human T cells. These results confirmed a direct regulatory effect of vitamin D itself on T cells (Mayne *et al.*,

2011, Peelen *et al.*, 2011) and thus failed to explain the enhanced proliferation and pro-inflammatory differentiation of T cells observed in high dose vitamin D-treated mice.

Calcium supplementation causes a direct and dose-dependent increase in activation, proliferation and pro-inflammatory differentiation of human and murine T cells

In search for an alternative explanation, we next investigated a possible T cell-excitatory effect of calcium (Quintana *et al.*, 2011, Monaco *et al.*, 2016) in our model. Purified human and murine T cells were exposed to various calcium concentrations ranging from 1 to 3 mM (**figure 7a-h**). Importantly, in these in vitro assays we extended the range to include lower concentrations of calcium, having in mind that in the serum of our vitamin D treated mice a substantial proportion is bound to protein (**figure 1b+c; suppl. figure 6a**), which may proportionally reduce its direct availability for T cells. As shown in **figure 7a+b**, calcium dose-dependently accelerated proliferation of both human and murine $CD4^+$ and $CD8^+$ T cells in this setting, while chloride levels, pH and T cell viability remained unaffected (**suppl. figure 6b-e**). Further dissecting this observation, we monitored the cellular calcium influx upon T cell activation (Gwack *et al.*, 2007). To account for a protein-reduced medium in these assays we used a lower range of total calcium concentrations (**suppl. figure 6f**) and checked again that chloride levels and pH remained unaffected (**suppl. figure 6g+h**). As indicated in **figure 7c+d**, raising extracellular calcium to concentrations again equivalent to the serum levels of ionized calcium in our vitamin D fed mice caused a significant increase in the mean calcium influx, triggering an upregulation of pro-inflammatory gene products (**figure 7e+f**). Lastly, we corroborated that this direct T cell stimulating effect of calcium also occurred in vivo. For this purpose, we repetitively and continuously injected mice with calcium gluconate, resulting in a hypercalcemia equivalent to the levels measured in high dose vitamin D-treated mice (**figure 8a+b**). As indicated in **figure 8c+d**, serum hypercalcemia by itself substantially increased the expression of activation markers on $CD4^+$ and $CD8^+$ T cells in these mice, confirming that this effect occurs in vivo independent of vitamin D. Taken together, our results indicate that development of encephalitogenic T cells and EAE exacerbation in high dose vitamin D-treated mice indeed reflected a direct increase in T cell-excitatory calcium.

Calcium supplementation increases human T cell transmigration across a blood-brain barrier model

To evaluate the impact of calcium on the capacity of T cells to cross the blood-brain barrier (BBB), we used an in vitro model in which activated human T cells migrate across a monolayer of inflamed human BBB endothelial cells (ECs). T cells exposed to higher calcium concentrations (2+3 mM) showed a significantly greater migration capacity when compared to the lower concentration (1 mM). High level calcium exposure of T cells furthermore resulted in an increased number of $CD4^+$ and $CD8^+$ T cells producing pro-inflammatory cytokines, such as IFN-γ, GM-CSF and IL-17 beyond the BBB-ECs monolayer (**figure 7g+h**). In context with the enhanced cellular CNS infiltration in EAE, these data suggest that secondary hypercalcemia occurring upon high-dose vitamin D treatment could enhance migration of pro-inflammatory effector T cells into the affected CNS.

Discussion

Geographical latitude correlates with MS incidence (Acheson *et al.*, 1960) which highlights the influence of environmental factors in MS (Ascherio and Munger, 2007). Lack of exposure to sunlight, UV radiation and hereby relatively low levels of vitamin D in the context of its emerging immunoregulatory properties provides one attractive explanation for this correlation (Nielsen *et al.*, 2017); the central question remaining though is whether lack of vitamin D is causal in triggering MS activity or an epiphenomenon of insufficient sun light exposure as the true risk factor (Schwarz *et al.*, 2012). A direct effect of vitamin D on MS activity is yet the conceptual requirement for all current efforts to therapeutically raise its level in affected patients. Empiric vitamin D supplementation studies thus far have provided conflicting results (Stein *et al.*, 2011, Loken-Amsrud *et al.*, 2012). For example, adding vitamin D3 to interferon treatment reduced MRI activity in a small trial with relapsing-remitting MS patients (Soilu-Hanninen *et al.*, 2012), which was recently confirmed by a larger phase II study. Unfortunately, the conclusions from these studies are limited as both interferon-beta (IFN b) and vitamin D interact in modulating MS disease activity, and data indicate that sufficient vitamin D is a pre-requisite for the benefit of IFN b (Stewart *et al.*, 2012). While available data indicate that moderate vitamin D supplementation is safe in MS (Sotirchos *et al.*, 2016), results of ongoing larger placebo-controlled trials are needed to clarify whether therapeutic vitamin D supplementation is beneficial in MS independent of concomitant disease modifying therapy.

Our results suggest that modest vitamin D supplementation may have a beneficial effect in EAE, while those data were not significant. We report here, to our knowledge for the first time, that continuous supplementation with high doses of vitamin D yet exerted a highly significant paradoxical effect, promoting exacerbation of clinical and histological EAE. This outcome was underpinned by an accentuated phenotype and function of myeloid APC as well as an unleashed development of pro-inflammatory T cells upon high dose vitamin D treatment. Further, high-dose vitamin D similarly accelerated activation and differentiation of both myeloid APC and T cells in unimmunized healthy mice (**suppl. figure 7; figure 5f+g**), indicating that the high vitamin D dose exerted a broad immune cell activating effect independent of an inflammatory context. At first sight, these findings appear to conflict with several other experimental studies, which mainly reported a clinical benefit of vitamin D treatment in EAE, also at higher doses (Lemire and Archer, 1991, Cantorna *et al.*, 1996, Nashold *et al.*, 2000); however, all of these studies evaluated short-term vitamin D supplementation. In most of these studies, hydroxylated forms of vitamin D were investigated in a brief intervention regimen. Most likely as a result, none of these studies reported development of hypercalcemia. Elevated serum calcium was

however observed in another study continuously exposing mice to high doses of vitamin D (Spach and Hayes, 2005), again suggesting that it may develop only after an extended period of exposure. The strength in our study is that we supplemented vitamin D for several months before assessing EAE susceptibility and that we fed cholecalciferol, the metabolite supplemented in humans. As a result, we measured serum levels of 25-(OH) vitamin D, again the molecule most commonly assessed in humans, reflective of MS patients considered vitamin D-deficient, with physiological or high vitamin D levels (Burton *et al.*, 2010, Smolders *et al.*, 2010), suggesting that our experimental setup including the doses chosen most suitably reflects vitamin D supplementation in humans.

Binding of vitamin D to immune cells and subsequent VDR signaling regulates pro-inflammatory immune functions (Peelen *et al.*, 2011) and is likely of benefit in suppression of CNS autoimmune disease (Meehan and DeLuca, 2002, Xie *et al.*, 2017). In line with these studies, our in vitro results confirm a direct beneficial effect of vitamin D and its metabolites on T cells (Peelen *et al.*, 2011), inhibiting their activation and pro-inflammatory differentiation. Of note, the extent of this effect was consistently greater on $CD8^+$ than on $CD4^+$ T cells, following the relative expression levels of the VDR on these cells (Veldman *et al.*, 2000). Interestingly, B cells can only react to vitamin D after initial activation and subsequent upregulation of the VDR, as their constitutive expression is relatively low (Provvedini *et al.*, 1983, Provvedini *et al.*, 1986). Nevertheless, $1,25(OH)_2D_3$ has been shown to reduce B cell proliferation, plasma and memory cell differentiation and induced apoptosis in proliferating B cells(Chen *et al.*, 2007).

These findings suggest that the direct effect of vitamin D on both human and murine lymphocytes is indeed of anti-inflammatory nature and most likely beneficial in an auto-immune setting.

Our results indicate that in contrast, a rise in the serum calcium exerts the opposite effect on T cells, which can apparently override any clinical benefit of vitamin D in EAE. This is in line with the earlier finding that adding the calcium-lowering hormone calcitonin additively augmented the therapeutic benefit of a vitamin D in EAE (Becklund *et al.*, 2009). Calcium acts as a second messenger promoting cell cycle progression in many cell types, including lymphocytes (Feske, 2007). T cell receptor signaling raises intracellular calcium at first by its release from the endoplasmatic reticulum, and to the greater extent by subsequent extracellular calcium influx through plasma membrane calcium channels (Kuno and Gardner, 1987, Lewis, 2001). Only the latter is capable of raising intracellular and nuclear calcium levels over an

extended period of time, which is required to promote activation, proliferation and differentiation of immune cells (Dolmetsch *et al.*, 1998, Vig and Kinet, 2009), including clonal expansion of T cells (Vaeth *et al.*, 2017). This is precisely the scenario and the sequence of events which we identified to underlie deterioration of EAE severity in our study. Modelling hypercalcemia at the levels observed upon continuous high dose vitamin D treatment in vivo activated T cells independent of vitamin D. Mechanistically, an elevated level of calcium triggered its increased influx into T cells upon activation, which led to an upregulation of pro-inflammatory gene products. These initial events were followed by an unleashed proliferation and encephalitogenic differentiation of both human and murine T cells, corroborating a causal sequence of high dose vitamin D treatment, secondary hypercalcemia and a promoted development of disease-driving encephalitogenic T cells. While there is currently no molecule to selectively interfere with the calcium influx into immune cells in vivo, genetically determined inability of these calcium channels to function in T cells completely blocked EAE by preventing development of myelin-reactive Th1 and Th17 cells (Ma *et al.*, 2010). Along the same lines, therapeutic blockade of calcium channels by nimodipine was recently reported to suppress EAE (Schampel *et al.*, 2017). This clinical benefit was primarily attributed to restored remyelination, but may furthermore relate to attenuated T cell activation. In conjunction, these findings indicate that worsening of EAE in our high vitamin D group indeed occurred as a consequence of raising the mean calcium level. In greater context, these data implicate that the clinically desirable effect of modest vitamin supplementation may be reflective of immune-regulatory VDR signaling, while exacerbation of T cell-mediated CNS autoimmunity at excessive vitamin D doses is primarily attributed to raising the mean calcium level.

Hypercalcemia in its extent comparable to the levels associated with deterioration of EAE commonly occurs in humans supplemented with high doses of vitamin D (Malihi et al., 2016), especially when combined with calcium intake (Jansen *et al.*, 1997, Wingerchuk *et al.*, 2005, Avenell *et al.*, 2014, Bjelakovic *et al.*, 2014). High dose vitamin D was also reported to cause hypercalcemia in treatment of MS (Marcus et al., 2012), which was associated with development of severely disabling relapses as well as increased MRI activity (Fragoso et al., 2014). Along the same lines, recent clinical trials revealed enhanced immune cell activation in MS patients supplemented with 50,000 IU of vitamin D3 every five days (Naghavi Gargari et al., 2015), whereas the functionally opposite outcome occurred at moderate vitamin D levels (Muris *et al.*, 2016, Sotirchos *et al.*, 2016). In conjunction with these observations, our novel findings highlight excessive vitamin D supplementation and resulting hypercalcemia as novel risk factors promoting worsening of CNS demyelinating disease. Our data caution that in light

of the currently limited information on a direct beneficial effect of vitamin D in MS, MS patients may be at danger of experiencing untoward immunological and/or clinical effects when vitamin D is supplemented excessively.

Acknowledgements

We thank Katja Grondey, Julian Koch and Audrey Daigneault for excellent technical support. Further, we thank Hana Janova for providing the protocol on testing phagocytosis in vitro. D.H. is supported by the Startprogramm of the Universitätsmedizin Göttingen. M.S. Weber is serving as an editor for PLoS One. He receives research support from the National Multiple Sclerosis Society (NMSS; PP 1660), the Deutsche Forschungsgemeinschaft (DFG; WE 3547/5-1), from Novartis, TEVA, Biogen-Idec, Roche, Merck and the ProFutura Programm of the Universitätsmedizin Göttingen.

Author contributions

D.H. and S.T. contributed equally to this work, carried out most of the experiments and analyzed the data. E.P. and C.L. performed the BBB transmigration experiments and analyzed the data. T.B. quantified the serum 25-OH-vitamin D3 concentrations. D.H. prepared the figures. M.S.W. supervised the research and wrote the manuscript. D.H., S.T., C.L., S.S.Z., W.B., E.P., T.B., M.D. and R.N. participated in reviewing and editing the manuscript.

References

Acheson ED, Bachrach CA, Wright FM. Some comments on the relationship of the distribution of multiple sclerosis to latitude, solar radiation, and other variables. Acta Psychiatr Scand Suppl. 1960;35(147):132-47.

Ascherio A, Munger KL. Environmental risk factors for multiple sclerosis. Part II: Noninfectious factors. Ann Neurol. 2007;61(6):504-13.

Ascherio A, Munger KL. Epstein-barr virus infection and multiple sclerosis: a review. J Neuroimmune Pharmacol. 2010;5(3):271-7.

Ascherio A, Munger KL, Simon KC. Vitamin D and multiple sclerosis. Lancet Neurol. 2010;9(6):599-612.

Avenell A, Mak JC, O'Connell D. Vitamin D and vitamin D analogues for preventing fractures in post-menopausal women and older men. Cochrane Database Syst Rev. 2014(4):CD000227.

Baaten BJ, Tinoco R, Chen AT, Bradley LM. Regulation of Antigen-Experienced T Cells: Lessons from the Quintessential Memory Marker CD44. Front Immunol. 2012;3:23.

Baranzini SE, Oksenberg JR. The Genetics of Multiple Sclerosis: From 0 to 200 in 50 Years. Trends Genet. 2017;33(12):960-70.

Barrat FJ, Cua DJ, Boonstra A, Richards DF, Crain C, Savelkoul HF, et al. In vitro generation of interleukin 10-producing regulatory CD4(+) T cells is induced by immunosuppressive drugs and inhibited by T helper type 1 (Th1)- and Th2-inducing cytokines. J Exp Med. 2002;195(5):603-16.

Becklund BR, Hansen DW, Jr., Deluca HF. Enhancement of 1,25-dihydroxyvitamin D3-mediated suppression of experimental autoimmune encephalomyelitis by calcitonin. Proc Natl Acad Sci U S A. 2009;106(13):5276-81.

Bhargava P, Cassard S, Steele SU, Azevedo C, Pelletier D, Sugar EA, et al. The vitamin D to ameliorate multiple sclerosis (VIDAMS) trial: study design for a multicenter, randomized, double-blind controlled trial of vitamin D in multiple sclerosis. Contemp Clin Trials. 2014;39(2):288-93.

Bhargava P, Fitzgerald KC, Calabresi PA, Mowry EM. Metabolic alterations in multiple sclerosis and the impact of vitamin D supplementation. JCI Insight. 2017;2(19).

Bjelakovic G, Gluud LL, Nikolova D, Whitfield K, Wetterslev J, Simonetti RG, et al. Vitamin D supplementation for prevention of mortality in adults. Cochrane Database Syst Rev. 2014(1):CD007470.

Bjornevik K, Riise T, Casetta I, Drulovic J, Granieri E, Holmoy T, et al. Sun exposure and multiple sclerosis risk in Norway and Italy: The EnvIMS study. Mult Scler. 2014;20(8):1042-9.

Bolton C, Gates J, Giovannoni G. Serum levels of 25-hydroxy vitamin D in normal Biozzi and C57BL/6 mice and during the course of chronic relapsing experimental autoimmune encephalomyelitis (CR EAE). Inflamm Res. 2013;62(7):659-67.

Burton JM, Kimball S, Vieth R, Bar-Or A, Dosch HM, Cheung R, et al. A phase I/II dose-escalation trial of vitamin D3 and calcium in multiple sclerosis. Neurology. 2010;74(23):1852-9.

Cantorna MT, Hayes CE, DeLuca HF. 1,25-Dihydroxyvitamin D3 reversibly blocks the progression of relapsing encephalomyelitis, a model of multiple sclerosis. Proc Natl Acad Sci U S A. 1996;93(15):7861-4.

Cantorna MT, Zhu Y, Froicu M, Wittke A. Vitamin D status, 1,25-dihydroxyvitamin D3, and the immune system. Am J Clin Nutr. 2004;80(6 Suppl):1717S-20S.

Chen S, Sims GP, Chen XX, Gu YY, Chen S, Lipsky PE. Modulatory effects of 1,25-dihydroxyvitamin D3 on human B cell differentiation. J Immunol. 2007;179(3):1634-47.

Djukic M, Sostmann N, Bertsch T, Mecke M, Nessler S, Manig A, et al. Vitamin D deficiency decreases survival of bacterial meningoencephalitis in mice. J Neuroinflammation. 2015;12:208.

Dolmetsch RE, Xu K, Lewis RS. Calcium oscillations increase the efficiency and specificity of gene expression. Nature. 1998;392(6679):933-6.

Dorr J, Ohlraun S, Skarabis H, Paul F. Efficacy of vitamin D supplementation in multiple sclerosis (EVIDIMS Trial): study protocol for a randomized controlled trial. Trials. 2012;13:15.

Feske S. Calcium signalling in lymphocyte activation and disease. Nat Rev Immunol. 2007;7(9):690-702.

Fragoso YD, Adoni T, Damasceno A, de Albuquerque Damasceno CA, Ferreira ML, Finkelzstejn A, et al. Unfavorable outcomes during treatment of multiple sclerosis with high doses of vitamin D. J Neurol Sci. 2014;346(1-2):341-2.
Gwack Y, Feske S, Srikanth S, Hogan PG, Rao A. Signalling to transcription: store-operated Ca2+ entry and NFAT activation in lymphocytes. Cell Calcium. 2007;42(2):145-56.
Holick MF. Photosynthesis of vitamin D in the skin: effect of environmental and life-style variables. Fed Proc. 1987;46(5):1876-82.
Holick MF. Sunlight and vitamin D for bone health and prevention of autoimmune diseases, cancers, and cardiovascular disease. Am J Clin Nutr. 2004;80(6 Suppl):1678S-88S.
Holick MF. Vitamin D deficiency. N Engl J Med. 2007;357(3):266-81.
Holick MF. Vitamin D status: measurement, interpretation, and clinical application. Ann Epidemiol. 2009;19(2):73-8.
Ifergan I, Wosik K, Cayrol R, Kebir H, Auger C, Bernard M, et al. Statins reduce human blood-brain barrier permeability and restrict leukocyte migration: relevance to multiple sclerosis. Ann Neurol. 2006;60(1):45-55.
J Smolders RH, R Vieth , T Holmøy , K Marhardt , M Schluep , J Killestein , F Barkhof , L.M.E Grimaldi , M Beelke High dose cholecalciferol (vitamin D3) oil as add-on therapy in subjects with relapsing-remitting multiple sclerosis receiving subcutaneous interferon beta-1a. ECTRIMS Online Library Hupperts R Sep 16, 2016; 147013

2016.
Jansen TL, Janssen M, de Jong AJ. Severe hypercalcaemia syndrome with daily low-dose vitamin D supplementation. Br J Rheumatol. 1997;36(6):712-3.
Kinzel S, Lehmann-Horn K, Torke S, Hausler D, Winkler A, Stadelmann C, et al. Myelin-reactive antibodies initiate T cell-mediated CNS autoimmune disease by opsonization of endogenous antigen. Acta Neuropathol. 2016.
Korf H, Wenes M, Stijlemans B, Takiishi T, Robert S, Miani M, et al. 1,25-Dihydroxyvitamin D3 curtails the inflammatory and T cell stimulatory capacity of macrophages through an IL-10-dependent mechanism. Immunobiology. 2012;217(12):1292-300.
Kuno M, Gardner P. Ion channels activated by inositol 1,4,5-trisphosphate in plasma membrane of human T-lymphocytes. Nature. 1987;326(6110):301-4.
Larochelle C, Cayrol R, Kebir H, Alvarez JI, Lecuyer MA, Ifergan I, et al. Melanoma cell adhesion molecule identifies encephalitogenic T lymphocytes and promotes their recruitment to the central nervous system. Brain. 2012;135(Pt 10):2906-24.
Larochelle C, Lecuyer MA, Alvarez JI, Charabati M, Saint-Laurent O, Ghannam S, et al. Melanoma cell adhesion molecule-positive CD8 T lymphocytes mediate central nervous system inflammation. Ann Neurol. 2015;78(1):39-53.
Laursen JH, Sondergaard HB, Albrechtsen A, Frikke-Schmidt R, Koch-Henriksen N, Soelberg Sorensen P, et al. Genetic and environmental determinants of 25-hydroxyvitamin D levels in multiple sclerosis. Mult Scler. 2015;21(11):1414-22.
Lemire JM, Archer DC. 1,25-dihydroxyvitamin D3 prevents the in vivo induction of murine experimental autoimmune encephalomyelitis. J Clin Invest. 1991;87(3):1103-7.
Lewis RS. Calcium signaling mechanisms in T lymphocytes. Annu Rev Immunol. 2001;19:497-521.
Loken-Amsrud KI, Holmoy T, Bakke SJ, Beiske AG, Bjerve KS, Bjornara BT, et al. Vitamin D and disease activity in multiple sclerosis before and during interferon-beta treatment. Neurology. 2012;79(3):267-73.
Ma J, McCarl CA, Khalil S, Luthy K, Feske S. T-cell-specific deletion of STIM1 and STIM2 protects mice from EAE by impairing the effector functions of Th1 and Th17 cells. Eur J Immunol. 2010;40(11):3028-42.
Malihi Z, Wu Z, Stewart AW, Lawes CM, Scragg R. Hypercalcemia, hypercalciuria, and kidney stones in long-term studies of vitamin D supplementation: a systematic review and meta-analysis. Am J Clin Nutr. 2016;104(4):1039-51.

Marcus JF, Shalev SM, Harris CA, Goodin DS, Josephson SA. Severe hypercalcemia following vitamin d supplementation in a patient with multiple sclerosis: a note of caution. Arch Neurol. 2012;69(1):129-32.
Mayne CG, Spanier JA, Relland LM, Williams CB, Hayes CE. 1,25-Dihydroxyvitamin D3 acts directly on the T lymphocyte vitamin D receptor to inhibit experimental autoimmune encephalomyelitis. Eur J Immunol. 2011;41(3):822-32.
Meehan TF, DeLuca HF. The vitamin D receptor is necessary for 1alpha,25-dihydroxyvitamin D(3) to suppress experimental autoimmune encephalomyelitis in mice. Arch Biochem Biophys. 2002;408(2):200-4.
Miyazono K, Olofsson A, Colosetti P, Heldin CH. A role of the latent TGF-beta 1-binding protein in the assembly and secretion of TGF-beta 1. EMBO J. 1991;10(5):1091-101.
Mokry LE, Ross S, Ahmad OS, Forgetta V, Smith GD, Goltzman D, et al. Vitamin D and Risk of Multiple Sclerosis: A Mendelian Randomization Study. PLoS Med. 2015;12(8):e1001866.
Monaco S, Jahraus B, Samstag Y, Bading H. Nuclear calcium is required for human T cell activation. J Cell Biol. 2016;215(2):231-43.
Munger KL, Levin LI, Hollis BW, Howard NS, Ascherio A. Serum 25-hydroxyvitamin D levels and risk of multiple sclerosis. JAMA. 2006;296(23):2832-8.
Muris AH, Smolders J, Rolf L, Thewissen M, Hupperts R, Damoiseaux J, et al. Immune regulatory effects of high dose vitamin D3 supplementation in a randomized controlled trial in relapsing remitting multiple sclerosis patients receiving IFNbeta; the SOLARIUM study. J Neuroimmunol. 2016;300:47-56.
Naghavi Gargari B, Behmanesh M, Shirvani Farsani Z, Pahlevan Kakhki M, Azimi AR. Vitamin D supplementation up-regulates IL-6 and IL-17A gene expression in multiple sclerosis patients. Int Immunopharmacol. 2015;28(1):414-9.
Nashold FE, Miller DJ, Hayes CE. 1,25-dihydroxyvitamin D3 treatment decreases macrophage accumulation in the CNS of mice with experimental autoimmune encephalomyelitis. J Neuroimmunol. 2000;103(2):171-9.
Nielsen NM, Munger KL, Koch-Henriksen N, Hougaard DM, Magyari M, Jorgensen KT, et al. Neonatal vitamin D status and risk of multiple sclerosis: A population-based case-control study. Neurology. 2017;88(1):44-51.
Nieves J, Cosman F, Herbert J, Shen V, Lindsay R. High prevalence of vitamin D deficiency and reduced bone mass in multiple sclerosis. Neurology. 1994;44(9):1687-92.
Peelen E, Knippenberg S, Muris AH, Thewissen M, Smolders J, Tervaert JW, et al. Effects of vitamin D on the peripheral adaptive immune system: a review. Autoimmun Rev. 2011;10(12):733-43.
Provvedini DM, Tsoukas CD, Deftos LJ, Manolagas SC. 1,25-dihydroxyvitamin D3 receptors in human leukocytes. Science. 1983;221(4616):1181-3.
Provvedini DM, Tsoukas CD, Deftos LJ, Manolagas SC. 1 alpha,25-Dihydroxyvitamin D3-binding macromolecules in human B lymphocytes: effects on immunoglobulin production. J Immunol. 1986;136(8):2734-40.
Quintana A, Pasche M, Junker C, Al-Ansary D, Rieger H, Kummerow C, et al. Calcium microdomains at the immunological synapse: how ORAI channels, mitochondria and calcium pumps generate local calcium signals for efficient T-cell activation. EMBO J. 2011;30(19):3895-912.
Runia TF, Hop WC, de Rijke YB, Buljevac D, Hintzen RQ. Lower serum vitamin D levels are associated with a higher relapse risk in multiple sclerosis. Neurology. 2012;79(3):261-6.
Salama AD, Chitnis T, Imitola J, Ansari MJ, Akiba H, Tushima F, et al. Critical role of the programmed death-1 (PD-1) pathway in regulation of experimental autoimmune encephalomyelitis. J Exp Med. 2003;198(1):71-8.
Schampel A, Volovitch O, Koeniger T, Scholz CJ, Jorg S, Linker RA, et al. Nimodipine fosters remyelination in a mouse model of multiple sclerosis and induces microglia-specific apoptosis. Proc Natl Acad Sci U S A. 2017;114(16):E3295-E304.
Schwarz A, Navid F, Sparwasser T, Clausen BE, Schwarz T. 1,25-dihydroxyvitamin D exerts similar immunosuppressive effects as UVR but is dispensable for local UVR-induced immunosuppression. J Invest Dermatol. 2012;132(12):2762-9.

Smolders J, Menheere P, Kessels A, Damoiseaux J, Hupperts R. Association of vitamin D metabolite levels with relapse rate and disability in multiple sclerosis. Mult Scler. 2008;14(9):1220-4.
Smolders J, Peelen E, Thewissen M, Cohen Tervaert JW, Menheere P, Hupperts R, et al. Safety and T cell modulating effects of high dose vitamin D3 supplementation in multiple sclerosis. PLoS One. 2010;5(12):e15235.
Soilu-Hanninen M, Aivo J, Lindstrom BM, Elovaara I, Sumelahti ML, Farkkila M, et al. A randomised, double blind, placebo controlled trial with vitamin D3 as an add on treatment to interferon beta-1b in patients with multiple sclerosis. J Neurol Neurosurg Psychiatry. 2012;83(5):565-71.
Sotirchos ES, Bhargava P, Eckstein C, Van Haren K, Baynes M, Ntranos A, et al. Safety and immunologic effects of high- vs low-dose cholecalciferol in multiple sclerosis. Neurology. 2016;86(4):382-90.
Spach KM, Hayes CE. Vitamin D3 confers protection from autoimmune encephalomyelitis only in female mice. J Immunol. 2005;175(6):4119-26.
Stein MS, Liu Y, Gray OM, Baker JE, Kolbe SC, Ditchfield MR, et al. A randomized trial of high-dose vitamin D2 in relapsing-remitting multiple sclerosis. Neurology. 2011;77(17):1611-8.
Stewart N, Simpson S, Jr., van der Mei I, Ponsonby AL, Blizzard L, Dwyer T, et al. Interferon-beta and serum 25-hydroxyvitamin D interact to modulate relapse risk in MS. Neurology. 2012;79(3):254-60.
Vaeth M, Maus M, Klein-Hessling S, Freinkman E, Yang J, Eckstein M, et al. Store-Operated Ca(2+) Entry Controls Clonal Expansion of T Cells through Metabolic Reprogramming. Immunity. 2017;47(4):664-79 e6.
Veldman CM, Cantorna MT, DeLuca HF. Expression of 1,25-dihydroxyvitamin D(3) receptor in the immune system. Arch Biochem Biophys. 2000;374(2):334-8.
Vieth R. Vitamin D supplementation, 25-hydroxyvitamin D concentrations, and safety. Am J Clin Nutr. 1999;69(5):842-56.
Vig M, Kinet JP. Calcium signaling in immune cells. Nat Immunol. 2009;10(1):21-7.
Wingerchuk DM. Smoking: effects on multiple sclerosis susceptibility and disease progression. Ther Adv Neurol Disord. 2012;5(1):13-22.
Wingerchuk DM, Lesaux J, Rice GP, Kremenchutzky M, Ebers GC. A pilot study of oral calcitriol (1,25-dihydroxyvitamin D3) for relapsing-remitting multiple sclerosis. J Neurol Neurosurg Psychiatry. 2005;76(9):1294-6.
Xie Z, Chen J, Zheng C, Wu J, Cheng Y, Zhu S, et al. 1,25-dihydroxyvitamin D3 -induced dendritic cells suppress experimental autoimmune encephalomyelitis by increasing proportions of the regulatory lymphocytes and reducing T helper type 1 and type 17 cells. Immunology. 2017;152(3):414-24.

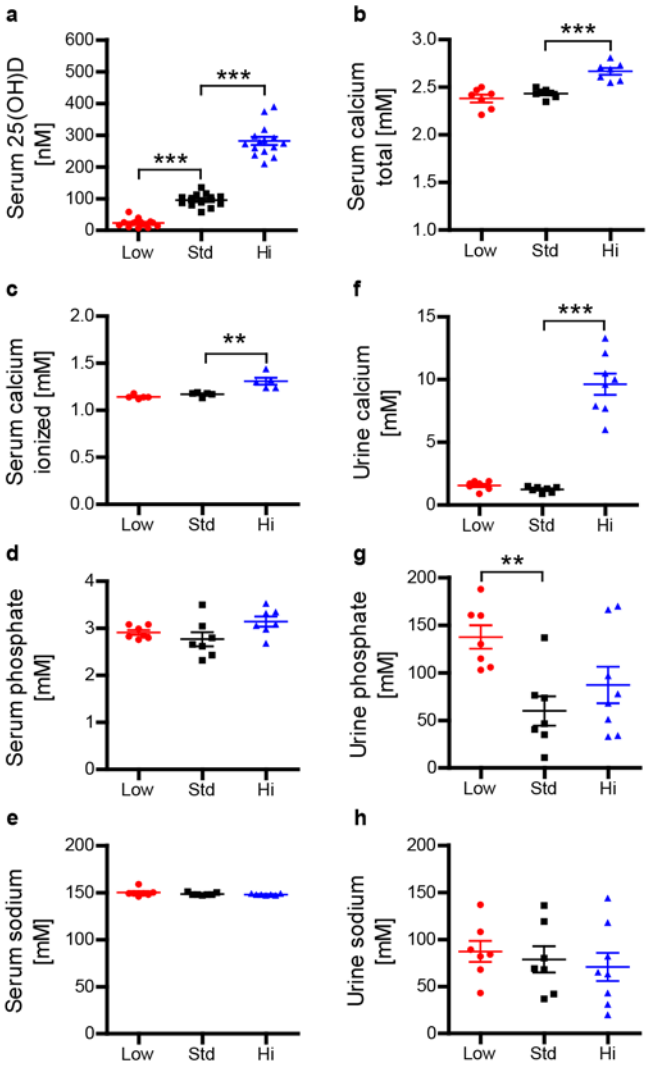

Figure 1. Vitamin D high excess supplementation raises serum 25-OH-vitamin D3 as well as serum and urine calcium concentrations. Mice were fed a diet containing low (< 5 IU/kg food), standard (1.500 IU/kg food) or high vitamin D concentrations (75.000 IU/kg food). **(a)** Serum 25-hydroxyvitamin D3 concentrations were measured using liquid chromatography-tandem mass spectrometry fifteen weeks after diet onset (representative plots of three independent experiments; data given as mean ± SEM; n = 13-15). Total calcium, total phosphate and total sodium in serum **(b+d+e)** and urine **(f-h)** were quantified on an ARCHITECT c 16000 analyzer ten weeks after vitamin D diet onset (representative plots of two independent experiments; data given as mean ± SEM; n = 7-8). **(c)** Ionized calcium was measured on a blood gas analyzer GEM Premier 4000 ten weeks after vitamin D diet onset (data given as mean ± SEM; n = 5).

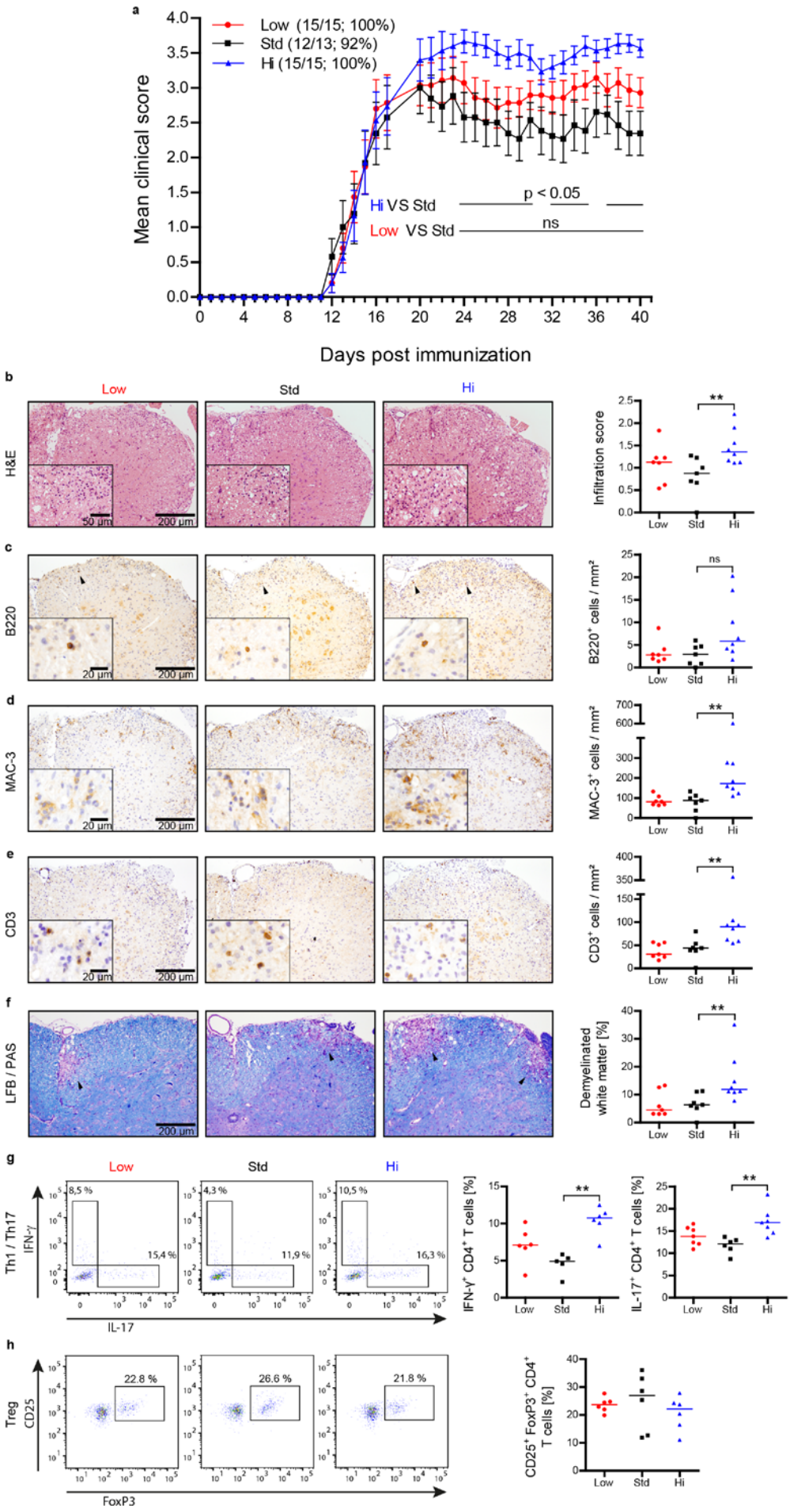
a
Low (15/15; 100%)
Std (12/13; 92%)
Hi (15/15; 100%)
Mean clinical score
Hi VS Std
p < 0.05
Low VS Std
ns
Days post immunization
b
Low
Std
Hi
H&E
Infiltration score
c
B220
B220+ cells / mm²
d
MAC-3
MAC-3+ cells / mm²
e
CD3
CD3+ cells / mm²
f
LFB / PAS
Demyelinated white matter [%]
g
Th1 / Th17
IFN-γ
IL-17
8,5 %
15,4 %
4,3 %
11,9 %
10,5 %
16,3 %
IFN-γ+ CD4+ T cells [%]
IL-17+ CD4+ T cells [%]
h
Treg
CD25
FoxP3
22.8 %
26.6 %
21.8 %
CD25+ FoxP3+ CD4+ T cells [%]

Figure 2. Vitamin D high excess supplementation enhances clinical severity of active EAE and increases CNS cellular infiltration by MAC-3$^+$ cells, encephalitogenic T cells and white matter demyelination. Mice were fed a diet containing low (< 5 IU/kg food), standard (1.500 IU/kg food) or high vitamin D concentrations (75.000 IU/kg food) for fifteen weeks. EAE was induced by MOG peptide 35-55 immunization fifteen weeks after diet onset. Spinal cords were isolated and analyzed forty days post immunization. **(a)** Mean group EAE severity is given as mean ± SEM; disease incidence is indicated in brackets; representative plots of two independent experiments; n = 13-15. **(b)** Overall spinal cord inflammation was evaluated by H&E staining and assessed on a scale from 0 to 3 as follows: 0 = no infiltration; 1 = minor infiltration; 2 = moderate infiltration; 3 = pronounced infiltration (representative sections; left); (inflammatory scores are depicted as median; n = 7-8; right). **(c-e)** Cellular CNS infiltration was assessed by immunohistochemical staining for **(c)** B220, (**d**) Mac-3 and **(e)** CD3 (representative sections; black arrowheads indicate individual cells; left); (quantitative comparison of groups given as median; n = 7-8; right). **(f)** Myelinated as well as demyelinated white matter areas were assessed by LFB / PAS staining (representative sections; black arrowheads indicate demyelinated white matter; left). The percentage of demyelinated white matter was calculated relative to the whole white matter area (data are shown as median; n = 7-8; right). Frequencies of **(g)** Th1- (IFN-γ^+CD4$^+$), Th17- (IL-17$^+$CD4$^+$) and **(h)** Treg cells (CD25$^+$FoxP3$^+$CD4$^+$) in the CNS were quantified by FACS analysis. Representative FACS plots of two independent experiments are shown left and frequencies of Th1-, Th17- and Treg cells are depicted on the right as median; n = 5-7.

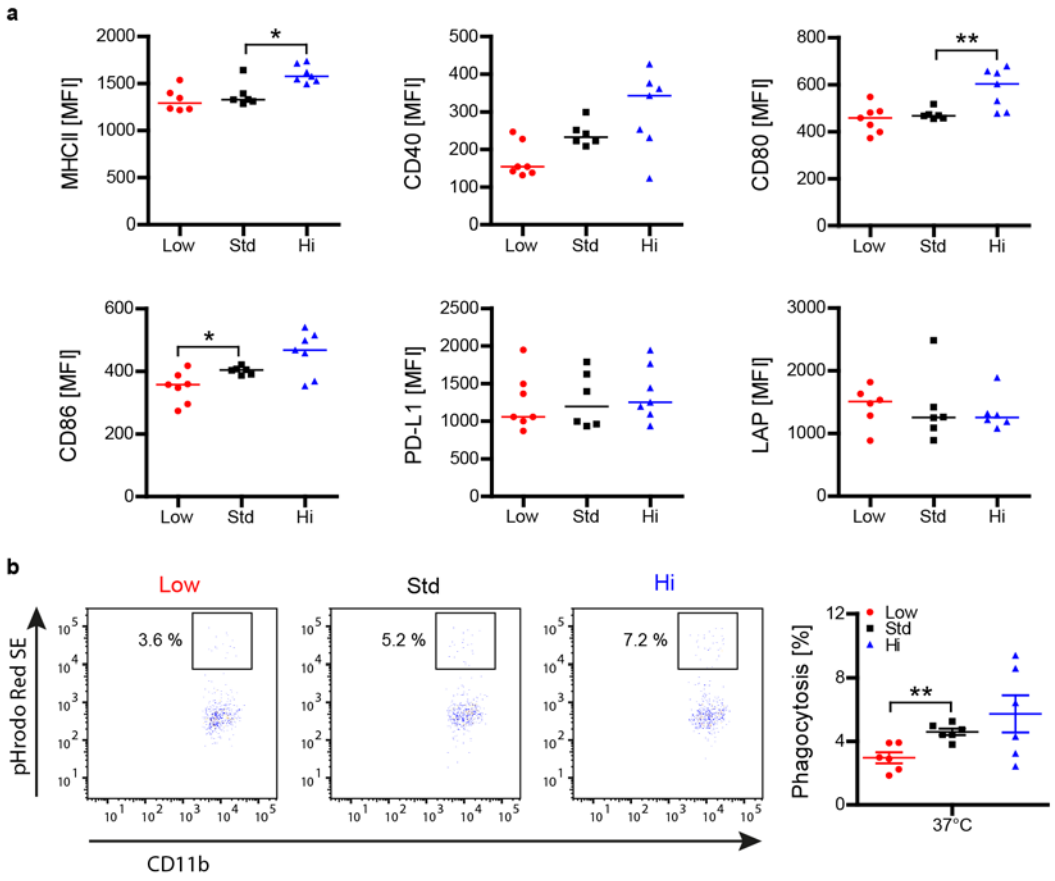

Figure 3. Vitamin D high excess supplementation increases activation of splenic monocytes and enhances phagocytosis by splenic macrophages. (a) Splenocytes were isolated and splenic monocyte activation / differentiation was analyzed by FACS fifteen weeks after vitamin D diet onset in EAE diseased mice (representative plots of two independent experiments; data are shown as median of MFI; n = 6-7). **(b)** Splenic macrophages were isolated nine weeks after vitamin D diet onset from EAE diseased mice and co-cultured with pHrodo Red SE labelled apoptotic thymocytes at 37°C for one hour. Phagocytosis of apoptotic thymocytes by splenic macrophages ($CD11b^+F4/80^+$) was determined by FACS. Representative FACS dot plots are shown left and percentage of phagocytosis by macrophages is depicted on the right as mean ± SEM; n = 6.

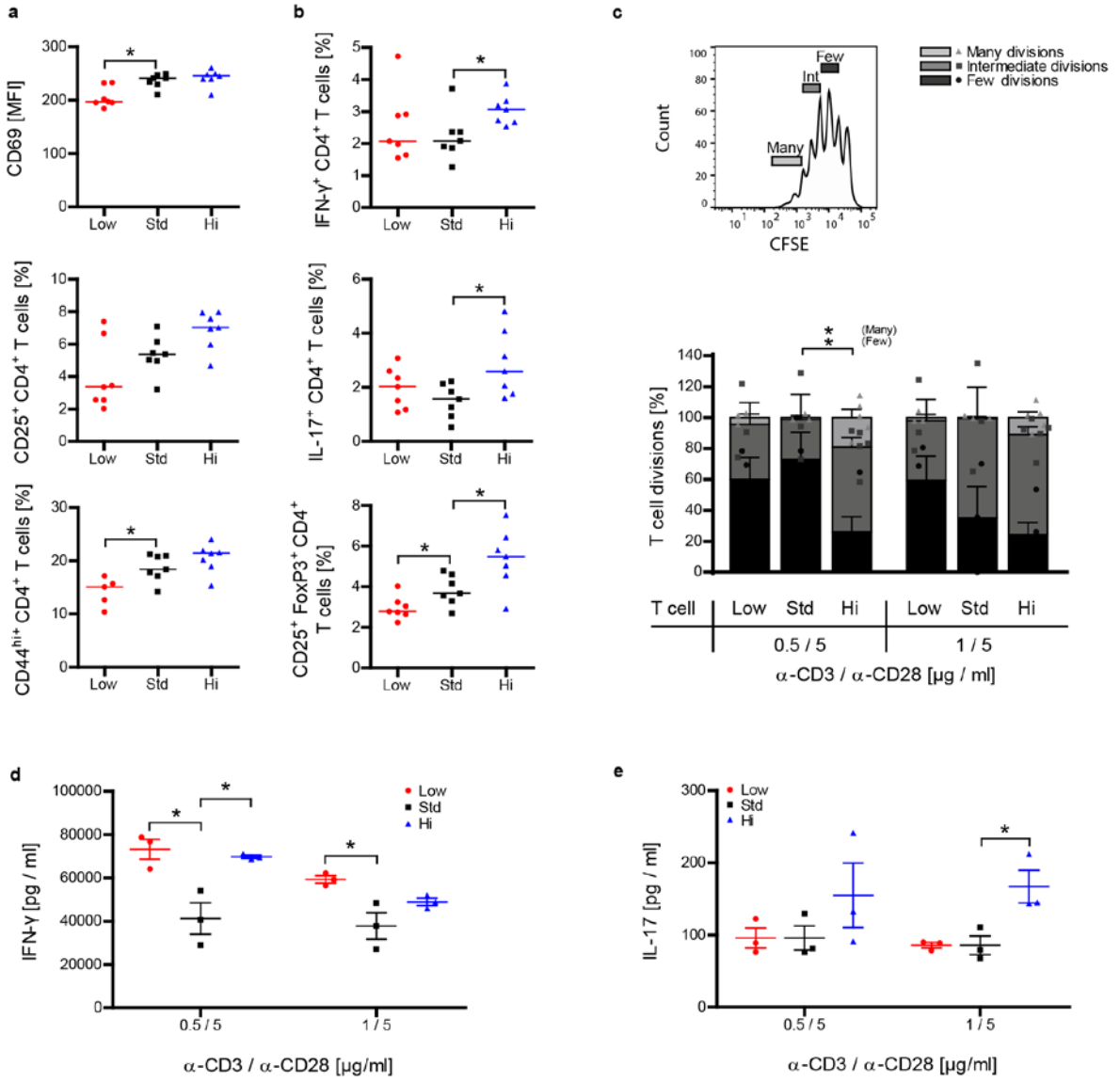

Figure 4. Vitamin D high excess supplementation enhances activation of peripheral T cells and promotes their encephalitogenic differentiation. (a+b) Splenocytes were isolated and T cell activation and differentiation was analyzed by FACS nine weeks after vitamin D diet onset and fifteen days post immunization (representative plots of two independent experiments; data given as median; n = 5-7). **(c-e)** Splenic T cells were MACS purified from WT mice fifty days post immunization and seventeen weeks after vitamin D diet onset. **(c)** T cells were CFSE labelled and incubated in anti-CD3 / anti-CD28 pre-coated wells for 72 hours. T cell proliferation was evaluated by CFSE dilution and stratified by division frequency as follows: few divisions (1-2; dark grey), intermediate divisions (3-4; medium grey) and many divisions (≥ 5; light grey). T cell divisions in the three groups are shown according to this setup as mean ± SEM; n = 3-5. **(d+e)** Differentiation of T cells into Th1- and Th17 -secreting T cells was analyzed by quantification of IFN-γ and IL-17 in culture supernatants by ELISA (data given as mean ± SEM; n = 3-5).

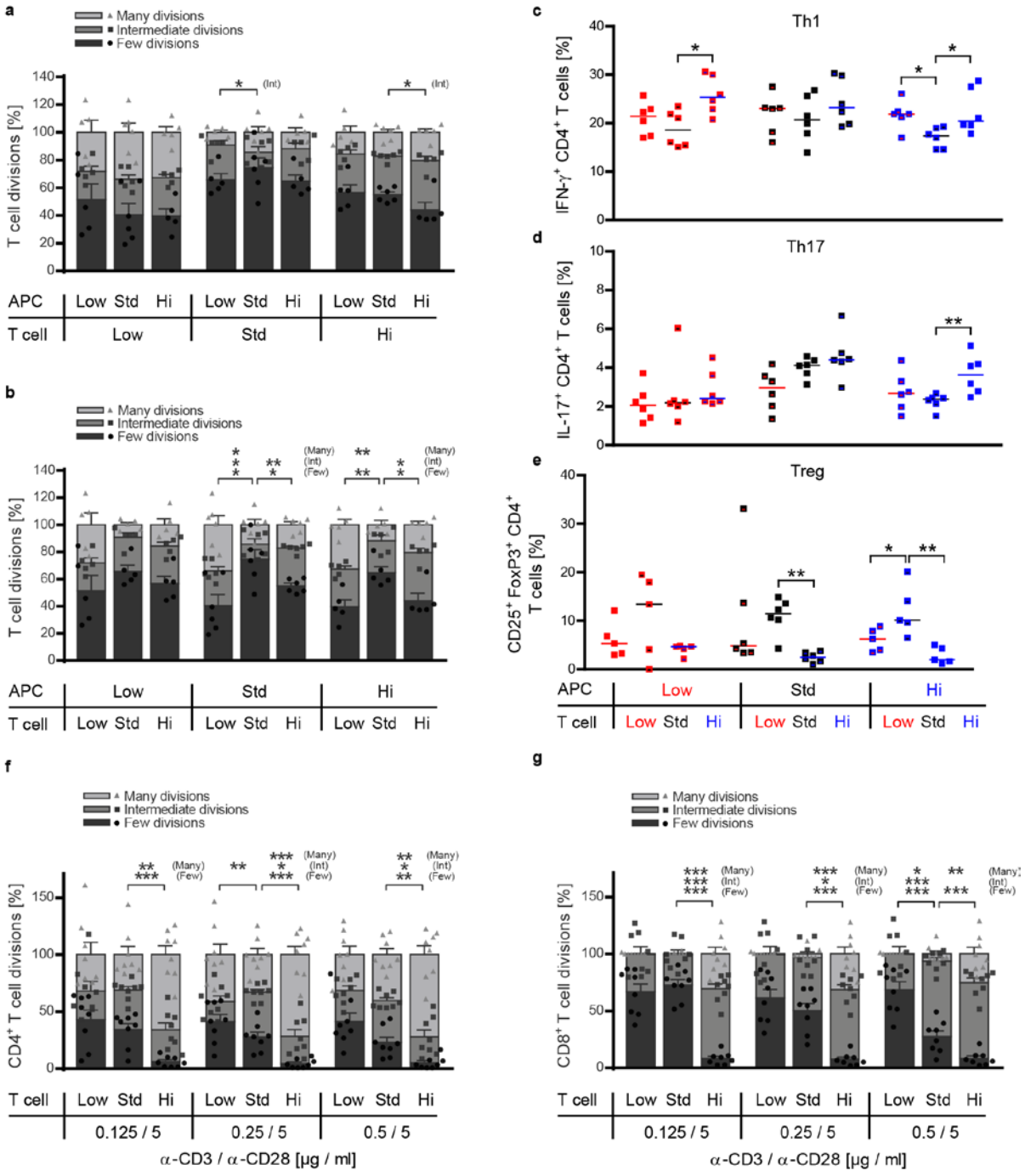
a
Many divisions
Intermediate divisions
Few divisions
T cell divisions [%]
(Int)
APC
Low Std Hi
T cell
Low
Std
Hi
b
(Many) (Int) (Few)
c
Th1
IFN-γ+ CD4+ T cells [%]
d
Th17
IL-17+ CD4+ T cells [%]
e
Treg
CD25+ FoxP3+ CD4+ T cells [%]
f
CD4+ T cell divisions [%]
0.125 / 5
0.25 / 5
0.5 / 5
α-CD3 / α-CD28 [µg / ml]
g
CD8+ T cell divisions [%]

Figure 5. Vitamin D high excess supplementation promotes proliferation and encephalitogenic differentiation of T cells independent of its effect on myeloid APCs. (a-e) $CD11b^+$ cells from donor mice, which were fed with vitamin D low, standard or high diet, were co-cultured in a criss-cross setup with myelin specific T cells originated from low, standard or high vitamin D supplemented 2D2 mice in the presence of MOG peptide 35-55 for 72 hours. WT splenic $CD11b^+$ cells were purified by MACS separation sixteen days post immunization and ten weeks after vitamin D diet onset. Myelin-specific T cells were isolated from 2D2 mice by MACS separation ten weeks after vitamin D diet onset. **(a+b)** Myelin-specific T cells were CFSE labelled prior to co-culture with $CD11b^+$ cells in the presence of MOG peptide 35-55. T cell proliferation was evaluated by CFSE dilution and stratified by division frequency as follows: few divisions (1-2; dark grey), intermediate divisions (3-4; medium grey) and many divisions (≥ 5; light grey). T cell divisions are shown as mean ± SEM; n = 5-6. **(c-e)** Differentiation of myelin-specific naïve T cells into Th1- ($IFN\text{-}\gamma^+CD4^+$), Th17- ($IL\text{-}17^+CD4^+$) or Treg cells ($CD25^+FoxP3^+CD4^+$) was analyzed by FACS (data given as median; n = 5-6). **(f+g)** Splenic T cells were isolated from naïve WT mice, which were fed with vitamin D low, standard or high diet for eight weeks. MACS purified $CD4^+$ and $CD8^+$ T cells were labelled with CFSE and separately incubated in anti-CD3 / anti-CD28 pre-coated wells for 72 hours. Proliferation of **(f)** $CD4^+$ and **(g)** $CD8^+$ T cells was evaluated by CFSE dilution and stratified by division frequency (data given as mean ± SEM; n = 8).

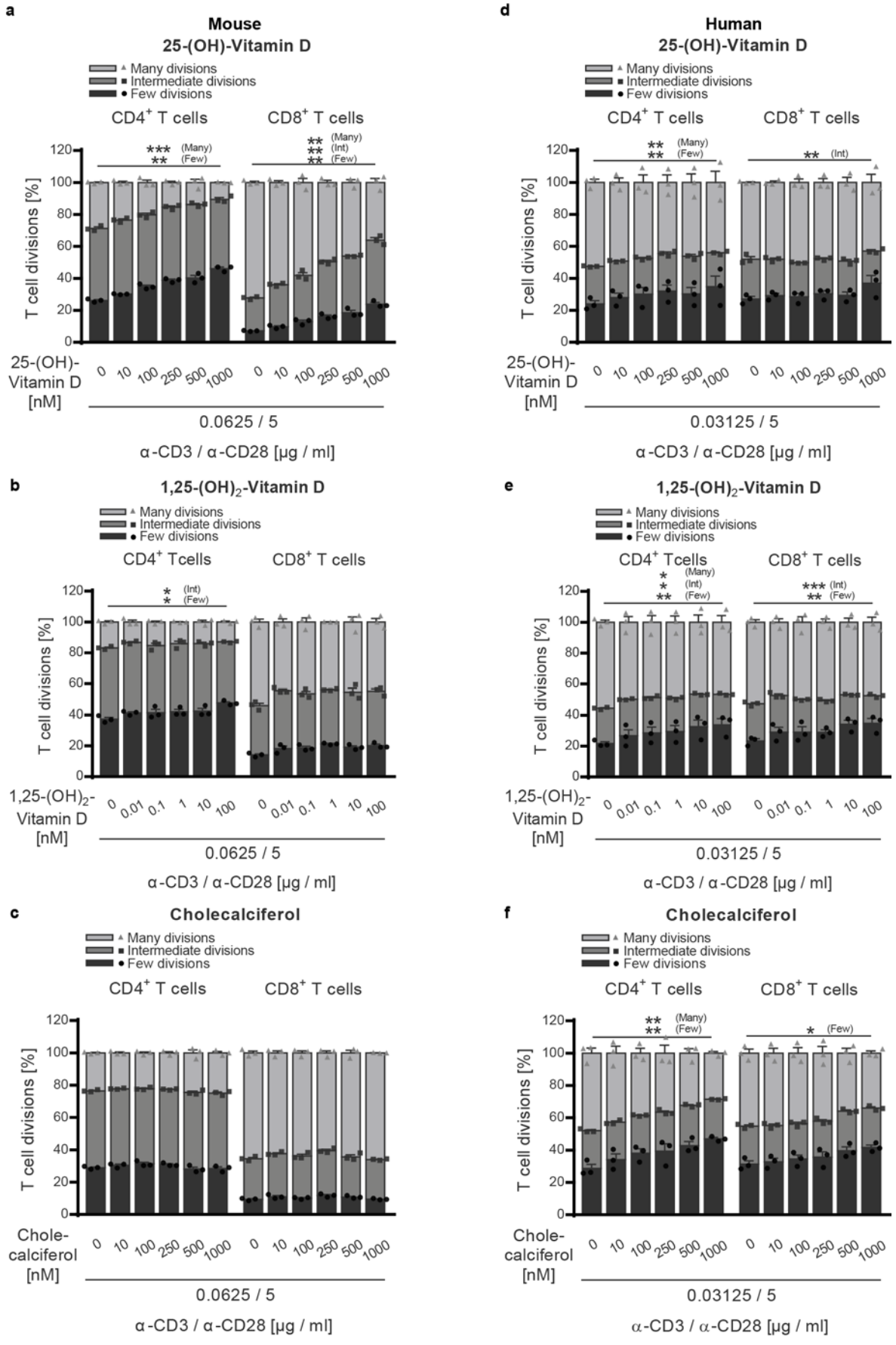
a
Mouse
25-(OH)-Vitamin D
Many divisions
Intermediate divisions
Few divisions
CD4+ T cells
CD8+ T cells
*** (Many)
** (Few)
** (Many)
** (Int)
** (Few)
T cell divisions [%]
25-(OH)-Vitamin D [nM]
0 10 100 250 500 1000 0 10 100 250 500 1000
0.0625 / 5
α-CD3 / α-CD28 [µg / ml]
b
1,25-(OH)2-Vitamin D
Many divisions
Intermediate divisions
Few divisions
CD4+ Tcells
CD8+ T cells
* (Int)
* (Few)
T cell divisions [%]
1,25-(OH)2-Vitamin D [nM]
0 0.01 0.1 1 10 100 0 0.01 0.1 1 10 100
0.0625 / 5
α-CD3 / α-CD28 [µg / ml]
c
Cholecalciferol
Many divisions
Intermediate divisions
Few divisions
CD4+ T cells
CD8+ T cells
T cell divisions [%]
Chole-calciferol [nM]
0 10 100 250 500 1000 0 10 100 250 500 1000
0.0625 / 5
α-CD3 / α-CD28 [µg / ml]
d
Human
25-(OH)-Vitamin D
Many divisions
Intermediate divisions
Few divisions
CD4+ T cells
CD8+ T cells
** (Many)
** (Few)
** (Int)
T cell divisions [%]
25-(OH)-Vitamin D [nM]
0 10 100 250 500 1000 0 10 100 250 500 1000
0.03125 / 5
α-CD3 / α-CD28 [µg / ml]
e
1,25-(OH)2-Vitamin D
Many divisions
Intermediate divisions
Few divisions
CD4+ Tcells
CD8+ T cells
* (Many)
* (Int)
** (Few)
*** (Int)
** (Few)
T cell divisions [%]
1,25-(OH)2-Vitamin D [nM]
0 0.01 0.1 1 10 100 0 0.01 0.1 1 10 100
0.03125 / 5
α-CD3 / α-CD28 [µg / ml]
f
Cholecalciferol
Many divisions
Intermediate divisions
Few divisions
CD4+ T cells
CD8+ T cells
** (Many)
** (Few)
* (Few)
T cell divisions [%]
Chole-calciferol [nM]
0 10 100 250 500 1000 0 10 100 250 500 1000
0.03125 / 5
α-CD3 / α-CD28 [µg / ml]

Figure 6. Vitamin D and its metabolites inhibit activation of both human and murine $CD4^+$ and $CD8^+$ T cells. (a-c) Splenocytes were isolated from naïve WT mice receiving standard vitamin D diet. **(d-f)** Human PBMCs were isolated from healthy donors after Ficoll gradient centrifugation. **(a-f)** MACS purified murine or human T cells were CFSE labelled and incubated with increasing concentrations of **(a+d)** 25-(OH)-vitamin D, **(b+e)** 1,25-$(OH)_2$-vitamin D or **(c+f)** cholecalciferol at 37°C. After 1 hour, T cells were transferred to anti-CD3 / anti-CD28 pre-coated wells and incubated for 48-72 hours (murine T cells) or 96-120 hours (human T cells). **(a-f)** T cell proliferation was evaluated by CFSE dilution and stratified by division frequency as follows: few divisions (1-2; dark grey), intermediate divisions (3-4; medium grey) and many divisions (≥ 5; light grey). T cell divisions are shown as mean ± SEM; representative plots of two independent experiments; n = 3.

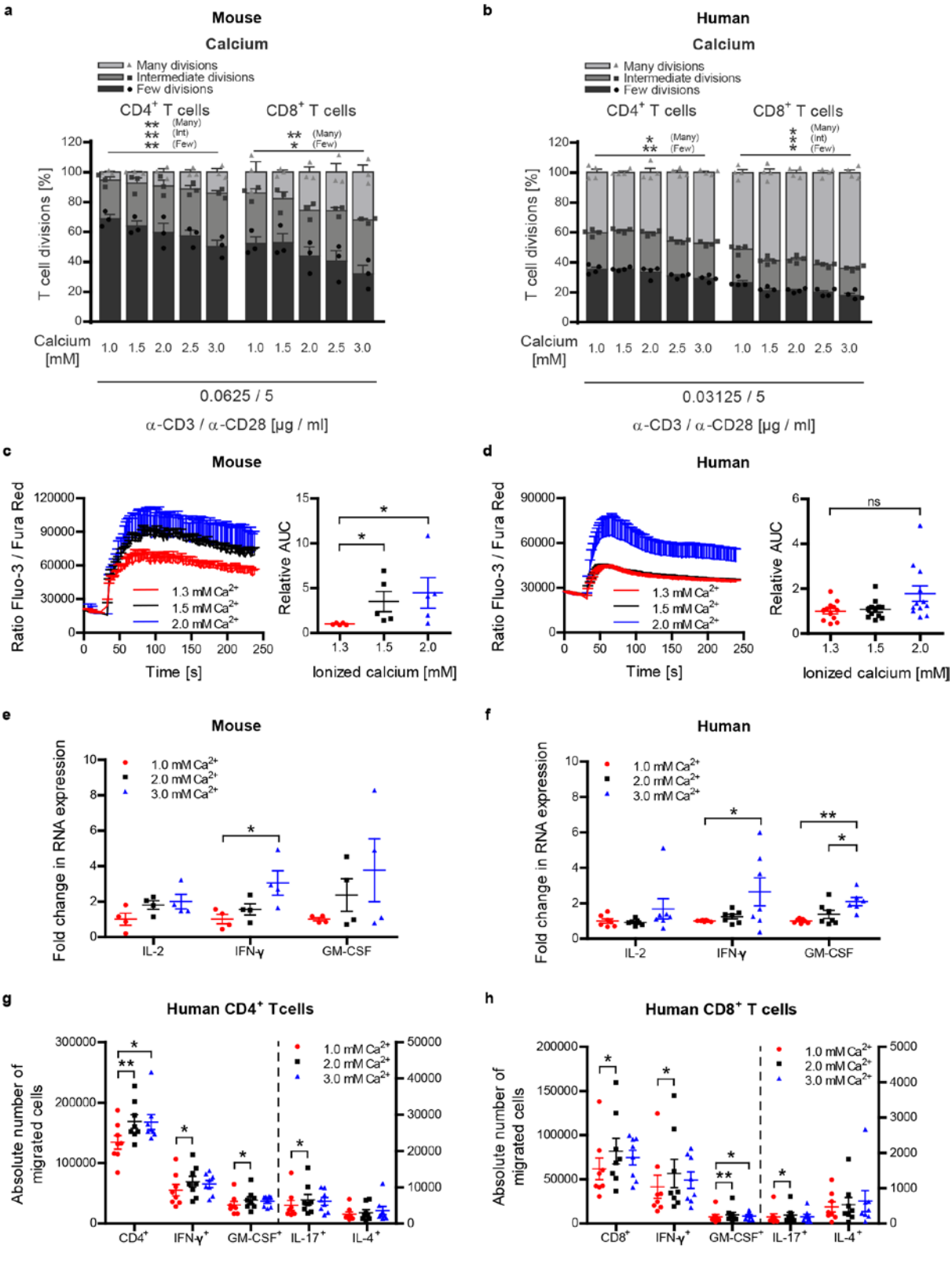
a
Mouse
Calcium
Many divisions
Intermediate divisions
Few divisions
CD4+ T cells
CD8+ T cells
T cell divisions [%]
Calcium [mM]
1.0 1.5 2.0 2.5 3.0
0.0625 / 5
α-CD3 / α-CD28 [µg / ml]
b
Human
Calcium
0.03125 / 5
c
Mouse
Ratio Fluo-3 / Fura Red
1.3 mM Ca2+
1.5 mM Ca2+
2.0 mM Ca2+
Time [s]
Relative AUC
Ionized calcium [mM]
d
Human
ns
e
Mouse
Fold change in RNA expression
1.0 mM Ca2+
2.0 mM Ca2+
3.0 mM Ca2+
IL-2
IFN-γ
GM-CSF
f
Human
g
Human CD4+ Tcells
Absolute number of migrated cells
CD4+
IFN-γ+
GM-CSF+
IL-17+
IL-4+
h
Human CD8+ T cells
CD8+

Figure 7. Hypercalcemia increases proliferation and encephalitogenic differentiation of both human and murine CD4$^+$ and CD8$^+$ T cells. (a, c, e) Splenocytes were isolated from naïve WT mice receiving standard vitamin D diet. **(b, d, f, g, h)** Human PBMCs were isolated from healthy donors after Ficoll gradient centrifugation. **(a-b)** MACS purified murine or human T cells were CFSE labelled and incubated with increasing calcium concentrations at 37°C. After 1 hour, T cells were transferred to anti-CD3 / anti-CD28 pre-coated wells and incubated for 48-72 hours (murine T cells) or 96-120 hours (human T cells). T cell proliferation was evaluated by CFSE dilution and stratified by division frequency as follows: few divisions (1-2; dark grey), intermediate divisions (3-4; medium grey) and many divisions (≥ 5; light grey). T cell divisions are shown as mean ± SEM; representative plots of two independent experiments; n = 3. MACS purified **(c)** murine or **(d)** human T cells were incubated with concentrations of ionized (free) calcium equivalent to concentrations measured in serum or culture medium. After 1 hour, T cells were stained with Fluo-3 AM and Fura Red AM and calcium flux was evaluated by FACS. Representative calcium flux is shown left and area under the curve is depicted on the right (data given as mean ± SEM; **(c)** pooled plots from two independent experiments; n = 5, **(d)** pooled plots from three independent experiments; n = 8). MACS purified **(e)** murine or **(f)** human T cells were incubated with increasing calcium concentrations at 37°C. After 1 hour, T cells were transferred to anti-CD3 / anti-CD28 pre-coated wells and incubated for 1-3 hours (murine T cells) or 3-20 hours (human T cells). Total RNA was isolated, transcribed into cDNA and analyzed by qPCR (data given as mean ± SEM; **(e)** pooled plots from two independent experiments; n = 4, **(f)** pooled plots from two independent experiments; n = 6-7). Number of CD4$^+$ **(g)** and CD8$^+$ **(h)** T cells in bottom chamber after 16 h migration over inflamed human BBB-ECs (modified Boyden chamber assay; left: total number of cells; right: number of cytokine-producing cells), following activation of T cells in the presence of various calcium concentrations. 1 million activated human T lymphocytes were seeded (data given as mean ± SEM; n = 6 different T cell donors, 2 different BBB-EC preparations).

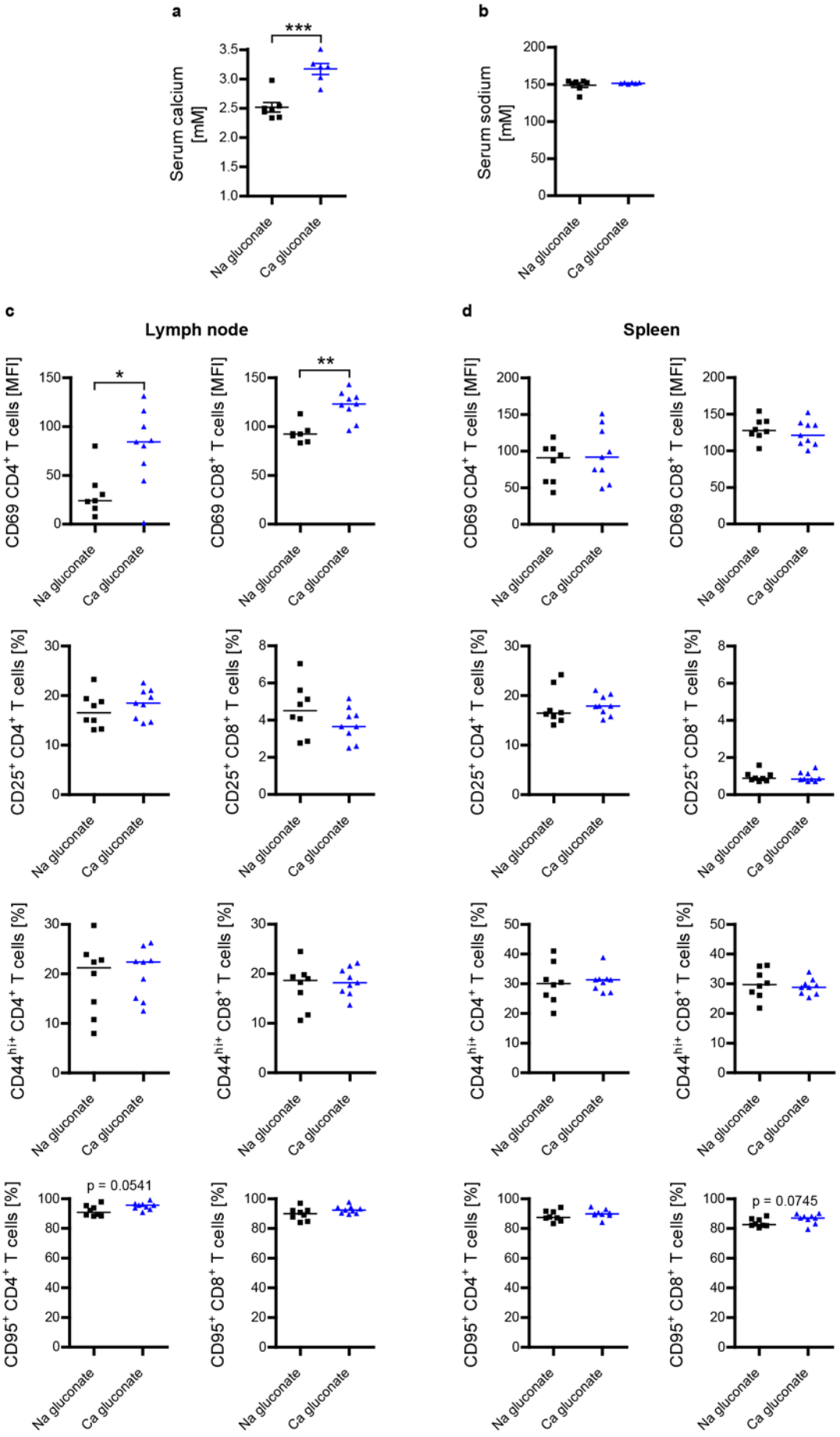
a
***
Serum calcium [mM]
3.5
3.0
2.5
2.0
1.5
1.0
Na gluconate
Ca gluconate
b
Serum sodium [mM]
200
150
100
50
0
Na gluconate
Ca gluconate
c
Lymph node
d
Spleen
CD69 CD4+ T cells [MFI]
CD69 CD8+ T cells [MFI]
CD25+ CD4+ T cells [%]
CD25+ CD8+ T cells [%]
CD44hi+ CD4+ T cells [%]
CD44hi+ CD8+ T cells [%]
CD95+ CD4+ T cells [%]
CD95+ CD8+ T cells [%]
*
**
p = 0.0541
p = 0.0745
Na gluconate
Ca gluconate

Figure 8. Calcium administration in vivo enhances activation of peripheral T cells. Hypercalcemia in mice was induced by daily intraperitoneal injection of calcium gluconate (2000 mg/kg/day) starting three days before immunization. Total calcium **(a)** and total sodium **(b)** in serum were quantified on an ARCHITECT c 16000 analyzer twenty-two days post immunization (representative plots of two independent experiments; data given as mean ± SEM; n = 6-7). Inguinal lymph node cells **(c)** and splenocytes **(d)** were isolated and analyzed for T cell activation by FACS twenty-two days post immunization (representative plots of two independent experiments; data given as median; n = 7-9).

Supplementary Material

Suppl. table 1. Primer used for real-time quantitative PCR

Primer mouse:

Target	Assay ID (Bio-Rad)	Amplicon length	Assay Design
IL-2	qMmuCID0015786	80	Intron-spanning
IFNgamma	qMmuCID0006268	175	Intron-spanning
GM-CSF (CSF2)	qMmuCED0025728	133	Exonic
Actin-beta	qMmuCED0027505	109	Exonic

Primer human:

Target	Assay ID (Thermo Fisher Scientific)	Amplicon length	Fw primer	Rv primer
IL-2	Hs00698651_CE	230	AAGGCCTGATATGTTTTAAGTGGGAA	GCCTATAAGACTTCAATTGGGAATAACTGTAT
IFNgamma	Hs00607988_CE	262	AAAACAAAGGATTAAGTGAGACAGTCACA	GGAAGCGAAAAAGGAGTCAGATG
GM-CSF (CSF2)	Hs00664932_CE	254	CCTCCCTGGCATTTTGTGGT	AGTGTCTCTACTCAGGTTCAGGAG
Actin-beta	Hs00800199_CE	254	ACAGGACTCCATGCCTGAGA	GCCCTGGACTTCGAGCAA

Mineral content in experimental diets			
	Low	Std	Hi
	%		
Calcium	0.9	1.0	0.9
Phosphorus	0.63	0.70	0.63
Sodium	0.19	0.24	0.21

Suppl. figure 1. Low-, standard- and high vitamin D diets have similar calcium, phosphorus and sodium contents. Low, standard or high vitamin D diets contained standard concentrations of calcium, phosphorus and sodium.

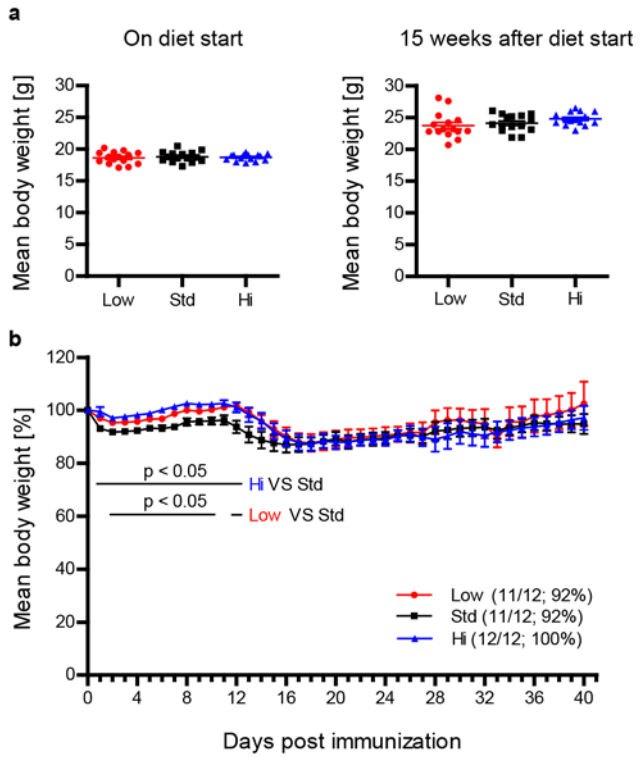

Suppl. figure 2. Vitamin D high excess supplementation has no impact on body weight. (a) Body weight was determined before and fifteen weeks after mice were fed a diet containing low (< 5 IU/kg food), standard (1.500 IU/kg food) or high vitamin D concentrations (75.000 IU/kg food); (data given as mean ± SEM; n = 15). **(b)** EAE was induced by MOG peptide 35-55 immunization fifteen weeks after diet onset. Body weights are shown as mean ± SEM; disease incidence is indicated in brackets; n = 12.

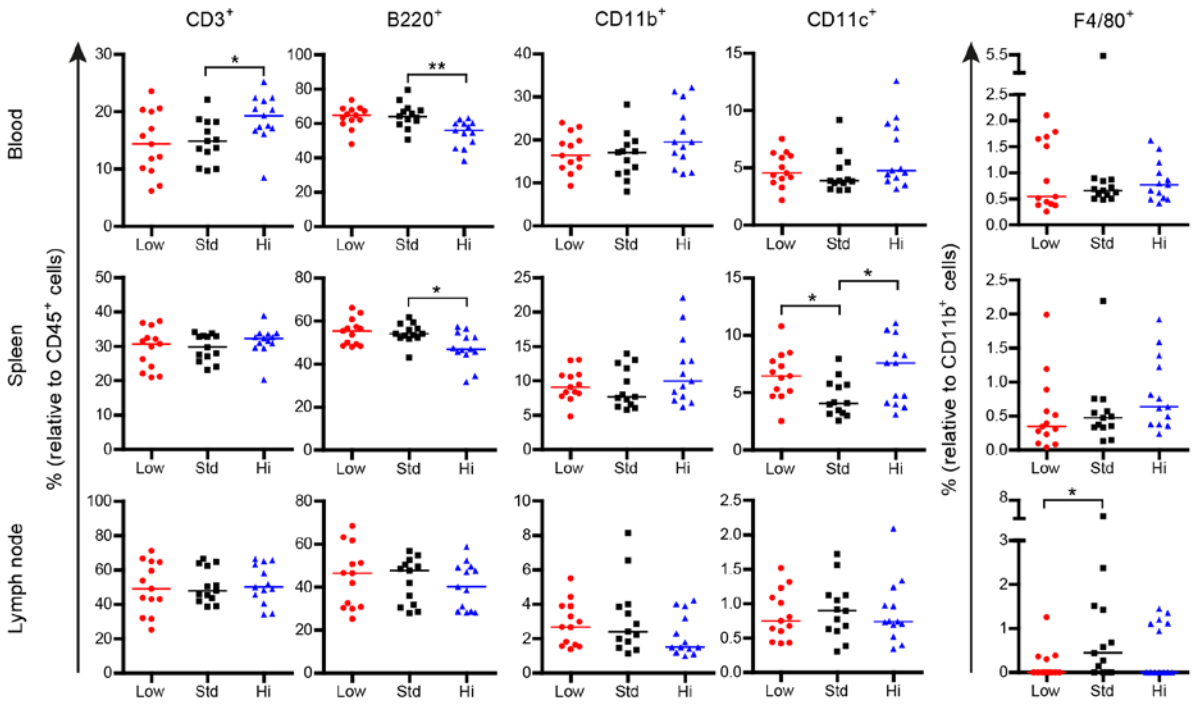

Suppl. figure 3. Vitamin D high excess supplementation increases the frequencies of T cells, CD11c$^+$ myeloid APCs as well as F4/80$^+$ macrophages. Frequencies of immune cells in blood, spleen and inguinal lymph node were analyzed by FACS forty-nine weeks after vitamin D diet onset (data given as median; representative plots of two independent experiments; n = 13).

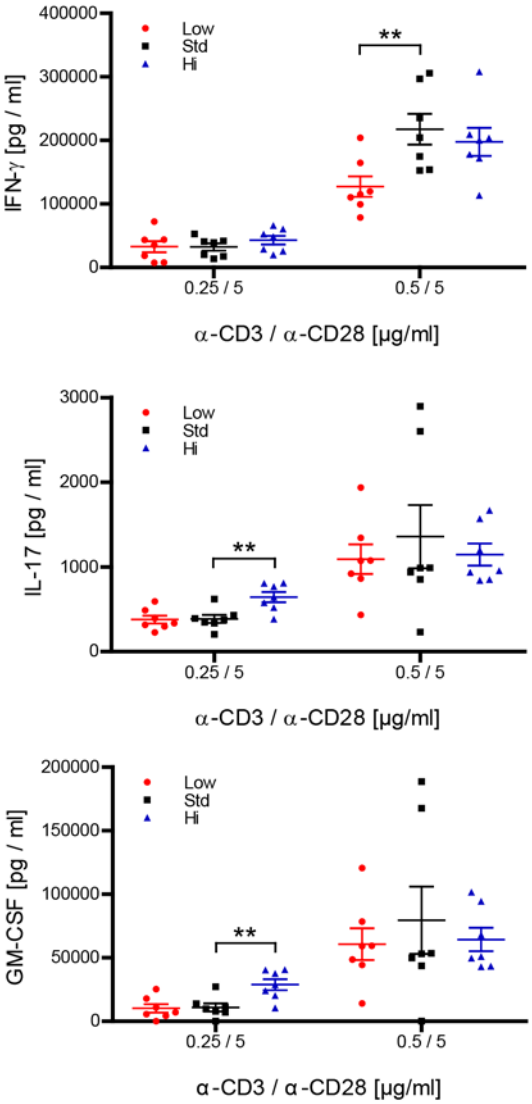

Suppl. figure 4. Vitamin D high excess supplementation promotes differentiation into encephalitogenic T cells. Splenic T cells were isolated from naïve WT mice, which were fed with vitamin D low, standard or high diet for eight weeks. MACS purified T cells were incubated in anti-CD3 / anti-CD28 pre-coated wells for 72 hours. Differentiation into Th1-, Th17- or GM-CSF-secreting T cells was analyzed by quantification of IFN-γ, IL-17 and GM-CSF concentrations in culture supernatants by ELISA (data given as mean ± SEM; n = 7).

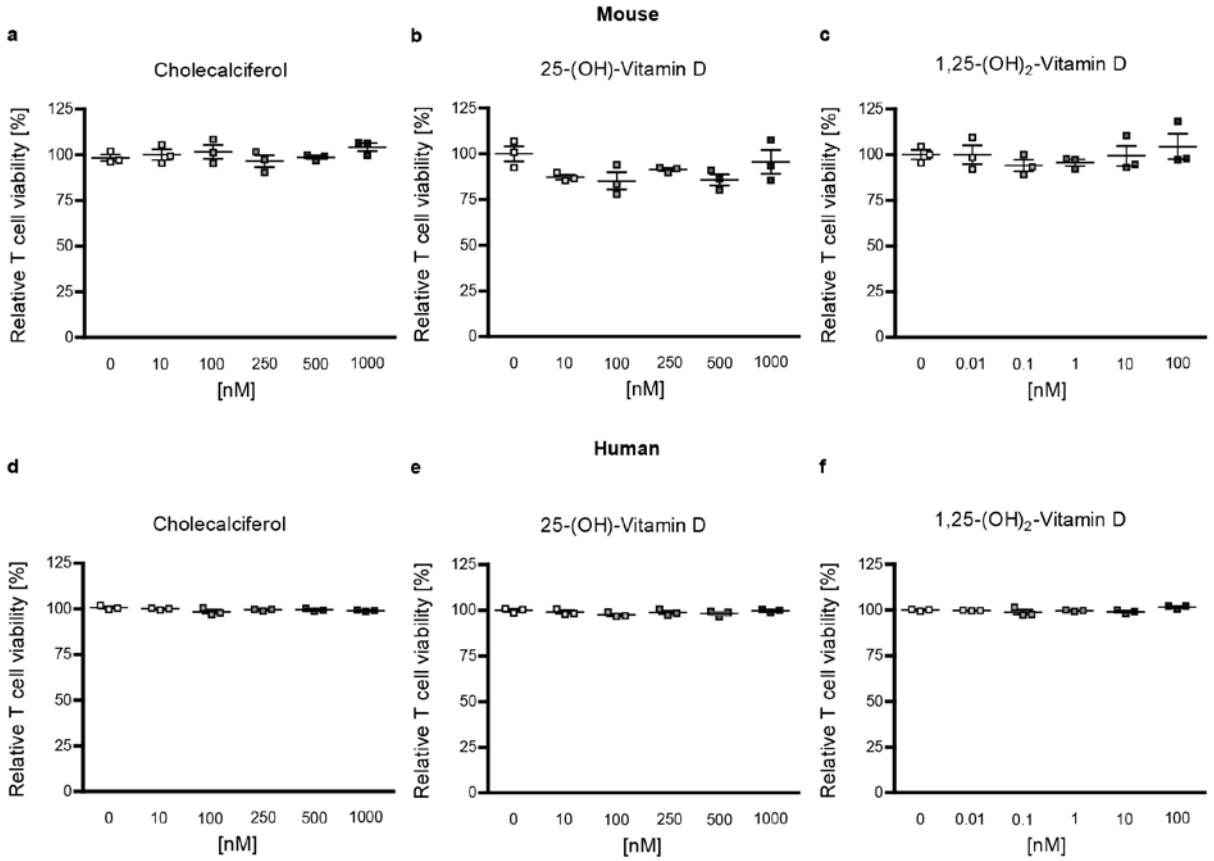

Suppl. figure 5. T cell viability is unaffected by incubation with cholecalciferol, 25-(OH)-vitamin D or 1,25-(OH)$_2$-vitamin D. (a-c) Splenocytes were isolated from naïve WT mice receiving standard vitamin D diet. **(d-f)** Human PBMCs were isolated from healthy donors after Ficoll gradient centrifugation. MACS purified T cells were incubated in anti-CD28 pre-coated wells in presence of increasing concentrations of **(a, d)** cholecalciferol, **(b, e)** 25-(OH)-vitamin D or **(c, f)** 1,25-(OH)$_2$-vitamin D for 48-72 hours (murine T cells) or 96-120 hours (human T cells). T cell viability was determined by FACS using a fixable live cell- / dead cell discrimination dye (data shown as mean ± SEM; representative plots of two independent experiments; n = 3).

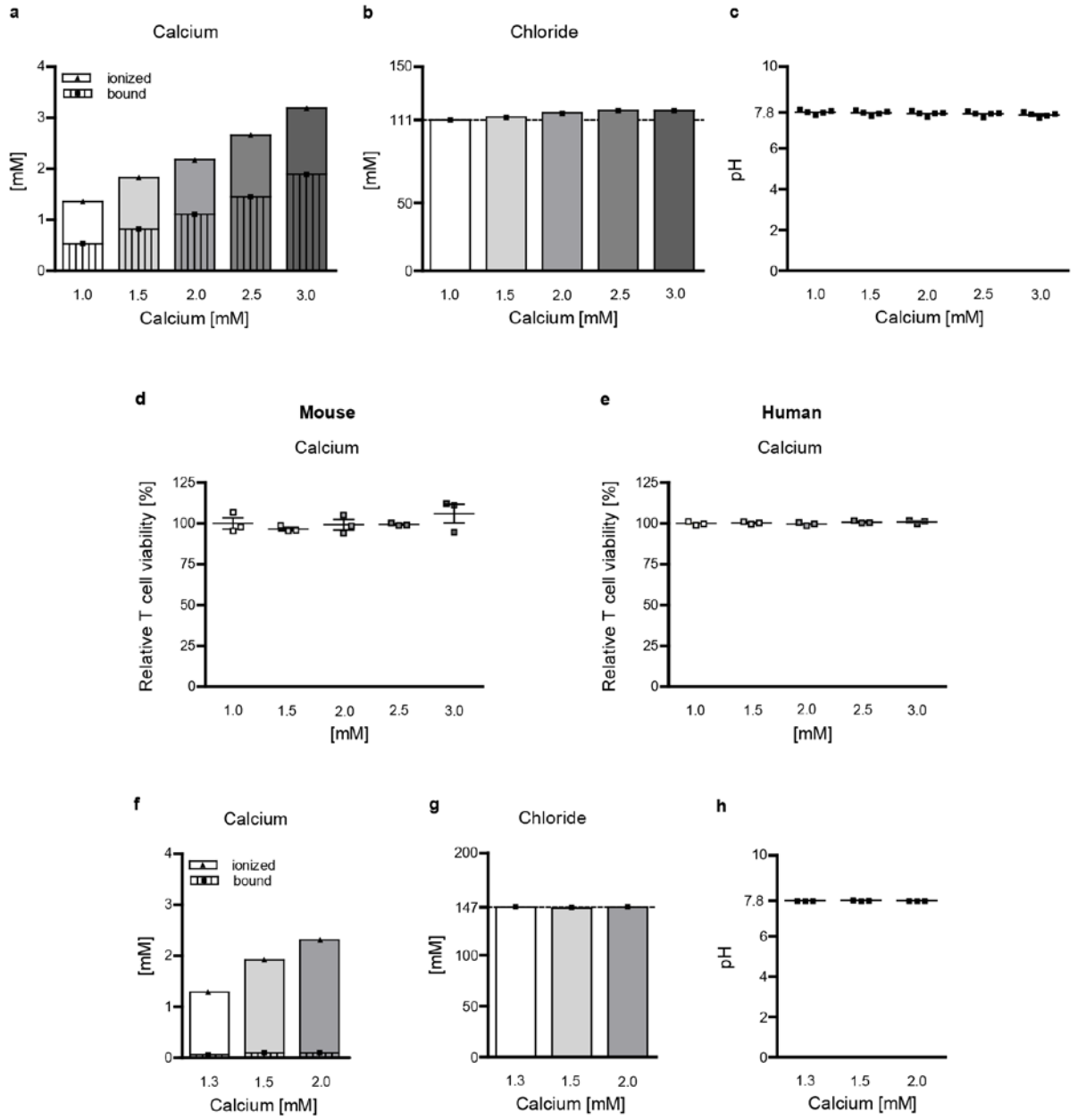

Suppl. figure 6. Increasing calcium concentrations in culture medium have no effect on chloride levels, pH or T cell viability. Calcium concentrations in **(a)** culture medium or **(f)** calcium flux assay medium were increased by dissolving calcium chloride. **(a, f)** Total calcium in culture medium was quantified on an ARCHITECT c 16000 analyzer. Ionized calcium was measured on a blood gas analyzer GEM Premier 4000. Bound calcium was calculated by subtracting the ionized calcium from the total calcium concentration. Data from one representative experiment are presented. Total chloride in **(b)** culture medium or **(g)** calcium flux assay medium was measured using ion-selective electrodes on an ARCHITECT c 16000 analyzer. Data from one representative experiment are presented. **(c, h)** pH in calcium-supplemented media was determined by inoLab pH Level 1 (data given as mean ± SEM; n = 3). **(d)** Splenocytes were isolated from naïve WT mice receiving standard vitamin D diet. **(e)** Human PBMCs were isolated from healthy donors after Ficoll gradient centrifugation. MACS purified T cells were incubated in anti-CD28 pre-coated wells in presence of increasing calcium concentrations for **(d)** 48-72 hours (murine T cells) or **(e)** 96-120 hours (human T cells). T cell viability was determined by FACS using a fixable live cell- / dead cell discrimination dye (data shown as mean ± SEM; representative plots of two independent experiments; n = 3).

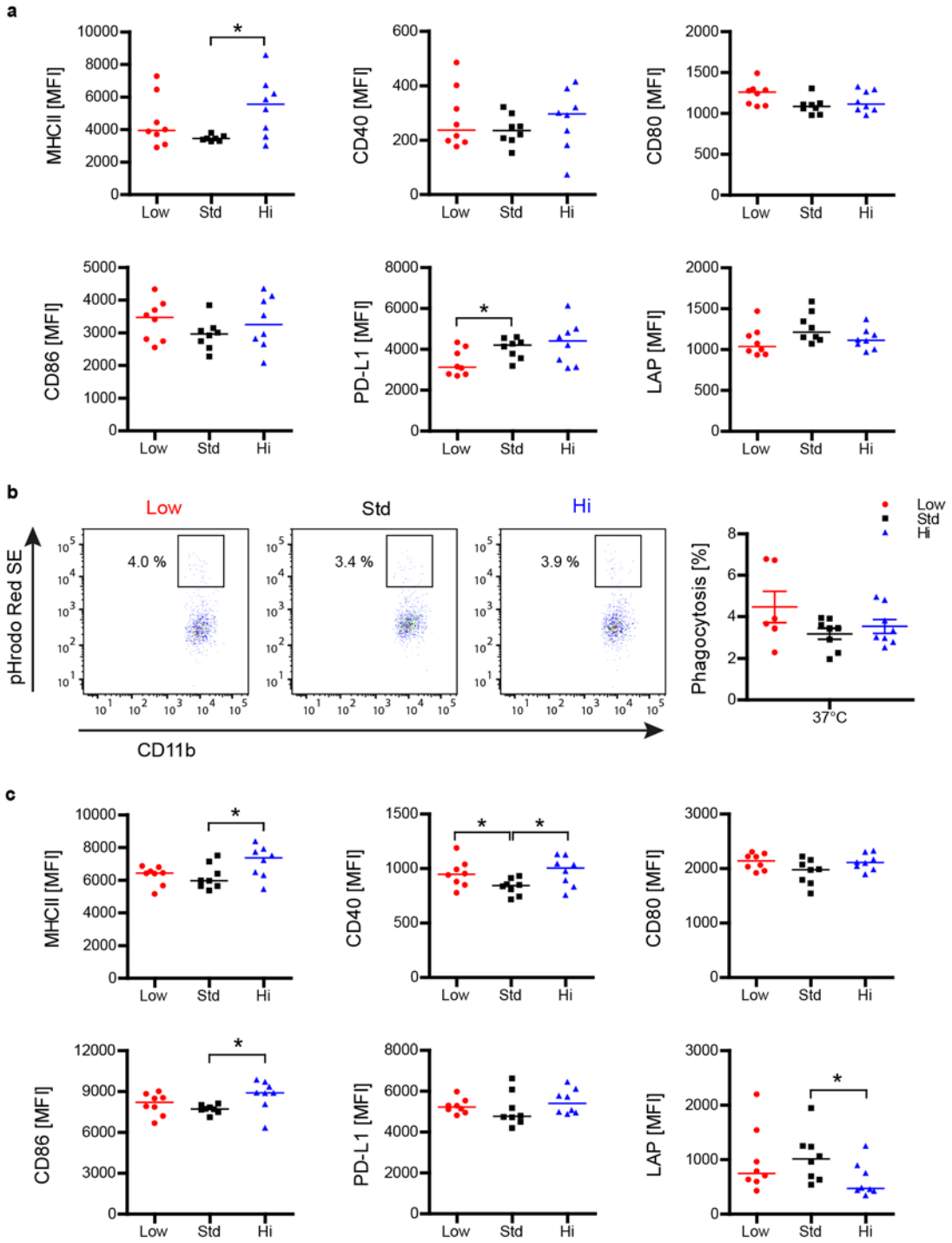

Suppl. figure 7. Vitamin D high excess supplementation increases activation of splenic monocytes and dendritic cells in naïve mice. (a) Splenocytes were isolated and splenic monocyte activation / differentiation was analyzed by FACS eight weeks after vitamin D diet onset in naïve mice (data are shown as median of MFI; n = 7-8). **(b)** Splenic macrophages were isolated eight weeks after vitamin D diet onset from naïve mice and co-cultured with pHrodo Red SE labelled apoptotic thymocytes at 37°C for one hour. Phagocytosis of apoptotic thymocytes by splenic macrophages ($CD11b^+F4/80^+$) was determined by FACS. Representative FACS dot plots are shown left and percentage of phagocytosis by macrophages is depicted on the right as mean ± SEM; n = 6-8. **(c)** Splenocytes were isolated and splenic dendritic cell activation / differentiation was analyzed by FACS eight weeks after vitamin D diet onset in naïve mice (data are shown as median of MFI; n = 8).

4. Myelin-reactive antibodies initiate T cell-mediated CNS autoimmune disease by opsonisation of endogenous antigen.

4.1. Background

Locally produced antibodies (Abs9 are a hallmark diagnostic criteria in a majority of MS patients (Schwenkenbecher et al., 2017). Therefore, B cells, plasma cells and Abs have been extensively studied as mediators of CNS demyelinating disease and have proven to be a valuable therapeutic target (Greenfield and Hauser, 2018). B cells constitutively express MHC class II and have the ability to present antigen after successful recognition via their BCR (Myers, 1991; Sartoris et al., 1990). Transgenic mice in which B cells express a BCR that recognizes MOG (Th mice) showed an accelerated disease course after immunization (Litzenburger et al., 1998). Crossing these mice with a second transgenic mouse strain containing MOG-specific T cells (2D2 mice) results in animals which spontaneously develop clinical and histological signs of CNS-demyelinating disease (Varrin-Doyer et al., 2016). Taken together with the fulminant success of B cell depleting therapies in EAE and MS proves the contribution of B cells to CNS pathogenicity. One important function of B cells is the production of antibodies (Alberts et al., 2002). Antibodies can opsonize antigens and thereby mark them for myeloid cells, which detect the immune complex via their Fc-receptors. This leads to the phagocytosis, processing and presentation of the antigen (HART et al., 2004). This work focused on the role of MOG-specific antibodies in the development of CNS autoimmunity.

4.2. Approach

Prophylactic B cell depletion leads to an amelioration of MOG protein EAE, however we did not observe an effect of anti-CD20 therapy in Th or the double transgenic Th x 2D2 mice. Injecting MOG_{1-117} immunized mice with serum from Th mice accelerated clinical and histological EAE. Additionally, disease could be initiated by injecting naïve 2D2 mice either with Th serum or the MOG-specific antibody 8.18C5. The accelerated proliferation of T cells in spleen and lymph nodes we observed and the increased expression of the activation marker CD69 on T cells and MHCII on myeloid APCs could be blocked by injecting an Fc-receptor blocking antibody in addition to 8.18C5. *In vitro* differentiated macrophages and dendritic cells showed an increase phagocytic ability of fluorescently-labelled antigen (MOG

or ovalbumin (OVA)) in the presence of specific antibodies (8.18C5 or anti-OVA) and depending on the availability of Fc-receptors. In co-culture experiments of macrophages and T cells, this increased phagocytosis translated into accelerated T cell proliferation. Additionally, the production of IFNγ, IL-17 and GM-CSF was increased, again depending on the presence of specific antibodies and Fc-receptor mediated recognition of the antigen. Lastly, using serum samples from patients either positive or negative for MOG-specific antibodies together with human macrophages we showed the same effect of Fc-receptor depending phagocytosis of opsonized antigen. These findings could be crucial to understand the involvement of antibodies in the initiation and progression of CNS disease.

4.3. Contribution

I conducted the experiments for figures 2, 4 and 6, and primarily carried out the experiments demanded in the review of the manuscript. I collected, analysed and interpreted the resulting data and was implicated in statistical analysis. I partially prepared the resulting figures and wrote the respective parts of the manuscript.

4.4. Original publication

Kinzel S*, Lehmann-Horn K*, Torke S, Häusler D, Winkler A, Stadelmann C, Payne N, Feldmann L, Saiz A, Reindl M, Lalive PH, Bernard CC, Brück W, Weber MS (2016): Myelin-reactive antibodies initiate T cell-mediated CNS autoimmune disease by opsonisation of endogenous antigen. Acta Neuropathol (Berl) 132, 43–58

*these authors contributed equally

Acta Neuropathol (2016) 132:43–58
DOI 10.1007/s00401-016-1559-8

ORIGINAL PAPER

Myelin-reactive antibodies initiate T cell-mediated CNS autoimmune disease by opsonization of endogenous antigen

Silke Kinzel[1] · Klaus Lehmann-Horn[2] · Sebastian Torke[1] · Darius Häusler[1] · Anne Winkler[1] · Christine Stadelmann[1] · Natalie Payne[3] · Linda Feldmann[1] · Albert Saiz[4] · Markus Reindl[5] · Patrice H. Lalive[6,7] · Claude C. Bernard[3] · Wolfgang Brück[1] · Martin S. Weber[1,8]

Received: 29 October 2015 / Revised: 5 March 2016 / Accepted: 5 March 2016 / Published online: 29 March 2016

Abstract In the pathogenesis of central nervous system (CNS) demyelinating disorders, antigen-specific B cells are implicated to act as potent antigen-presenting cells (APC), eliciting waves of inflammatory CNS infiltration. Here, we provide the first evidence that CNS-reactive antibodies (Ab) are similarly capable of initiating an encephalitogenic immune response by targeting endogenous CNS antigen to otherwise inert myeloid APC. In a transgenic mouse model, constitutive production of Ab against myelin oligodendrocyte glycoprotein (MOG) was sufficient to promote spontaneous experimental autoimmune encephalomyelitis (EAE) in the absence of B cells, when mice endogenously contained MOG-recognizing T cells. Adoptive transfer studies corroborated that anti-MOG Ab triggered activation and expansion of peripheral MOG-specific T cells in an Fc-dependent manner, subsequently causing EAE. To evaluate the underlying mechanism, anti-MOG Ab were added to a co-culture of myeloid APC and MOG-specific T cells. At otherwise undetected concentrations, anti-MOG Ab enabled Fc-mediated APC recognition of intact MOG; internalized, processed and presented MOG activated naïve T cells to differentiate in an encephalitogenic manner. In a series of translational experiments, anti-MOG Ab from two patients with an acute flare of CNS inflammation likewise facilitated detection of human MOG. Jointly, these observations highlight Ab-mediated opsonization of endogenous CNS auto-antigen as a novel disease- and/or relapse-triggering mechanism in CNS demyelinating disorders.

Keywords Auto-antibodies · Opsonization · Myeloid antigen-presenting cells · Fc receptor · Experimental autoimmune encephalomyelitis · Multiple sclerosis

Introduction

B cells, plasma cells and antibodies (Ab) are increasingly recognized as key players in inflammatory central nervous system (CNS) demyelinating diseases, such as multiple

S. Kinzel and K. Lehmann-Horn contributed equally and are listed in alphabetical order.

Electronic supplementary material The online version of this article (doi:10.1007/s00401-016-1559-8) contains supplementary material, which is available to authorized users.

✉ Martin S. Weber
martin.weber@med.uni-goettingen.de

[1] Department of Neuropathology, University Medical Center, Georg August University, Göttingen, Germany

[2] Department of Neurology, Klinikum rechts der Isar, Technische Universität München and Munich Cluster for Systems Neurology, Munich, Germany

[3] Monash Regenerative Medicine Institute, Multiple Sclerosis Research Group, Monash University, Melbourne, Australia

[4] Service of Neurology, Hospital Clinic, University of Barcelona, Barcelona, Spain

[5] Clinical Department of Neurology, Medical University of Innsbruck, Innsbruck, Austria

[6] Division of Neurology, Department of Clinical Neurosciences, University Hospital of Geneva, Geneva, Switzerland

[7] Department of Pathology and Immunology, Faculty of Medicine, University Hospital of Geneva, Geneva, Switzerland

[8] Department of Neurology, University Medical Center, Georg August University, Göttingen, Germany

sclerosis (MS), neuromyelitis optica (NMO) and related disorders. Within the cerebrospinal fluid of the majority of MS patients, locally supported plasma cells continuously produce oligoclonal immunoglobulin (Ig) [36, 51], which remain a hallmark diagnostic finding. B and plasma cells are commonly found in MS lesions [41] and Ab deposition co-localizes with complement activation and ongoing demyelination [16]. In NMO, compelling evidence suggests that anti-aquaporin (AQP)-4-Ab selectively target astrocytes resulting in subsequent demyelination [29].

B cells constitutively express major histocompatibility complex (MHC) class II and act as powerful antigen-presenting cells (APC) when they recognize conformational protein antigen via their B cell receptor (BCR) [9]. B cells from MS patients reveal signs of chronic activation with a differential shift toward antigen-experienced memory B cells producing pro-inflammatory cytokines, such as interleukin-6 [12] and granulocyte-macrophage colony-stimulating factor (GM-CSF) [25]. These properties, along with the fulminant success of the clinical trials testing anti-CD20 monoclonal Ab [18, 19], suggest that antigen-experienced B cells may act as potent APC in MS.

A series of recent experimental investigations aimed to directly address the role of B cells, plasma cells and Ab in development of inflammatory CNS demyelinating disease. First, transgenic mice were generated in which B cells recognize myelin oligodendrocyte protein (MOG) and plasma cells constitutively produce high titers of pathogenic anti-MOG Ab (Th mice); upon active immunization, these mice showed a fulminant course of experimental autoimmune encephalomyelitis (EAE) with enhanced CNS demyelination [27]. When Th mice were further crossed with MOG T cell receptor (TCR) transgenic mice (2D2 mice) [4], the resulting line (Thx2D2) even spontaneously developed EAE [3, 21]. A similar observation was reported on the SJL/J background, furthermore, demonstrating that transgenic T cells can recruit endogenous MOG-specific B cells [39]. In an attempt to elucidate which immunological components were required for spontaneous EAE development, a pivotal recent report demonstrated that myelin-recognizing B and T cells sufficed to trigger EAE development in C57BL/6 mice [34], corroborating that auto-reactive B cells are an essential APC population in this model.

Notwithstanding these results, we here report on a crucial complementary role of CNS-reactive Ab likely completing the scenario how initial recognition of auto-antigen in development of CNS autoimmune disease can occur. We show that traces of CNS antigen are opsonized by myelin-reactive Ab, making them recognizable for Fc receptor carrying myeloid APC. Subsequent to internalization, processed myelin antigen is presented to myelin-recognizing T cells triggering their expansion and encephalitogenic differentiation. We demonstrate that this mechanism indeed sparks experimental CNS autoimmunity; first, we show that in the absence of B cells, Thx2D2 mice develop spontaneous EAE indistinguishable from its course in mice containing B cells. Second, and most importantly, adoptive transfer of serum from Th mice or of purified anti-MOG Ab 8.18C5 into naïve 2D2 recipients triggered activation and expansion of T cells followed by severe and robust EAE, suggesting that the mechanism of Ab-mediated opsonization of auto-antigen may indeed contribute to initiation and propagation of CNS demyelinating disease.

Materials and methods

Mice

MOG p35-55 TCR transgenic 2D2 mice were kindly provided by Dr. Kuchroo (Boston, USA). MOG Ig heavy chain knockin (Th) mice were kindly provided by Dr. Wekerle (Munich, Germany). Fcγ receptor knockout (Fcγ$R^{-/-}$) mice were kindly provided by Dr. Nimmerjahn (Erlangen, Germany). Wild-type (WT) C57BL/6 mice were purchased from Charles River (Sulzfeld, Germany). All murine experiments were carried out as approved by the government of Upper Bavaria (protocol number 55.2-1-54-2531-67-09) and the government of lower Saxony (protocol number 33.9-42502).

B cell depletion

B cell depletion was achieved by weekly intraperitoneal (i.p.) injections of 200 µg of murine anti-CD20 or anti-ragweed isotype control Ab (both provided by Genentech, South San Francisco, USA) in 200 µl PBS.

Antigens and EAE induction regiments

Mouse MOG peptide (p) 35-55 (MEVGWYRSPFSRVVHLYRNGK) was synthesized by Auspep (Parkville, Australia). Murine MOG protein 1-117 (mMOG) and human MOG protein (hMOG) were kindly provided by C.C.A. Bernard and synthesized, purified and refolded as previously reported [8]. 8–10 week-old-female Th or WT mice were immunized subcutaneously with either a suboptimal dose of 35 µg mMOG or an optimal dose of 50 µg mMOG in Complete Freund's Adjuvant (CFA) followed by 200 ng of pertussis toxin (Sigma-Aldrich, St. Louis, USA) i.p. at the day of immunization and 2 days thereafter. Alternatively, WT mice were immunized with 100 µg MOG p35-55 in CFA followed by two injections of 300 ng pertussis toxin. For spontaneous EAE experiments, Th mice were bred with 2D2 mice (Thx2D2). To induce EAE by transfer of MOG-specific Ab, a serum preparation containing anti-MOG Ab or monoclonal Ab clone 8.18C5 were injected

into the tail vein of WT or 2D2 recipients. 150 µl Th serum or control serum was injected twice a week up to a total of five injections; 150 µg 8.18C5 Ab or isotype control Ab (clone: MOPC-21, Bio X cell, West Lebanon, USA) was injected twice a week up to a total of ten injections. In recipients, no immunization or adjuvant treatment was added.

Evaluation of EAE

Mice were assessed for clinical signs of EAE as follows: 0 = no clinical disease, 1 = tail weakness, 2 = hind limb weakness, 3 = one paralyzed hind limb, 4 = two paralyzed hind limbs, 5 = moribund or dead. To evaluate balance and general motor function the elevated beam test was used; mice were placed on a raised beam with a maximal height of 40–50 cm and a length of 100 cm and the time needed to traverse was measured. Mice were evaluated daily starting 2 weeks prior to the respective treatment.

Intrathecal injection of mMOG

Mice were injected with 40 µg mMOG in 10 µl PBS or 10 µl of 10 % Evans blue percutaneously into the cisterna magna with a 30-gauge needle in 45° anteflexion of the head.

Generation of anti-MOG Ab containing serum

Serum containing high titers of pathogenic anti-MOG Ab or control serum was obtained from Th mice immunized with 100 µg mMOG (Th serum) or from WT mice immunized with 100 µg MOG p35-55 (control serum), respectively. Donor mice were immunized to ensure the maximum capacity of obtained myelin-specific Ab. 14 days after immunization, blood was obtained by puncture of the left ventricle; serum was separated by centrifugation, pooled for further use and stored at −20 °C.

Preparation and digestion of 8.18C5

Anti-MOG monoclonal Ab clone 8.18C5 was generated by hybridoma cells kindly provided by Dr. Linington (Glasgow, UK). Hybridoma cells were cultured in complete medium (RPMI, 5–10 % fetal calf serum, 50 U/ml penicillin, 50 µg/ml streptomycin, 2 mM L-glutamine, 1 mM sodium pyruvate, 0.05 mM β-mercaptoethanol) in large-scale flasks (Greiner bio-one, Kremsmuenster, Austria) and Ab was purified using rProtein A/Protein G Sepharose columns (rProtein A/Protein G GraviTrap, GE Healthcare, Little Chalfont, UK), according to manufacturer's recommendations. 8.18C5 IgG was digested by ficin (Pierce Mouse IgG1 Fab and $F(ab')_2$ Preparation Kit, Thermo Scientific, Waltham, USA), according to manufacturer's recommendations; integrity and binding capacity of 8.18C5 Ab and resulting 8.18C5 $F(ab')_2$ fragments were verified by 6 % sodium dodecyl sulfate polyacrylamide gel electrophoresis (SDS-PAGE) under non-reducing conditions, followed by protein staining with Coomassie brilliant blue G250 (Biorad, Munich, Germany) and competitive anti-MOG enzyme linked immunosorbent assay (ELISA), respectively.

IgG preparation from patients with demyelinating CNS inflammation

IgG Ab preparations were isolated by Protein G Sepharose 4 Fast Flow (GE Healthcare) from plasma exchange fluid obtained from two patients with neuromyelitis optica spectrum disorders (NMOSD), and plasma from one healthy blood donor. One patient was a 62-year-old Caucasian woman with past history of relapsing bilateral optic neuritis. The patient was admitted because of a severe brainstem relapse that was treated with corticosteroids and plasma exchange followed by rituximab. The other patient was a 55-year-old Caucasian woman with a relapsing disease since the age of 48, who presented with a severe optic neuritis relapse in January 2016 that was treated with corticosteroids and plasma exchange followed by rituximab. In both cases, cerebrospinal fluid showed no oligoclonal bands, and serum samples were negative for anti-AQP-4 Ab but positive for anti-MOG Ab (titer 1:1280, patient #1; 1:5120, patient #2) measured by a recombinant live cell-based immunofluorescence assay with HEK293 cells as previously described [30]. Prior to our in vitro assay, the general ability to bind soluble recombinant hMOG was tested by ELISA using an anti-MOG Ab positive IgG preparation. The healthy blood donor was tested anti-MOG Ab negative, and IgG preparation served as negative control. Samples were kindly provided by Dr. Reindl (Innsbruck, Austria) and Dr. Saiz (Barcelona, Spain). The use of the patient's material was approved by the Ethic Committee of the Hospital Clinic of Barcelona, written consent was obtained.

Fc blocking in vivo

To block Fcγ receptors in vivo, mice were injected i.p. daily with 100 µg anti-CD16/CD32 Ab (Clone: 2.4G2, TONBO bioscience, San Diego, USA) in 100 µl 1xPBS starting 2 days prior to further treatment.

Assessment of in vivo proliferation of T cells

In vivo proliferation of T cells was evaluated by i.p injection of 200 µl Bromdesoxyuridin (BrdU; 10 mg/ml) 24 h before flow cytometry evaluation using a BrdU Flow kit (BD Pharmingen, San Diego, USA), according to manufacturer´s recommendations.

Generation of bone marrow-derived myeloid APC

To generate bone marrow-derived macrophages (BMDM), bone marrow isolated from hind limbs of WT or FcγR$^{-/-}$ mice was cultured at 37 °C for 7 days in medium containing 30 % conditioned L929 cell supernatant (DMEM, 30 % L929 supernatant, 10 % fetal calf serum, 5 % horse serum, 50 U/ml penicillin, 50 µg/ml streptomycin, 0.05 mM β-mercaptoethanol). For bone marrow-derived dendritic cell (BMDC) generation, bone marrow was isolated from hind limbs of WT mice and cultured for 7 days in complete medium (RPMI, 10 % fetal calf serum, 50 U/ml penicillin, 50 µg/ml streptomycin, 2 mM L-glutamine, 1 mM sodium pyruvate, 0.05 mM β-mercaptoethanol) containing 25 ng/ml GM-CSF (Sigma-Aldrich).

Evaluation of antigen uptake by myeloid APC

Adherent BMDM or BMDC were harvested using cell scraper, 0.5×10^5 cells/well were plated into 96-well flat-bottom plates (Sarstedt, Nuembrecht, Germany) and pre-stimulated with 500 ng/ml lipopolysaccharide (LPS, Sigma-Aldrich). 24 h thereafter, cells were incubated for 2 h with DyLight-405 labeled conformational mMOG (mMOG-DyLight-405) or ovalbumin (OVA)-FITC (Life Technologies, Thermo Fisher Scientific) in the presence of 50 µg/ml 8.18C5 Ab, 8.18C5 F(ab′)$_2$ fragment, anti-OVA Ab (clone: TOSG1C6, BioLegend, San Diego, USA) or isotype control Ab (clone: MOPC-21). To investigate phagocytosis of conformational hMOG, murine BMDM which are known to recognize human IgG via their Fc receptor [37] were incubated with hMOG-DyLight-405 for 2 h in the presence of 15 µg/ml of the respective IgG preparation. Where indicated, Fcγ receptors were blocked using anti-mouse CD16/CD32 Ab (Clone: 2.4G2, 1:100 dilution).

Assessment of T cell proliferation and differentiation in vitro

Adherent BMDM were harvested using cell scraper, 0.5×10^5 cells/well were plated into 96-well flat-bottom plates and pre-stimulated with 50 ng/ml LPS and mMOG in the presence of 50 µg/ml 8.18C5 Ab, 8.18C5 F(ab′)$_2$ fragment or isotype control Ab. Where indicated, Fcγ receptors were blocked using anti-mouse CD16/CD32 Ab (Clone: 2.4G2, 1:100 dilution). 24 h thereafter, 1×10^5 MACS-purified (Pan T cell Isolation Kit, Miltenyi, Bergisch Gladbach, Germany) carboxyfluorescein succinimidyl ester (CFSE)-stained (CFSE Cell Division Tracker Kit, BioLegend) or unstained T cells from 2D2 mice were added per well. 72 h thereafter, T cell proliferation and differentiation were evaluated by flow cytometry or ELISA, respectively.

Flow cytometric analysis

To obtain single cell suspensions of lymphoid tissues, respective spleens and lymph nodes were carefully dissected and passed through 70 µm strainer. Freshly obtained blood was mixed 1:2 with 1 mM EDTA and erythrocytes were lysed using BD Pharm Lyse Buffer, according to manufacturer's recommendation. B cells were stained for B220 (BioLegend) CD19 (BioLegend) and/or CD20 (BioLegend), T cells for CD3 and/or CD4 (all BD Bioscience). T cell activation was determined by expression of CD69 (BD Bioscience). T cell differentiation was evaluated by intracellular cytokine staining for IFN-γ (eBioscience, San Diego, USA) and IL-17A (BD Bioscience) after 4-h incubation with phorbol 12-myristate 13-acetate (PMA, 50 ng/ml) and ionomycin (0.5 µg/ml) in the presence of monensin (1 µl Golgi-Stop per ml cell suspension, BD Bioscience). Dead cells were excluded using an Aqua Dead Cell Stain Kit (Invitrogen, Thermo Fisher Scientific, 405 nm excitation). CNS-infiltrating cells were isolated by discontinuous density gradient (Percoll) [24] and stained in a similar manner for CD3, CD4, IFN-γ and IL-17A. Myeloid APC were stained for CD11b and CD11c (both BioLegend). Expression of Fcγ receptor (FcγR) I and III of BMDM and BMDC was determined using anti-CD64 Ab (FcγRI, BioLegend) and anti-CD16 Ab (FcγRIII, BioLegend). APC secretion of IL-1α and IL-23 (both BioLegend) was determined after 5-h incubation with 500 ng/ml LPS in the presence of monensin (1 µl Golgi-Stop per ml cell suspension. BD Bioscience).

ELISA for cytokine analysis

ELISA for IFN-γ, IL-17 or GM-CSF was performed using paired monoclonal Ab per manufacturer's recommendations (DuoSet, R&D Systems, Wiesbaden-Nordstadt, Germany). The results are expressed as an average of duplicates/triplicates ± SEM. iMark microplate reader and software was used for data analysis (Bio-Rad Laboratories Inc., Hercules, CA, USA).

ELISA for detection of MOG Ab

96-well plates were coated with 10 µg/ml conformational mMOG or conformational hMOG in 1xPBS overnight. Diluted samples were added for 2 h. After washing, plate-bound Ab of murine samples and 8.18C5 Ab were detected with horseradish peroxidase (HRP)-conjugated anti-mouse IgG, directed against the Fc part of the bound Ab (1:6000; Sigma-Aldrich) or against the whole molecule (1:5000; Sigma-Aldrich). Anti-MOG Ab in human samples were detected with HRP-conjugated anti-human IgG (1:1000; Sigma-Aldrich). Plates were read at 450 nm wavelength by

a Tecan Genios plate reader and analyzed using Magellan6 software or iMark microplate reader and software.

Histology

Brain and spinal cord tissue was PBS-perfused and cryo-fixed or perfused and fixed with 4 % paraformaldehyde and paraffin embedded. To determine myelin loss and inflammatory infiltration, vertically or horizontally oriented sections were stained with Luxol Fast Blue and periodic acid Schiff (LFB/PAS) or hematoxylin and eosin (H&E), respectively. Infiltration of immune cells was determined by immunohistochemistry using Ab against CD3 (1:150 dilution; DCS, Hamburg, Germany), B220 (1:200 dilution; BD Pharmingen) or MAC3 (1:200 dilution, BD Bioscience). Evaluation of histologic samples was performed in a blinded manner.

Statistical analysis

EAE experiments were evaluated for significance using the Mann–Whitney test. The Student *t* test was used for all other statistical comparison. A value of $p < 0.05$ was considered significant. Data are presented as mean ± SEM.

Results

Depletion of CD20 positive B cells does not alter severity of induced EAE in Th mice nor spontaneous EAE development in Thx2D2 mice

To delineate the relative pathogenic contribution of myelin-specific Ab from myelin-specific B cells, we first investigated the effect of preventive B cell depletion on actively induced EAE in Th mice constitutively containing a high frequency of MOG-recognizing B cells as well as plasma cells producing pathogenic anti-MOG Ab (Suppl. Figure 1a). Results were compared to WT mice, in which only a comparably small fraction of B cells can respond to mouse MOG protein immunization, and developing Ab titers are non-pathogenic [32]. As shown in suppl. Figure 1b, three injections of anti-mouse CD20 Ab efficiently depleted virtually all CD20 positive ($^+$) B cells from blood, bone marrow, lymph node and spleen of WT mice, sparing only CD20 negative B cells in the bone marrow. Corresponding results were obtained in secondary lymphoid organs of Th mice following anti-CD20 Ab treatment (Suppl. Figure 1c). Upon immunization with a suboptimal dose of mMOG protein, WT mice developed mild but consistent EAE with a slight benefit in the B cell-depleted group [52]; using the identical induction regimen, Th mice developed fulminant EAE irrespective of anti-CD20 Ab treatment prior to immunization (Fig. 1a) or after EAE onset (Suppl. Figure 1d). These findings were closely reflected by a massive CNS demyelination and inflammation in both B cell-depleted and isotype-treated Th mice (Fig. 1b), along with an unhindered Th1/Th17 differentiation in the absence of B cells (Suppl. Figure 1e). In line with the fact that anti-CD20 Ab spare CD20 negative plasma cells, constitutively produced anti-MOG Ab remained high in preventatively anti-CD20 Ab treated Th mice during the priming- and CNS-infiltration period (Fig. 1c).

Next, we applied anti-CD20 Ab treatment to Thx2D2 mice (Suppl. Figure 1f) containing MOG-recognizing B cells, MOG-specific T cells and high titers of constitutively produced pathogenic anti-MOG Ab. To our surprise, preventative B cell depletion at the age of 3–4 weeks neither affected incidence of spontaneous EAE (18 anti-CD20-treated vs. 22 isotype-treated in equally sized groups) nor its severity (Fig. 1d). As in immunized Th mice, depletion of $CD20^+$ B cells did not affect generation of encephalitogenic Th1 and Th17 cells (Fig. 1e) nor lower endogenous anti-MOG Ab production at the time of disease induction (Fig. 1f); analogous clinical and immunological results were obtained when anti-CD20 Ab treatment was initiated in fully established spontaneous EAE (Suppl. Figure 1g–h).

Transfer of serum from Th mice exacerbates experimental autoimmune encephalomyelitis in wild-type mice

These findings endorsed a prominent pathogenic role of myelin-reactive Ab independent of B cells, which we next investigated directly and independent of anti-CD20 Ab treatment by adoptive transfer. At first, serum from immunized Th mice (Th serum) was transferred into MOG p35-55-immunized WT mice. As shown in Fig. 1g, repeated intravenous (i.v.) injections of Th serum indeed substantially accelerated EAE severity in WT recipients and, of note, onset and severity closely resembled EAE in immunized Th mice. Histologic analysis revealed accentuated CNS inflammation and demyelination in Th serum recipients (Fig. 1h, left and middle), which is in line with the reported demyelinating nature of anti-MOG Ab in ongoing EAE [26, 46]. Exceeding this anticipated result, Th serum recipients furthermore displayed a massive CNS infiltration of $CD3^+$ T cells (Fig. 1h, right).

Transfer of anti-MOG antibodies triggers spontaneous experimental autoimmune encephalomyelitis in MOG T cell receptor transgenic 2D2 mice

Together with the observation that early B cell depletion failed to halt spontaneous EAE development in Thx2D2

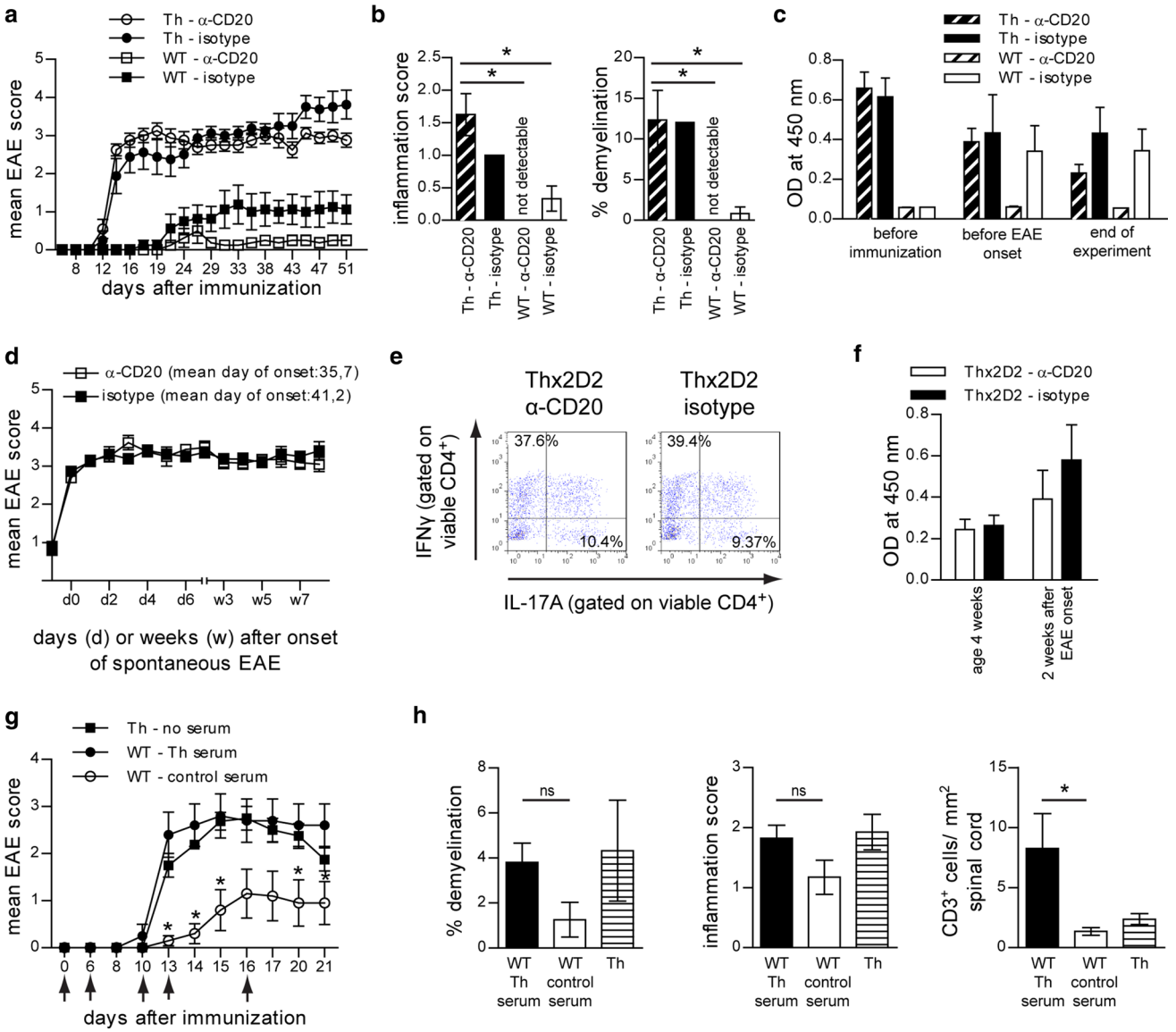

Fig. 1 B cells are not required for fulminant induced EAE in Th mice nor for spontaneous EAE in Thx2D2. **a–c** Th or WT mice were treated weekly with anti (α)-CD20 or isotype control Ab starting 3 weeks prior to immunization with mMOG. **a** Mean group EAE score ± SEM; $n = 10$ mice/group; * = $p < 0.05$ (Mann–Whitney; data represent five independent experiments). **b** CNS inflammatory damage at day 48 after immunization. Indicated is the mean group score ± SEM of spinal cord inflammation (H&E; *left*), determined as: 0 = no inflammation, 1 = slight inflammation. 2 = moderate inflammation, 3 = strong inflammation and the mean % ± SEM of demyelinated spinal cord area per group (LFB/PAS; right); $n = 3$–4 mice/group; * = $p < 0.05$ (Mann–Whitney). **c** Anti-mMOG IgG Ab serum levels determined by ELISA (dilution 1:40,500); $n = 10$ mice/group. **d–f** Thx2D2 mice were treated weekly with anti (α)-CD20 or isotype control Ab starting 28 days after birth. **d** Mean group score and mean day of onset of spontaneous EAE in anti (α)-CD20 ($n = 18$) and isotype Ab treated mice ($n = 22$) ± SEM; p = ns (Mann–Whitney). **e** Frequency of IFN-γ and IL-17A producing T cells isolated from the CNS at the end of experiment. **f** Anti-mMOG IgG Ab determined by ELISA (serum dilution 1:13,500); $n = 6$–16 mice/group. **g**, **h** EAE was induced in WT mice by immunization with MOG p35-55. *Arrows* indicate i.v. injections of serum containing pathogenic anti-mMOG Ab (Th serum) or non-pathogenic Ab (control serum). Immunized Th mice not receiving any serum, served as positive control. **g** Mean group EAE score ± SEM; $n = 8$–10 mice/group; * = $p < 0.05$ (WT Th serum recipients vs. WT control; Mann–Whitney; data represent three independent experiments). **h** CNS inflammatory damage at day 25 after immunization. Indicated is the mean % ± SEM of demyelinated spinal cord white matter area per group (LFB/PAS; *left*), the mean group score ± SEM of inflammation (H&E; *middle*), determined as follows: 0 = no inflammation, 1 = slight inflammation. 2 = moderate inflammation, 3 = strong inflammation and the number of T cells/mm^2 spinal cord ± SEM per group determined by CD3$^+$ immunostaining (*right*); $n = 4$ mice/group; * = $p < 0.05$ (Mann–Whitney)

mice, these findings fueled our hypothesis that in lieu of antigen-specific B cells, anti-MOG Ab may be capable of triggering activation and expansion of myelin-reactive T cells in a manner sufficient to cause EAE. To test this hypothesis, we transferred serum from Th mice or purified 8.18C5 Ab into otherwise naïve 2D2 recipients, which contain MOG-specific T cells but no transgenic B cells (Fig. 2a). Strikingly, five out of fourteen 2D2 mice receiving Th serum developed classical EAE with ascending paralysis, one mouse developed atypical EAE with severe ataxia (Table 1). Histologic analysis confirmed that all EAE-diseased Th serum recipients showed extensive CNS demyelination, inflammation and infiltration by $CD3^+$ T cells (Fig. 2b), while none of the twelve 2D2 mice receiving control serum showed signs of clinical or histological EAE. To confirm that myelin-reactive Ab and not any other serum component had triggered EAE, we next transferred 150 µg of purified 8.18C5 Ab, the amount equivalent to its content in 150 µl Th serum. As indicated in Fig. 2c, 2D2 mice receiving a total of 10 injections showed a rapid increase in anti-MOG Ab, comparable to the level observed in Thx2D2 mice with spontaneous EAE (gray area). Again, thirteen out of twenty-three 8.18C5 Ab recipients, but none of the seventeen 2D2 mice receiving control Ab, developed severe clinical or histologic EAE (Table 1; Fig. 2d). When evaluated by the more sensitive elevated beam test, 8.18C5 Ab recipients without paralysis yet showed a significant decline in their agility (Table 1; Fig. 2e). CNS damage was quantified in all 8.18C5 Ab-transferred 2D2 mice, which revealed a pronounced inflammation and CNS infiltration by both B and T cells in the majority of these mice, while extensive demyelination was restricted to the paralyzed subgroup (Fig. 2f + g). Here, all histologic parameters were in their extent comparable to Thx2D2 mice with spontaneous fulminant EAE, while in some cases, the degree of infiltration by highly activated $MAC3^+$ macrophages even exceeded the level in diseased Thx2D2 mice. To investigate in which sequence peripherally applied anti-MOG Ab, MOG-reactive T cells and activated myeloid APC may have triggered EAE, we transferred anti-MOG Ab into naïve WT mice (Suppl. Figure 2a). Recipients showed no signs of paralysis, impaired agility or, importantly, CNS demyelination (Suppl. Table 1; Suppl. Figure 2b + c), suggesting that in the absence of ongoing CNS inflammation, myelin within the CNS is not recognized by peripherally applied myelin-reactive Ab. Alternatively, myelin-reactive Ab could have triggered activation of peripheral myelin-reactive T cells prior to CNS entry. To investigate this hypothesis, we evaluated proliferation of T cells in lymph nodes and spleen of healthy, naïve 2D2 mice after peripheral injection of 8.18C5 Ab and co-administration of mMOG protein intrathecally (Fig. 3a; Suppl. Figure 3a + c). As shown in Fig. 3b–d, 8.18C5 Ab triggered in vivo expansion of $CD4^+$ T cells in spleen, inguinal and cervical lymph nodes 4 days after mMOG injection and 6 days after the initial administration of 8.18C5 Ab. While at this early time point only a trend toward an enhanced Th17 differentiation could be observed, administration of 8.18C5 Ab lead to a distinct upregulation of the early activation marker CD69 on $CD4^+$ T cells (Fig. 3e). Further, co-administration of 8.18C5 Ab and mMOG was associated with a concomitant upregulation of MHC class II and an enhanced release of IL-1α by $CD11b^+$ myeloid APC (Fig. 3f). To a lesser extent, T cell proliferation and activation of myeloid APC were also observed in 2D2 mice receiving control Ab, which may be reflective of endogenous anti-MOG Ab development in these mice when MOG is administered intrathecally. Irrespectively, 8.18C5 Ab-mediated in vivo activation and proliferation of T cells as well as activation of myeloid APC could be completely abolished by addition of an in vivo Fc-blocking Ab (Suppl. Figure 3b; Fig. 3b–f). In conjunction, these findings indicate that myelin-specific Ab trigger activation of peripheral myelin-specific T cells and highlight Fc-mediated opsonization of antigen as most plausible mechanism.

Anti-MOG antibodies promote low dose recognition of MOG by myeloid antigen-presenting cells permitting activation of MOG-reactive T cells

Activation of $CD4^+$ T cells requires antigen presentation in the context of MHC class II. Prior to its presentation, antigen must be taken up and presented by the immune system, which, particularly at low concentrations, can be facilitated by specific binding to B cells [9, 17, 38] or Ab [22, 31]. In the latter case, Ab-decoration triggers Fc receptor-mediated internalization and processing of the antigen by APC [49], followed by its presentation to adaptive immune cells. This mechanism of Ab-mediated antigen opsonization is believed to be central for instance in development of systemic lupus erythematosus (SLE) [15]. To investigate whether in our setting, MOG-specific Ab may have triggered in vivo activation of myelin-specific T cells [35] by opsonization of rare CNS auto-antigen, we developed an in vitro setting capable of dissecting the respective components; we generated BMDM or BMDC from WT mice expressing high levels of Fc receptors or from knockout mice lacking Fcγ receptors ($Fc\gamma R^{-/-}$) (Fig. 4a + b). Further, we digested the 8.18C5 Ab to obtain an antigen-recognizing, but Fc-cleaved $F(ab')_2$ fragment (Fig. 4c; Suppl. Figure 4a + b). Using these tools, we demonstrated that intact 8.18C5 Ab strongly promoted recognition and internalization of fluorescence-labeled mMOG by either BMDC or BMDM (Fig. 4d + e, left). This effect strictly depended

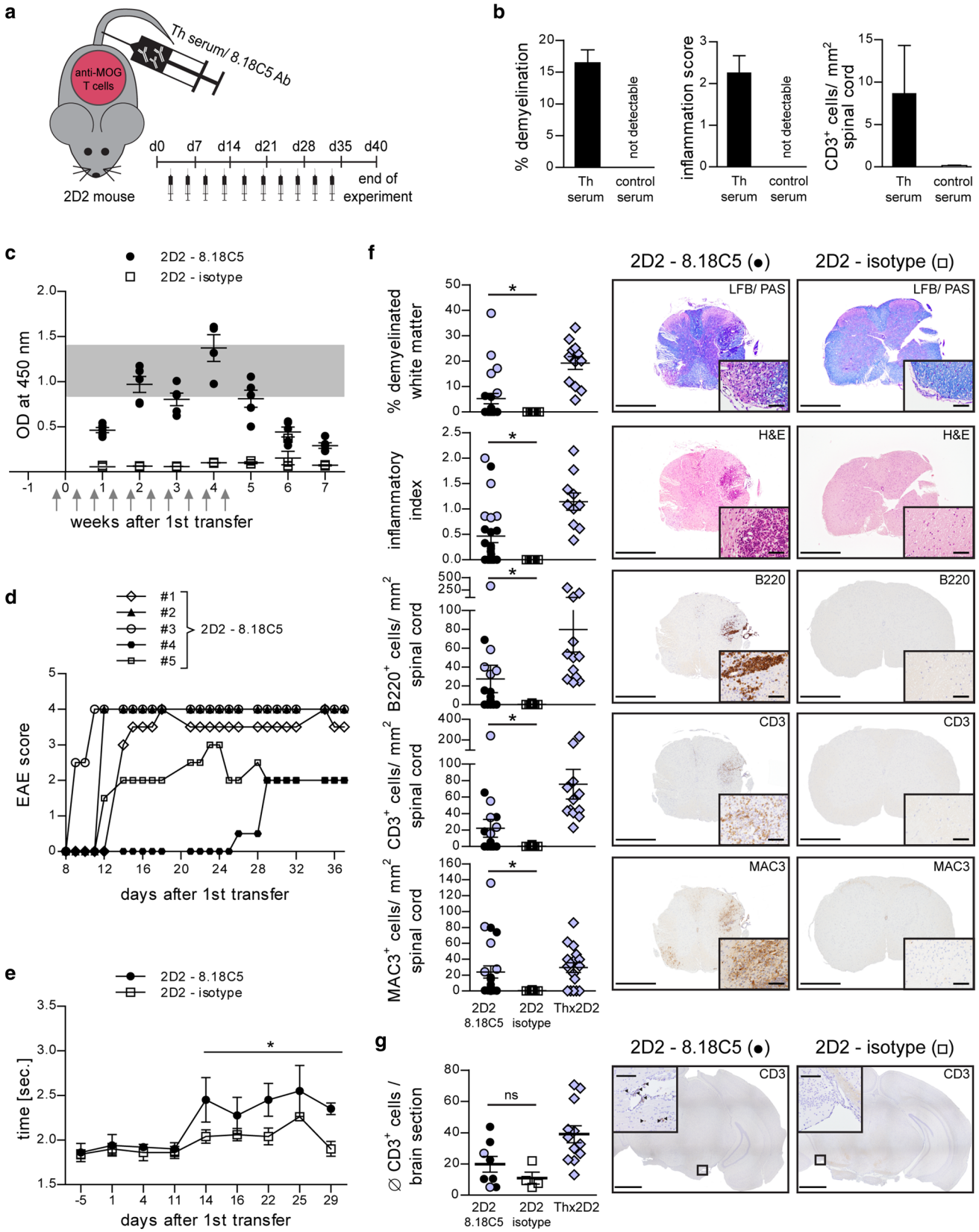
a
Th serum/ 8.18C5 Ab
anti-MOG T cells
2D2 mouse
d0 d7 d14 d21 d28 d35 d40
end of experiment
b
% demyelination
not detectable
Th serum
control serum
inflammation score
not detectable
Th serum
control serum
CD3+ cells/ mm2 spinal cord
Th serum
control serum
c
2D2 - 8.18C5
2D2 - isotype
OD at 450 nm
weeks after 1st transfer
d
#1
#2
#3
#4
#5
2D2 - 8.18C5
EAE score
days after 1st transfer
e
2D2 - 8.18C5
2D2 - isotype
time [sec.]
days after 1st transfer
f
2D2 - 8.18C5 (●)
2D2 - isotype (□)
% demyelinated white matter
inflammatory index
B220+ cells/ mm2 spinal cord
CD3+ cells/ mm2 spinal cord
MAC3+ cells/ mm2 spinal cord
LFB/ PAS
H&E
B220
CD3
MAC3
2D2 8.18C5
2D2 isotype
Thx2D2
g
2D2 - 8.18C5 (●)
2D2 - isotype (□)
∅ CD3+ cells / brain section
ns
CD3
2D2 8.18C5
2D2 isotype
Thx2D2

◀ **Fig. 2** Transfer of anti-mMOG Ab containing serum or purified anti-mMOG Ab triggers spontaneous EAE in 2D2 recipients. **a** Overview of experimental setup. **b** Naïve 2D2 mice received i.v. injections of Th serum or control serum. CNS inflammatory damage determined at day 18 after EAE onset. Indicated is the mean % ± SEM of demyelinated spinal cord area per group (LFB/PAS; *left*), the mean group score ± SEM of spinal cord inflammation (H&E; *middle*), determined as follows: 0 = no inflammation, 1 = slight inflammation. 2 = moderate inflammation, 3 = strong inflammation and the number of T cells/mm^2 spinal cord ± SEM per group determined by CD3$^+$ immunostaining (*right*); $n = 2$ mice/group. **c**–**g** Naïve 2D2 mice received i.v. injections of 8.18C5 or isotype control Ab. **c** Anti-mMOG Ab serum levels in recipients determined by ELISA (dilution 1:13,500). *Arrows* indicate injections of 8.18C5 or isotype control Ab. *Gray area* represents the range of anti-mMOG Ab predetermined in spontaneously EAE-diseased Thx2D2 mice; $n = 5$ mice/group. **d** Individual EAE courses of 2D2 mice receiving 8.18C5 Ab. **e** Elevated beam test of 2D2 mice receiving 8.18C5 or isotype control Ab. Indicated is the mean time in seconds (sec.) per group ± SEM required to traverse the beam; $n = 4$–5 mice/group; * = $p < 0.05$ (Mann–Whitney). **f** Demyelination (LFB/PAS), overall inflammation (H&E) and immune cell infiltration of the spinal cord evaluated by CD3-, B220- and MAC3-immunohistochemistry 40 days after first Ab transfer. Representative sections (*right*) and group mean % ± SEM of demyelinated white matter area, number of inflammatory spots per spinal cord section (inflammatory index) and of infiltrating immune cells/mm^2 spinal cord (*left*). Mice with paralysis in *purple*; for comparison, Thx2D2 mice with EAE are depicted. *Scale bar* overview = 500 µm, *scale bar* inlay = 50 µm; $n = 12$–23 mice/group; * = $p < 0.05$ (Mann–Whitney). **g** CD3 immunostaining of T cells in the brain at day 40 after first transfer. Representative sections (*right*) and absolute number of infiltrating T cells/section (*left*). Mice with paralysis in purple; for comparison Thx2D2 mice with EAE are depicted. *Scale bar* overview = 1000 µm, *scale bar* inlay = 100 µm; $n = 4$–12 mice/group; p = ns (Mann–Whitney)

on cellular expression of Fcγ receptors (Fig. 4e, right); along the same lines, the Fc-cleaved 8.18C5 F(ab′)$_2$ fragment failed to enhance internalization and rather neutralized antigen recognition (Fig. 4f). Of interest, Ab-mediated opsonization similarly occurred when the random control antigen OVA was used in combination with anti-OVA Ab (Fig. 4g), corroborating that Ab opsonize any fitting antigen.

To understand the downstream immunological consequences of Ab-mediated antigen opsonization we co-cultured WT BMDM with naïve 2D2 T cells, again in the presence of mMOG. In line with our in vivo findings, addition of 8.18C5 Ab specifically accelerated T cell proliferation and differentiation into encephalitogenic T cells, while blockade of Fcγ receptors on APC reversed this effect (Fig. 5a–c; Suppl. Figure 4c). Along the same lines, the 8.18C5 F(ab′)$_2$ fragment again failed to enhance internalization and subsequent presentation of mMOG to myelin-specific T cells (Fig. 5d). In summary, these results indicate that in development of CNS autoimmune disease, systemic auto-Ab facilitate APC recognition of otherwise undetected CNS antigen, resulting in activation, pro-inflammatory differentiation and CNS infiltration of autoreactive T cells.

Table 1 Summary of clinical and histological results upon transfer of anti-MOG Ab containing serum or of purified anti-mMOG Ab into naïve 2D2 mice

	Animals with histological or clinical signs of EAE				Animals with impaired agility[a]
	Number of animals with CNS inflammation	Number of animals with clinical symptoms	Mean max. EAE severity (range)	Onset of EAE; mean days after 1st serum/Ab transfer (range)	Number of mice with ≥25 % deterioration in agility testing; measured by increase in time
2D2—Th serum	6/14	6/14	3.1 (2.5–3.5)	12.8 (5–24)	n.a.
2D2—control serum	0/12	0/12	n.a.	n.a.	n.a.
2D2—8.18C5	13/23	5/23	3.4 (2.0–4.0)	14.2 (9–26)	6/8
2D2—isotype control	0/17	0/17	n.a.	n.a.	2/9

[a] Only mice without signs of classical EAE (paralysis) tested

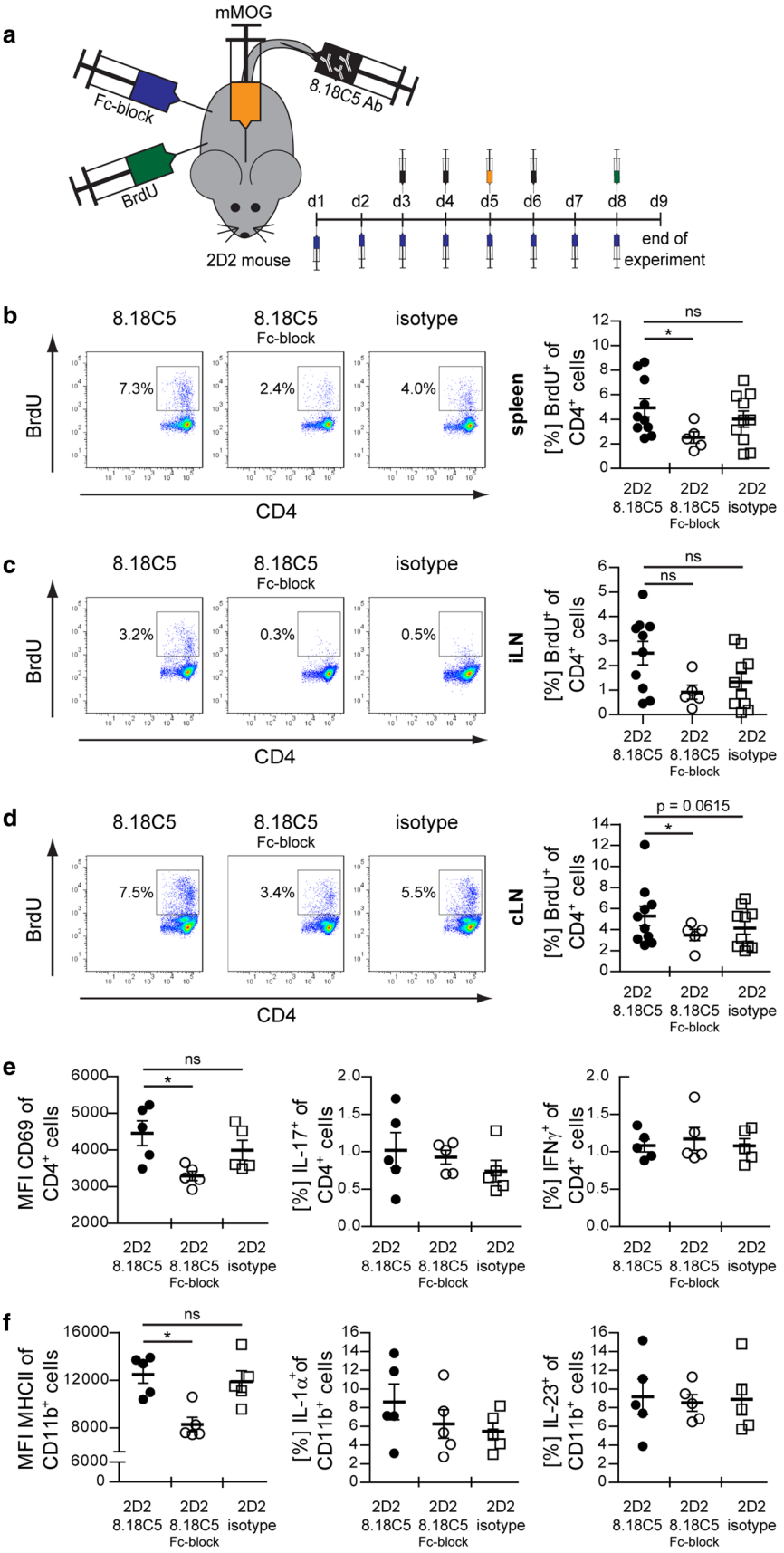

Fig. 3 Transfer of anti-mMOG Ab into 2D2 mice triggers in vivo activation and expansion of peripheral myelin-reactive T cells in an Fc-dependent manner. **a** Overview of experimental setup. **a–f** Naïve 2D2 mice were treated daily with Fc receptor blocking anti-CD16/CD32 or control Ab i.p. during the entire experiment. Starting at day (d)3, mice received three consecutive i.v. injections of 8.18C5 or control Ab. mMOG was injected intrathecally at d5. 24 h before evaluation, mice received BrdU i.p. (d8). In vivo proliferation of $CD4^+$ T cells (pre-gated on viable $CD4^+$ cells) analyzed by BrdU uptake in **b** spleen, **c** inguinal lymph nodes (iLN) and **d** cervical lymph nodes (cLN). **b–d** Representative FACS plots (*left*) and frequency of $BrdU^+$ $CD4^+$ cells in % ± SEM (*right*); $n = 5$–10 mice/group; $* = p < 0.05$ (*t* test). **e** Expression of CD69 (mean fluorescence intensity; MFI) and % of IL-17A and IFN-γ producing $CD4^+$ cells ± SEM isolated from cLN (pre-gated on intact cells). **f** Expression of MHC class II (MHCII; MFI) and % of IL-1α and IL-23 producing $CD11b^+$ cells ± SEM isolated from cLN (pre-gated on intact cells)

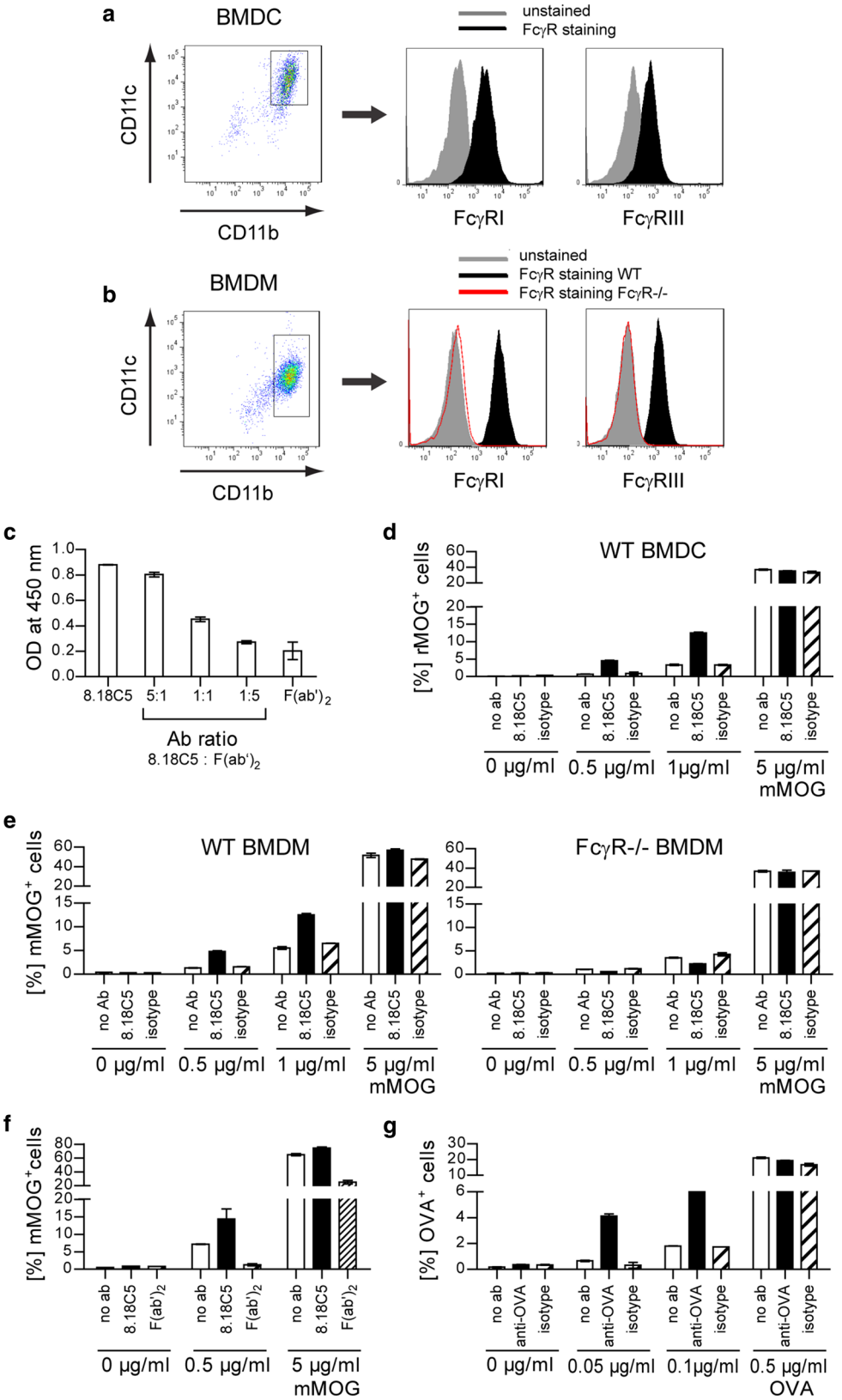

Fig. 4 Opsonization of conformational mMOG by anti-mMOG Ab fosters Fc-mediated antigen uptake. Mean expression of Fcγ receptor (FcγR)I and FcγRIII by **a** WT BMDC and **b** WT or FcγR$^{-/-}$ BMDM. **c** Competitive binding of 8.18C5 F(ab′)$_2$ and intact 8.18C5 Ab at various ratios to mMOG; plate-bound Ab detected by anti-mouse IgG Ab against the Fc part. **d–f** Phagocytosis of mMOG-DyLight-405 by APC. APC were incubated with mMOG-DyLight-405 in the presence of 8.18C5, or isotype control Ab (mean % of mMOG-DyLight-405 positive (mMOG$^+$) APC ± SEM, gated on intact CD11b$^+$/CD11c$^+$ cells). **d** Phagocytosis of mMOG by WT BMDC. Representative data set shown; combined statistical analysis of two independent experiments: $p < 0.05$ for 8.18C5 vs. isotype Ab at 0.5 and 1 µg/ml mMOG (*t* test). **e** Phagocytosis of mMOG by WT (*left*) or FcγR$^{-/-}$ (*right*) BMDM. Representative data set shown; combined statistical analysis of two independent experiments: $p < 0.05$ for 8.18C5 vs. isotype control Ab at 0.5, 1 and 5 µg/ml mMOG of WT BMDM (*t* test). **f** Phagocytosis of mMOG by WT BMDM, additionally in the presence of 8.18C5 F(ab′)$_2$ fragments. Representative data set shown; combined statistical analysis of two independent experiments: $p < 0.05$ for 8.18C5 Ab vs. 8.18C5 F(ab′)$_2$ at 0.5 and 5 µg/ml mMOG (*t* test). **g** Phagocytosis of OVA-FITC by BMDM. BMDM were incubated with OVA-FITC in the presence of anti-OVA Ab or isotype control Ab (mean % of OVA-FITC positive (OVA$^+$) BMDM, gated on intact CD11b$^+$/CD11c$^+$ cells). Representative data set shown; combined statistical analysis of two independent experiments: $p < 0.05$ for anti-OVA vs. isotype control Ab at 0.05 and 0.1 µg/ml OVA (*t* test)

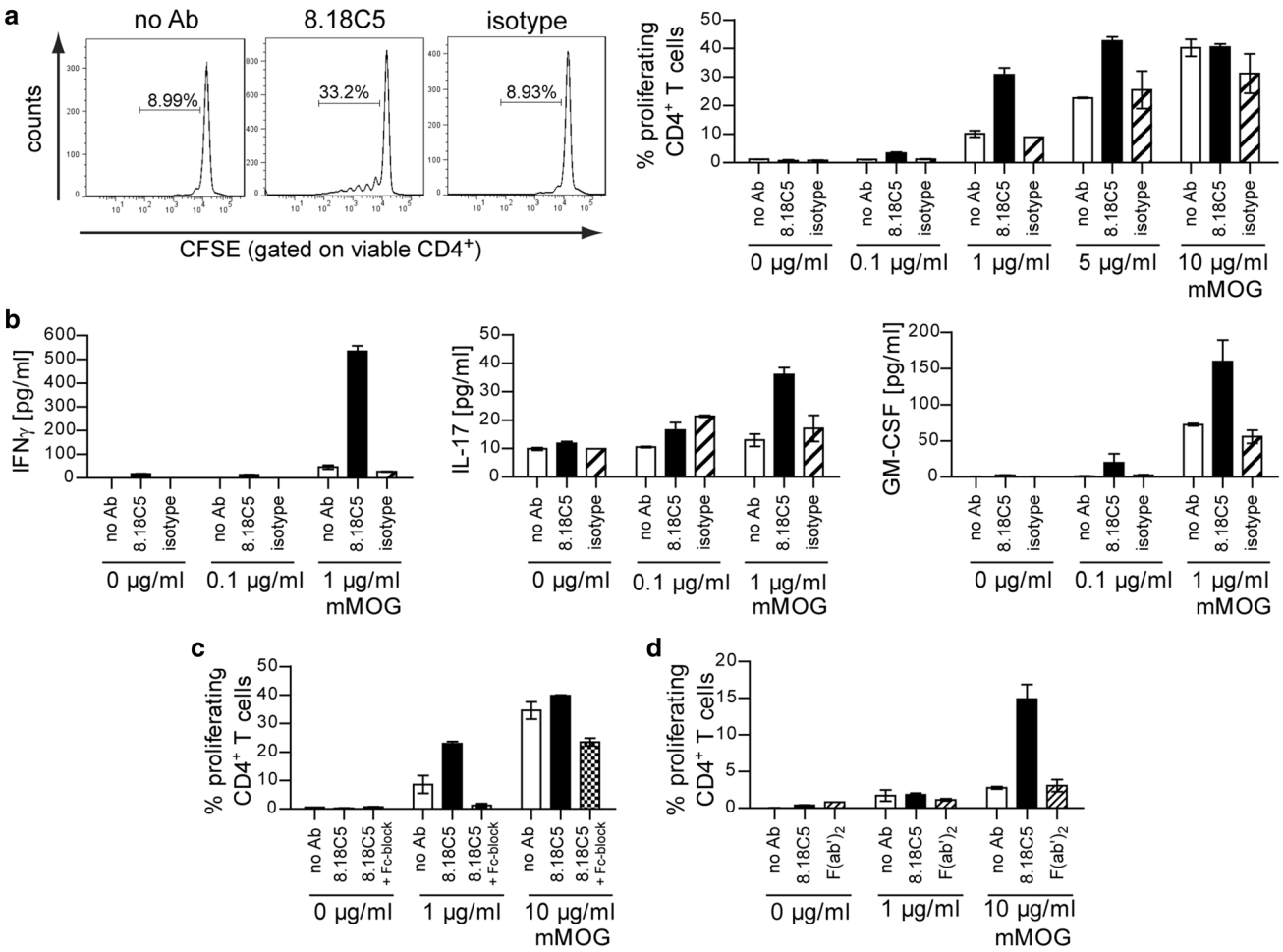

Fig. 5 Opsonization-triggered antigen uptake results in an increased capability of myeloid APC to generate encephalitogenic T cells. **a**–**d** WT BMDM co-cultured with CFSE-labeled MOG-specific 2D2 T cells in the presence of mMOG. **a** Proliferation of $CD4^+$ T cells in the presence of 8.18C5 or isotype control Ab determined by CFSE dilution (representative FACS plot, *left*; mean % of proliferating T cells in duplicates ± SEM, *right*). Representative data set shown; combined statistical analysis of four independent experiments: $p < 0.05$ for 8.18C5 vs. isotype control Ab at 0.1 µg/ml mMOG (*t* test). **b** Differentiation of naïve T cells into Th1-, Th17- or GM-CSF-producing T cells determined by production of IFN-γ, IL-17 or GM-CSF in the presence of 8.18C5 or isotype control Ab (duplicates ± SEM). **c** Proliferation of $CD4^+$ T cells in the presence of 8.18C5 Ab or a combination of 8.18C5 Ab and Fcγ receptor blocking anti-CD16/CD32 Ab (8.18C5 + Fc-block) determined by CFSE dilution (mean % of proliferating T cells in duplicates ± SEM). Representative data set shown; combined statistical analysis of two independent experiments: $p < 0.05$ for 8.18C5 Ab vs. 8.18C5 $F(ab')_2$ at 1 µg/ml mMOG and $p = 0.054$ at 10 µg/ml mMOG (*t* test). **d** Proliferation of $CD4^+$ T cells in the presence of 8.18C5 Ab or the 8.18C5 $F(ab')_2$ fragment determined by CFSE dilution (mean % of proliferating T cells in duplicates ± SEM)

Patient-derived anti-MOG antibodies mediate opsonization of human MOG protein

To exemplify that human IgG is capable of opsonizing human myelin protein, we next investigated IgG preparations obtained from two NMOSD patients with high titers of anti-MOG Ab determined in an established cell-based assay [30]. As a prerequisite to be tested in our in vitro assay, we first ensured that patient-derived anti-MOG Ab recognized soluble hMOG in vitro by a conventional ELISA (Fig. 6a). Applying the IgG preparations to our phagocytosis assay, we indeed observed that both anti-MOG Ab containing IgG preparations significantly enhanced the APC uptake of hMOG, when compared to an anti-MOG Ab negative IgG preparation obtained from a healthy individual (Fig. 6b). Ab-mediated opsonization could be largely reversed by addition of an Fc receptor blocking Ab (Fig. 6c), mechanistically corroborating that under these conditions human anti-MOG Ab facilitate APC uptake of human CNS antigen in an Fc-dependent manner.

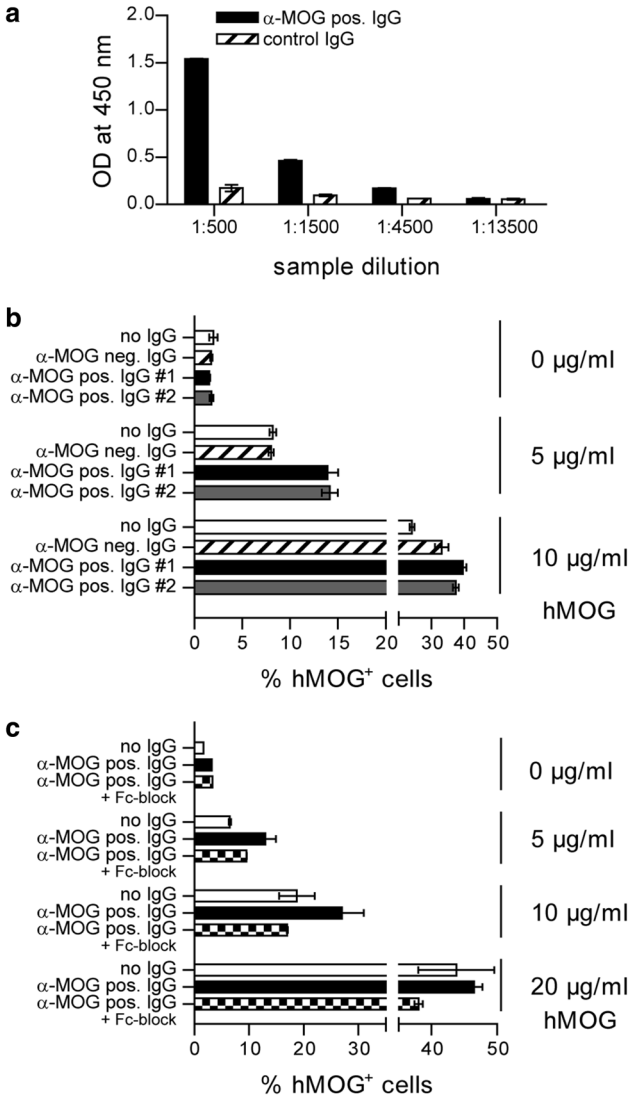

Fig. 6 IgG isolated from patients with NMOSD facilitate recognition of hMOG protein. **a** Detection of Ab against hMOG in a purified IgG fraction of a patient with NMOSD (α-MOG pos. IgG) by ELISA. Plate-bound Ab were detected with anti-human IgG Ab directed against the Fc part. For ELISA, intravenous IgG (control IgG) served as negative control. **b** Phagocytosis of hMOG-DyLight-405 by WT BMDM. Cells were incubated with hMOG-DyLight-405 in the presence of IgG samples from NMOSD patients containing anti-MOG Ab (α-MOG pos. IgG #1 and #2) or an anti (α)-MOG Ab negative (neg.) IgG preparation from a healthy individual (mean % of hMOG-DyLight-405 positive ($hMOG^+$) APC, gated on intact $CD11b^+/CD11c^+$ cells). Representative data set shown; $p < 0.05$ for α-MOG pos. IgG #1 vs. α-MOG neg. IgG and α-MOG pos. IgG #2 vs. α-MOG neg. IgG at 5 µg/ml hMOG (*t* test). **c** Phagocytosis of hMOG-DyLight-405 by WT BMDM. Cells were incubated with hMOG-DyLight-405 in the presence of anti-MOG positive IgG #2 or a combination of anti-MOG positive IgG #2 and Fcγ receptor blocking anti-CD16/CD32 Ab (8.18C5 + Fc-block; mean % of $hMOG^+$ APC, gated on intact $CD11b^+/CD11c^+$ cells)

Discussion

Antigen-specific B cells are increasingly recognized to act as important APC in models of human CNS demyelinating diseases. High affinity BCR binding of antigen triggers B cell activation and enables subsequent presentation of processed antigen to T cells. Thus, when B cells and T cells share antigen recognition, B cells are the dominant APC population and mere co-existence of antigen-specific B and T cells can prompt spontaneous CNS autoimmune disease [3, 21, 39]. A recent publication demonstrated that in this setting, spontaneous EAE can occur without the requirement of myelin-specific Ab [34]. Here, we investigated the inverse scenario, and report that in the absence of antigen-specific B cells, myelin-specific Ab in conjunction with T cells recognizing MOG suffice to trigger spontaneous EAE. At first sight, these two reports on the relevance of B cells versus myelin-specific Ab appear conflicting; upon closer view though, the link between both observations is specific recognition of endogenously rare antigen, which can be achieved by two distinct, yet related mechanisms: by binding to the BCR of B cells or alternatively to the corresponding Ab, which permits Fc-mediated antigen recognition by myeloid APC. Both mechanisms result in antigen uptake, processing and presentation by B cells or myeloid APC, respectively. This concept is supported by several mechanistic observations; in Thx2D2 mice, very low concentrations of mMOG added to a single cell suspension of purified splenocytes stimulated T cell proliferation [3, 21], while this effect was abolished when B cells were removed. Correspondingly, in our study, the addition of MOG-specific Ab enabled myeloid APC to recognize antigen at very low concentrations in an Fc-dependent manner and to activate co-cultured T cells. Antigen-specific B cells and antigen-specific Ab may thus independently contribute to the risk to develop CNS autoimmune disease, while the common element of disease initiation is specific recognition of rare CNS antigen subsequently boosting a disease-driving auto-reactive T cell response.

In line with this concept, we could show that anti-CD20 Ab-mediated depletion of myelin-specific B cells did not affect development of encephalitogenic T cells and failed to prevent or ameliorate EAE in the presence of endogenously produced myelin-specific Ab. Transfer of serum obtained from Th mice containing high levels of anti-MOG Ab exacerbated EAE in WT recipients in an extent indistinguishable from the fulminant course in Th mice containing both myelin-specific Ab and B cells. Furthermore, Th serum or purified anti-MOG Ab triggered spontaneous EAE in naïve 2D2 recipients. In conjunction, these findings evidently

support a crucial role of myelin-specific Ab independent of myelin-specific B cells, which is further corroborated by the observation that in the absence of an immediate clinical benefit, Th mice receiving anti-CD20 Ab either in prevention or reversal showed a slight amelioration late in the chronic course of EAE, when levels of myelin-specific Ab declined (Fig. 1a + c; Suppl. Figure 1d). It is unclear and rightful to question whether in patients with MS, endogenous self-reactive Ab titers can reach corresponding functional relevance. Nevertheless, it could be important to recognize the general concept that Ab-mediated opsonization can functionally bypass antigen-specific B cells and that this alternative pathway of self-antigen recognition is not targeted and likely not affected by the soon to be approved MS treatment of anti-CD20 Ab. Accordingly, Ab-mediated antigen recognition by myeloid APC may become particularly important when antigen-specific B cells are extinguished, a notion to be kept in mind when individuals fail to respond to anti-CD20 Ab treatment [2, 7].

One central and widely unanswered question in the pathogenesis of CNS autoimmune disease remains where and how CNS antigens are initially recognized. In the absence of ongoing inflammation, the CNS is a well-protected, immune-privileged site and molecularly large Ab should not be capable of crossing the intact blood–brain barrier in a meaningful manner. Therefore, it is rather unlikely that peripherally administered myelin-reactive Ab can recognize and possibly degrade intact myelin within the otherwise healthy CNS. One of our control settings, in which anti-MOG Ab were transferred into naïve WT mice, consolidates this notion as despite intensive investigation, no CNS damage was observed. Alternatively, a plausible site of initial recognition of CNS antigen is cervical lymph nodes [10, 40], where vessels drain brain interstitial fluid [1, 28]. Supporting this concept, traces of myelin have been detected in CNS draining deep cervical lymph nodes of patients with MS [13]. A paralleling observation was reported in EAE-diseased mice [53], and surgical excision of cervical lymph nodes reduced relapse severity in chronic EAE [50]. To corroborate this possible path of CNS drainage we first injected 10 % Evans blue intrathecally and indeed retrieved the blue dye 1 h after its injection from cervical lymph nodes (suppl. Figure 3c). We next applied MOG protein intrathecally and in addition injected 8.18C5 Ab peripherally into healthy, naïve 2D2 recipients. Four days after MOG injection and 6 days after initial application of anti-MOG Ab, this regimen caused a marked in vivo expansion of $CD4^+$ T cells in lymph nodes and spleen of otherwise healthy mice. In conjunction, these data point toward peripheral lymphoid organs as the most plausible site where CNS-reactive Ab facilitated initial recognition of CNS-drained antigen, which subsequently triggered development of an encephalitogenic T cell response.

Using human IgG preparations in our in vitro setting was meant to exemplify that peripherally produced human anti-CNS Ab are generally capable of opsonizing human CNS antigen. To date, it remains unknown whether this effect occurs in patients with CNS demyelinating disorders in a functionally meaningful manner, although early development of anti-MOG Ab in MS [23] as well as the pronounced peripheral production of Ab against AQP-4 or MOG in NMO and NMOSD patients [20] highlights this possibility. Ab-decoration of auto-antigen is indeed known to occur in a variety of paraneoplastic disorders [44] and to enhance severity of systemic autoimmune conditions, such as SLE [42, 47]. In its pathogenesis, Ab directed against nuclear antigens are believed to opsonize apoptotic cells enhancing their uptake by dendritic cells [14], which in return may augment an autoimmune T cell response [15]. Further paralleling our findings in patients in an intriguing manner, serum from SLE patients specifically enhanced in vitro phagocytosis of apoptotic Jurkat cells by normal healthy donor macrophages [45]. The clinical relevance of this effect is further supported by the observation that the effectiveness of anti-CD20 Ab treatment negatively correlates with an expanded auto-Ab profile in patients with SLE [6]. Besides inducing or promoting autoimmunity, the general concept of Ab-mediated opsonization can also be applied therapeutically, when monoclonal Ab are used to alert the immune system to tumor cells enhancing cell-mediated cytotoxicity [43] as well as priming of an adaptive immune response [48]. Lastly, immunotherapy via Ab-mediated opsonization is currently pioneered to target pathological protein deposits in treatment of neurodegenerative disorders [5, 33]. In summary, Ab-mediated opsonization widely occurs in development and progression of systemic autoimmune conditions and is therapeutically harnessed to enhance clearance of potentially harmful antigen.

To date, the role of self-reactive Ab in MS has been primarily projected into enhancing CNS demyelination in ongoing acute disease flares [16], while in NMO, anti-AQP-4 Ab are believed to selectively target astrocytes, followed by severe secondary demyelination [29]. Our findings reported here extend this view and suggest that in addition, CNS-reactive Ab may be crucial for initiating and amplifying an adaptive autoimmune response to traces of otherwise unrecognized CNS auto-antigen. This novel concept has several important implications: first, while CNS-reactive Ab may initiate this chain of events, they require responding T cells to hereby cause harm. This may explain why myelin-specific Ab can also be found in controls and healthy volunteers, which do not develop CNS demyelination [23]. Second, in the context of MS, a serum auto-Ab response, particularly against MOG, widely occurs at early disease stages and in children with MS [11, 23]. In light of our new findings and opposite to our current understanding, this humoral response could be tremendously important for

initial activation of myelin-specific T cells as well as for development of first clinical relapses, when the availability of CNS auto-antigen is still limited. Third and most importantly, our data implicate that independent of current B cell-oriented therapeutic approaches, inhibiting or modulating the auto-reactive humoral response or interfering with its downstream signaling may be of enormous, vastly unrecognized therapeutic potential for prevention of early relapses and disease progression in MS, NMO and related disorders.

Acknowledgments We thank Veronika Husterer, Caroline Jaß, Jan Einar Albin, Katja Grondey and Julian Koch for excellent technical support. KLH is supported by a fellowship from the Deutsche Forschungsgemeinschaft (DFG; Le 3079/1-1). AS is supported by Marató de TV3 (20141830). CCAB is supported by grants from the National Health and Medical Research Council of Australia (APP1053621), and the Department of Industry, Commonwealth of Australia (AISRF06680). MSW is supported by grants from the National Multiple Sclerosis Society (NMSS; PP 1660), the DFG (WE 3547/4-1), and the ProFutura Programm of the Universitätsmedizin Göttingen.

References

1. Aspelund A, Antila S, Proulx ST, Karlsen TV, Karaman S, Detmar M, Wiig H, Alitalo K (2015) A dural lymphatic vascular system that drains brain interstitial fluid and macromolecules. J Exp Med 212:991–999. doi:10.1084/jem.20142290
2. Benedetti L, Franciotta D, Vigo T, Grandis M, Fiorina E, Ghiglione E, Roccatagliata L, Mancardi GL, Uccelli A, Schenone A (2007) Relapses after treatment with rituximab in a patient with multiple sclerosis and anti myelin-associated glycoprotein polyneuropathy. Arch Neurol 64:1531–1533. doi:10.1001/archneur.64.10.1531
3. Bettelli E, Baeten D, Jager A, Sobel RA, Kuchroo VK (2006) Myelin oligodendrocyte glycoprotein-specific T and B cells cooperate to induce a Devic-like disease in mice. J Clin Invest 116:2393–2402
4. Bettelli E, Pagany M, Weiner HL, Linington C, Sobel RA, Kuchroo VK (2003) Myelin oligodendrocyte glycoprotein-specific T cell receptor transgenic mice develop spontaneous autoimmune optic neuritis. J Exp Med 197:1073–1081
5. Boutajangout A, Ingadottir J, Davies P, Sigurdsson EM (2011) Passive immunization targeting pathological phospho-tau protein in a mouse model reduces functional decline and clears tau aggregates from the brain. J Neurochem 118:658–667. doi:10.1111/j.1471-4159.2011.07337.x
6. Cambridge G, Isenberg DA, Edwards JC, Leandro MJ, Migone TS, Teodorescu M, Stohl W (2008) B cell depletion therapy in systemic lupus erythematosus: relationships among serum B lymphocyte stimulator levels, autoantibody profile and clinical response. Ann Rheum Dis 67:1011–1016. doi:10.1136/ard.2007.079418
7. Capobianco M, Malucchi S, di Sapio A, Gilli F, Sala A, Bottero R, Marnetto F, Doriguzzi Bozzo C, Bertolotto A (2007) Variable responses to rituximab treatment in neuromyelitis optica (Devic's disease). Neurol Sci 28:209–211. doi:10.1007/s10072-007-0823-z
8. Clements CS, Reid HH, Beddoe T, Tynan FE, Perugini MA, Johns TG, Bernard CC, Rossjohn J (2003) The crystal structure of myelin oligodendrocyte glycoprotein, a key autoantigen in multiple sclerosis. Proc Natl Acad Sci USA 100:11059–11064
9. Constant S, Schweitzer N, West J, Ranney P, Bottomly K (1995) B lymphocytes can be competent antigen-presenting cells for priming CD4 + T cells to protein antigens in vivo. J Immunol 155:3734–3741
10. Cserr HF, Knopf PM (1992) Cervical lymphatics, the blood-brain barrier and the immunoreactivity of the brain: a new view. Immunol Today 13:507–512. doi:10.1016/0167-5699(92)90027-5
11. Di Pauli F, Mader S, Rostasy K, Schanda K, Bajer-Kornek B, Ehling R, Deisenhammer F, Reindl M, Berger T (2011) Temporal dynamics of anti-MOG antibodies in CNS demyelinating diseases. Clin Immunol 138:247–254. doi:10.1016/j.clim.2010.11.013
12. Duddy M, Niino M, Adatia F, Hebert S, Freedman M, Atkins H, Kim HJ, Bar-Or A (2007) Distinct effector cytokine profiles of memory and naive human B cell subsets and implication in multiple sclerosis. J Immunol 178:6092–6099
13. Fabriek BO, Zwemmer JN, Teunissen CE, Dijkstra CD, Polman CH, Laman JD, Castelijns JA (2005) In vivo detection of myelin proteins in cervical lymph nodes of MS patients using ultrasound-guided fine-needle aspiration cytology. J Neuroimmunol 161:190–194. doi:10.1016/j.jneuroim.2004.12.018
14. Fransen JH, van der Vlag J, Ruben J, Adema GJ, Berden JH, Hilbrands LB (2010) The role of dendritic cells in the pathogenesis of systemic lupus erythematosus. Arthritis Res Ther 12:207. doi:10.1186/ar2966
15. Frisoni L, McPhie L, Colonna L, Sriram U, Monestier M, Gallucci S, Caricchio R (2005) Nuclear autoantigen translocation and autoantibody opsonization lead to increased dendritic cell phagocytosis and presentation of nuclear antigens: a novel pathogenic pathway for autoimmunity? J Immunol 175:2692–2701
16. Genain CP, Cannella B, Hauser SL, Raine CS (1999) Identification of autoantibodies associated with myelin damage in multiple sclerosis. Nat Med 5:170–175
17. Harvey BP, Gee RJ, Haberman AM, Shlomchik MJ, Mamula MJ (2007) Antigen presentation and transfer between B cells and macrophages. Eur J Immunol 37:1739–1751. doi:10.1002/eji.200636452
18. Hauser SL, Waubant E, Arnold DL, Vollmer T, Antel J, Fox RJ, Bar-Or A, Panzara M, Sarkar N, Agarwal S et al (2008) B-cell depletion with rituximab in relapsing-remitting multiple sclerosis. N Engl J Med 358:676–688
19. Kappos L, Li D, Calabresi PA, O'Connor P, Bar-Or A, Barkhof F, Yin M, Leppert D, Glanzman R, Tinbergen J et al (2011) Ocrelizumab in relapsing-remitting multiple sclerosis: a phase 2, randomised, placebo-controlled, multicentre trial. Lancet. doi:10.1016/S0140-6736(11)61649-8
20. Kitley J, Waters P, Woodhall M, Leite MI, Murchison A, George J, Kuker W, Chandratre S, Vincent A, Palace J (2014) Neuromyelitis optica spectrum disorders with aquaporin-4 and myelin-oligodendrocyte glycoprotein antibodies: a comparative study. JAMA Neurol 71:276–283. doi:10.1001/jamaneurol.2013.5857
21. Krishnamoorthy G, Lassmann H, Wekerle H, Holz A (2006) Spontaneous opticospinal encephalomyelitis in a double-transgenic mouse model of autoimmune T cell/B cell cooperation. J Clin Invest 116:2385–2392
22. Kuhlmann T, Wendling U, Nolte C, Zipp F, Maruschak B, Stadelmann C, Siebert H, Bruck W (2002) Differential regulation of

myelin phagocytosis by macrophages/microglia, involvement of target myelin, Fc receptors and activation by intravenous immunoglobulins. J Neurosci Res 67:185–190
23. Lalive PH, Menge T, Delarasse C, Della Gaspera B, Pham-Dinh D, Villoslada P, von Budingen HC, Genain CP (2006) Antibodies to native myelin oligodendrocyte glycoprotein are serologic markers of early inflammation in multiple sclerosis. Proc Natl Acad Sci USA 103:2280–2285
24. Lehmann-Horn K, Kinzel S, Feldmann L, Radelfahr F, Hemmer B, Traffehn S, Bernard CC, Stadelmann C, Bruck W, Weber MS (2014) Intrathecal anti-CD20 efficiently depletes meningeal B cells in CNS autoimmunity. Ann Clin Transl Neurol 1:490–496. doi:10.1002/acn3.71
25. Li R, Rezk A, Miyazaki Y, Hilgenberg E, Touil H, Shen P, Moore CS, Michel L, Althekair F, Rajasekharan S et al (2015) Proinflammatory GM-CSF-producing B cells in multiple sclerosis and B cell depletion therapy. Sci Transl Med 7:310ra166. doi:10.1126/scitranslmed.aab4176
26. Linington C, Bradl M, Lassmann H, Brunner C, Vass K (1988) Augmentation of demyelination in rat acute allergic encephalomyelitis by circulating mouse monoclonal antibodies directed against a myelin/oligodendrocyte glycoprotein. Am J Pathol 130:443–454
27. Litzenburger T, Fassler R, Bauer J, Lassmann H, Linington C, Wekerle H, Iglesias A (1998) B lymphocytes producing demyelinating autoantibodies: development and function in gene-targeted transgenic mice. J Exp Med 188:169–180
28. Louveau A, Smirnov I, Keyes TJ, Eccles JD, Rouhani SJ, Peske JD, Derecki NC, Castle D, Mandell JW, Lee KS et al (2015) Structural and functional features of central nervous system lymphatic vessels. Nature. doi:10.1038/nature14432
29. Lucchinetti CF, Guo Y, Popescu BF, Fujihara K, Itoyama Y, Misu T (2014) The pathology of an autoimmune astrocytopathy: lessons learned from neuromyelitis optica. Brain Pathol 24:83–97. doi:10.1111/bpa.12099
30. Mader S, Gredler V, Schanda K, Rostasy K, Dujmovic I, Pfaller K, Lutterotti A, Jarius S, Di Pauli F, Kuenz B et al (2011) Complement activating antibodies to myelin oligodendrocyte glycoprotein in neuromyelitis optica and related disorders. J Neuroinflamm 8:184. doi:10.1186/1742-2094-8-184
31. Manca F, Fenoglio D, Li Pira G, Kunkl A, Celada F (1991) Effect of antigen/antibody ratio on macrophage uptake, processing, and presentation to T cells of antigen complexed with polyclonal antibodies. J Exp Med 173:37–48
32. Marta CB, Oliver AR, Sweet RA, Pfeiffer SE, Ruddle NH (2005) Pathogenic myelin oligodendrocyte glycoprotein antibodies recognize glycosylated epitopes and perturb oligodendrocyte physiology. Proc Natl Acad Sci USA 102:13992–13997
33. Menendez-Gonzalez M, Perez-Pinera P, Martinez-Rivera M, Muniz AL, Vega JA (2011) Immunotherapy for Alzheimer's disease: rational basis in ongoing clinical trials. Curr Pharm Des 17:508–520
34. Molnarfi N, Schulze-Topphoff U, Weber MS, Patarroyo JC, Prod'homme T, Varrin-Doyer M, Shetty A, Linington C, Slavin AJ, Hidalgo J et al (2013) MHC class II-dependent B cell APC function is required for induction of CNS autoimmunity independent of myelin-specific antibodies. J Exp Med 210:2921–2937. doi:10.1084/jem.20130699
35. Myers KJ, Sprent J, Dougherty JP, Ron Y (1992) Synergy between encephalitogenic T cells and myelin basic protein-specific antibodies in the induction of experimental autoimmune encephalomyelitis. J Neuroimmunol 41:1–8
36. Obermeier B, Mentele R, Malotka J, Kellermann J, Kumpfel T, Wekerle H, Lottspeich F, Hohlfeld R, Dornmair K (2008) Matching of oligoclonal immunoglobulin transcriptomes and proteomes of cerebrospinal fluid in multiple sclerosis. Nat Med 14:688–693. doi:10.1038/nm1714
37. Overdijk MB, Verploegen S, Ortiz Buijsse A, Vink T, Leusen JH, Bleeker WK, Parren PW (2012) Crosstalk between human IgG isotypes and murine effector cells. J Immunol 189:3430–3438. doi:10.4049/jimmunol.1200356
38. Parker Harp CR, Archambault AS, Sim J, Ferris ST, Mikesell RJ, Koni PA, Shimoda M, Linington C, Russell JH, Wu GF (2015) B cell antigen presentation is sufficient to drive neuroinflammation in an animal model of multiple sclerosis. J Immunol 194:5077–5084. doi:10.4049/jimmunol.1402236
39. Pollinger B, Krishnamoorthy G, Berer K, Lassmann H, Bosl MR, Dunn R, Domingues HS, Holz A, Kurschus FC, Wekerle H (2009) Spontaneous relapsing-remitting EAE in the SJL/J mouse: MOG-reactive transgenic T cells recruit endogenous MOG-specific B cells. J Exp Med 206:1303–1316
40. Prineas JW (1979) Multiple sclerosis: presence of lymphatic capillaries and lymphoid tissue in the brain and spinal cord. Science 203:1123–1125
41. Prineas JW, Connell F (1978) The fine structure of chronically active multiple sclerosis plaques. Neurology 28:68–75
42. Rahman A, Isenberg DA (2008) Systemic lupus erythematosus. N Engl J Med 358:929–939. doi:10.1056/NEJMra071297
43. Redman JM, Hill EM, AlDeghaither D, Weiner LM (2015) Mechanisms of action of therapeutic antibodies for cancer. Mol Immunol 67:28–45. doi:10.1016/j.molimm.2015.04.002
44. Rosenfeld MR, Dalmau J (2013) Diagnosis and management of paraneoplastic neurologic disorders. Curr Treat Options Oncol 14:528–538. doi:10.1007/s11864-013-0249-1
45. Sarmiento LF, Munoz LE, Chirinos P, Bianco NE, Zabaleta-Lanz ME (2007) Opsonization by anti-dsDNA antibodies of apoptotic cells in systemic lupus erythematosus. Autoimmunity 40:337–339. doi:10.1080/08916930701356663
46. Schluesener HJ, Sobel RA, Linington C, Weiner HL (1987) A monoclonal antibody against a myelin oligodendrocyte glycoprotein induces relapses and demyelination in central nervous system autoimmune disease. J Immunol 139:4016–4021
47. ter Borg EJ, Horst G, Hummel EJ, Limburg PC, Kallenberg CG (1990) Measurement of increases in anti-double-stranded DNA antibody levels as a predictor of disease exacerbation in systemic lupus erythematosus. A long-term, prospective study. Arthritis Rheum 33:634–643
48. Trivedi S, Jie HB, Ferris RL (2014) Tumor antigen-specific monoclonal antibodies and induction of T-cell immunity. Semin Oncol 41:678–684. doi:10.1053/j.seminoncol.2014.08.003
49. Trotter J, DeJong LJ, Smith ME (1986) Opsonization with antimyelin antibody increases the uptake and intracellular metabolism of myelin in inflammatory macrophages. J Neurochem 47:779–789
50. van Zwam M, Huizinga R, Heijmans N, van Meurs M, Wierenga-Wolf AF, Melief MJ, Hintzen RQ, tHart BA, Amor S, Boven LA et al (2009) Surgical excision of CNS-draining lymph nodes reduces relapse severity in chronic-relapsing experimental autoimmune encephalomyelitis. J Pathol 217:543–551. doi:10.1002/path.2476
51. von Budingen HC, Gulati M, Kuenzle S, Fischer K, Rupprecht TA, Goebels N (2010) Clonally expanded plasma cells in the cerebrospinal fluid of patients with central nervous system autoimmune demyelination produce "oligoclonal bands". J Neuroimmunol 218:134–139. doi:10.1016/j.jneuroim.2009.10.005
52. Weber MS, Prod'homme T, Patarroyo JC, Molnarfi N, Karnezis T, Lehmann-Horn K, Danilenko DM, Eastham-Anderson J, Slavin AJ, Linington C et al (2010) B-cell activation influences T-cell polarization and outcome of anti-CD20 B-cell depletion in central nervous system autoimmunity. Ann Neurol 68:369–383. doi:10.1002/ana.22081
53. Weller RO, Engelhardt B, Phillips MJ (1996) Lymphocyte targeting of the central nervous system: a review of afferent and efferent CNS-immune pathways. Brain Pathol 6:275–288

Supplemental material

Myelin-reactive antibodies initiate T cell-mediated CNS autoimmune disease by opsonization of endogenous antigen

Silke Kinzel[1*], Klaus Lehmann-Horn[2*], Sebastian Torke[1], Darius Häusler[1], Anne Winkler[1], Christine Stadelmann[1], Natalie Payne[3], Linda Feldmann[1], Albert Saiz[4], Markus Reindl[5], Patrice H. Lalive[6,7], Claude C. Bernard[3], Wolfgang Brück[1], Martin S. Weber[1,8]

[1]Department of Neuropathology, University Medical Center, Georg August University, Göttingen, Germany; [2]Department of Neurology, Klinikum rechts der Isar, Technische Universität München and Munich Cluster for Systems Neurology, Munich, Germany; [3]Monash Regenerative Medicine Institute, Multiple Sclerosis Research Group, Monash University, Melbourne, Australia; [4]Service of Neurology, Hospital Clinic, University of Barcelona, Barcelona, Spain; [5]Clinical Department of Neurology, Medical University of Innsbruck, Innsbruck, Austria; [6]Department of Clinical Neurosciences, Division of Neurology, University Hospital of Geneva, Geneva, Switzerland; [7]Department of Pathology and Immunology , Faculty of Medicine, University Hospital of Geneva, Geneva, Switzerland; [8]Department of Neurology, University Medical Center, Georg August University, Göttingen, Germany

* These authors contributed equally and are listed in alphabetical order

Address correspondence to:
Martin S. Weber, MD
Department of Neuropathology
Department of Neurology
University Medical Center, Georg August University
Robert-Koch-Str. 40, 37099 Göttingen, Germany
Phone +49-551 39-7706
Fax +49-551-39-10800
E-mail: martin.weber@med.uni-goettingen.de

Supplemental table 1 Summary of clinical and histological results upon transfer of purified anti-MOG Ab 8.18C5 or isotype control Ab into WT mice

	animals with histological or clinical signs of EAE			
	number of animals with CNS inflammation	number of animals with clinical symptoms	mean max. EAE severity (range)	onset of EAE; mean days after 1st serum/ ab transfer (range)
WT – 8.18C5	0/5	0/5	n.a.	n.a.
WT – isotype control	0/5	0/5	n.a.	n.a.

Supplemental Figure 1

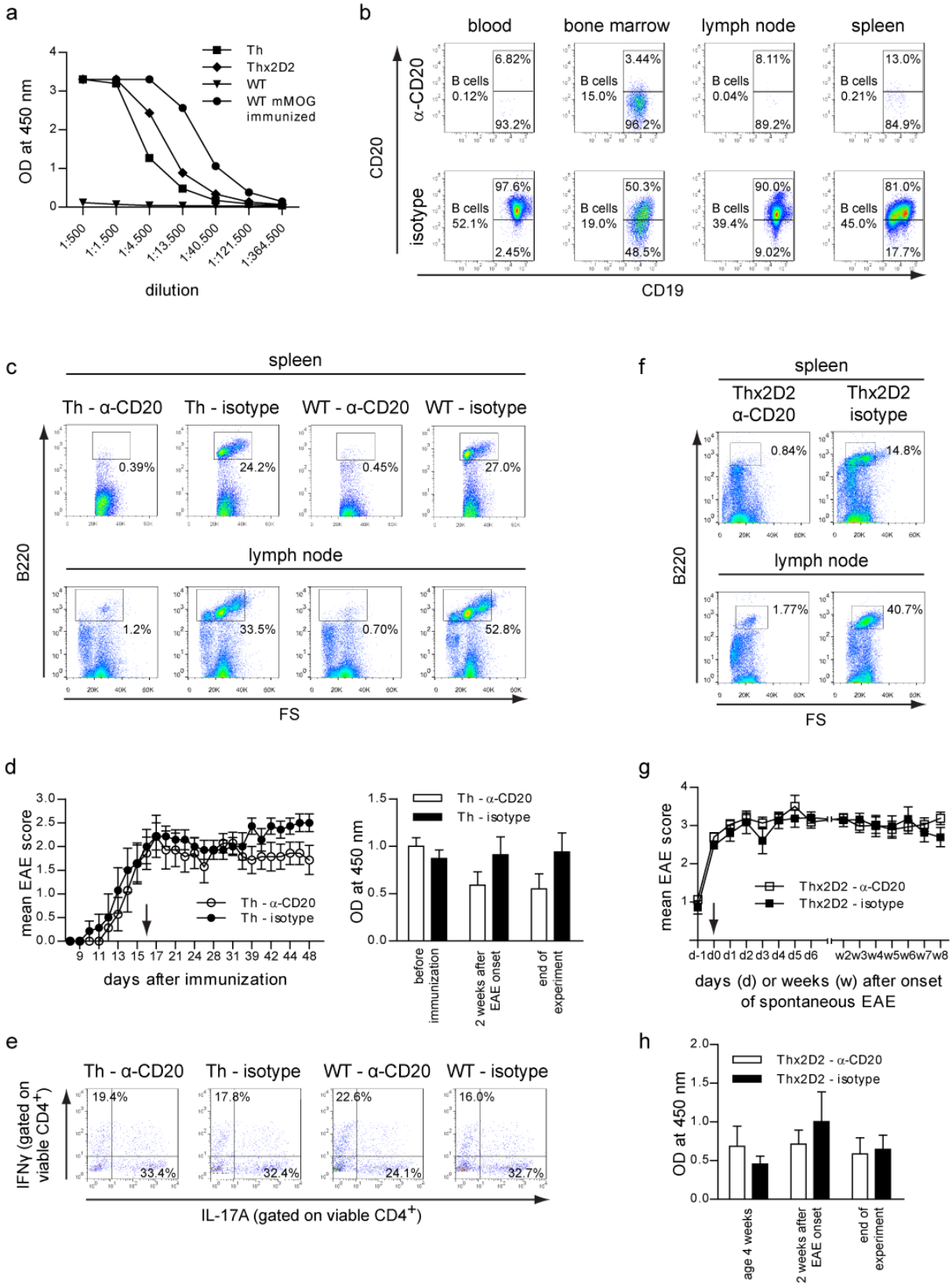

Suppl. Fig. 1 Depletion of B cells does not ameliorate established induced or spontaneous EAE when mMOG-specific Ab are present. **a** Detection of Ab against mMOG in Th, Thx2D2, WT and WT mice immunized with mMOG by ELISA at serial dilutions. **b** Frequency of $CD19^+$ B cells (left number) with corresponding CD20 expression in blood, bone marrow, lymph node and spleen of WT mice injected i.p. with anti (α)-CD20 or isotype control Ab once per week for 3 weeks. **c** Th or WT mice were injected with anti (α)-CD20 or isotype control Ab once per week, starting 3 weeks prior to immunization with mMOG. Frequency of $B220^+$ B cells in spleen (upper panel) and lymph node (lower panel) at the end of the experiment; n = 10 mice/group. **d** Th mice were immunized with mMOG and randomized to receive weekly anti-(α) CD20 or isotype control Ab at an EAE score $\geq$ 2. Initiation of anti-CD20 Ab treatment is depicted by arrow. Mean group EAE score ± SEM (left); p = ns (Mann-Whitney) and anti-mMOG IgG Ab serum levels determined by ELISA (dilution 1:40,500; right); n = 7 mice/group. **e** Th or WT mice were injected weekly with anti (α)-CD20 or isotype Ab starting 3 weeks prior to immunization with mMOG. Frequency of IFN-γ and IL-17A producing T cells isolated from the CNS at the end of the experiment; n = 10 mice/group. **f** Thx2D2 mice were injected weekly with anti (α)-CD20 or isotype control Ab starting 28 days after birth. Frequency of $B220^+$ B cells in spleen (upper panel) and lymph node (lower panel) at the end of the experiment. **g, h** Thx2D2 mice were randomized to receive weekly anti (α)-CD20 (n = 23) or isotype control Ab (n = 22) when spontaneous EAE was fully established (individual EAE score of $\geq$ 2). **g** Mean group EAE score ± SEM. Initiation of treatment is depicted by arrow; p = ns (Mann-Whitney). **h** Anti-mMOG IgG Ab serum levels determined by ELISA (dilution 1:13,500); p = ns (t test).

Supplemental Figure 2

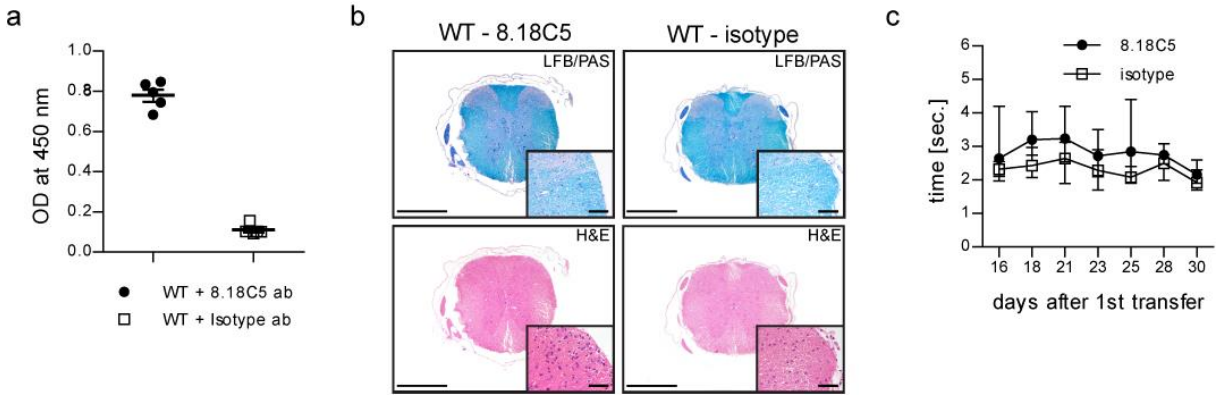

Suppl. Fig. 2 Transfer of anti-mMOG Ab containing serum or of purified anti-mMOG Ab triggers histologic EAE in 2D2 recipients, while WT recipients show no signs of CNS infiltration or demyelination. **a-c** Naïve WT mice were treated with 8.18C5 or isotype control Ab; *n* = 5 mice/group. **a** Anti-mMOG Ab serum levels determined by ELISA (dilution 1:13,500) at the end of the experiment. **b** Demyelination (LFB/PAS; upper panel) and overall inflammation (H&E; lower panel) of the spinal cord; one representative section of an 8.18C5 Ab-receiving vs. an isotype Ab-receiving animal is depicted. Scale bar overview = 500 µm, scale bar inlay = 50 µm. **c** Elevated beam test of WT mice receiving 8.18C5 or isotype control Ab. Indicated is the mean time in seconds (sec.) per group ± SEM required to traverse the beam; *p* = ns (Mann-Whitney).

Supplemental Figure 3

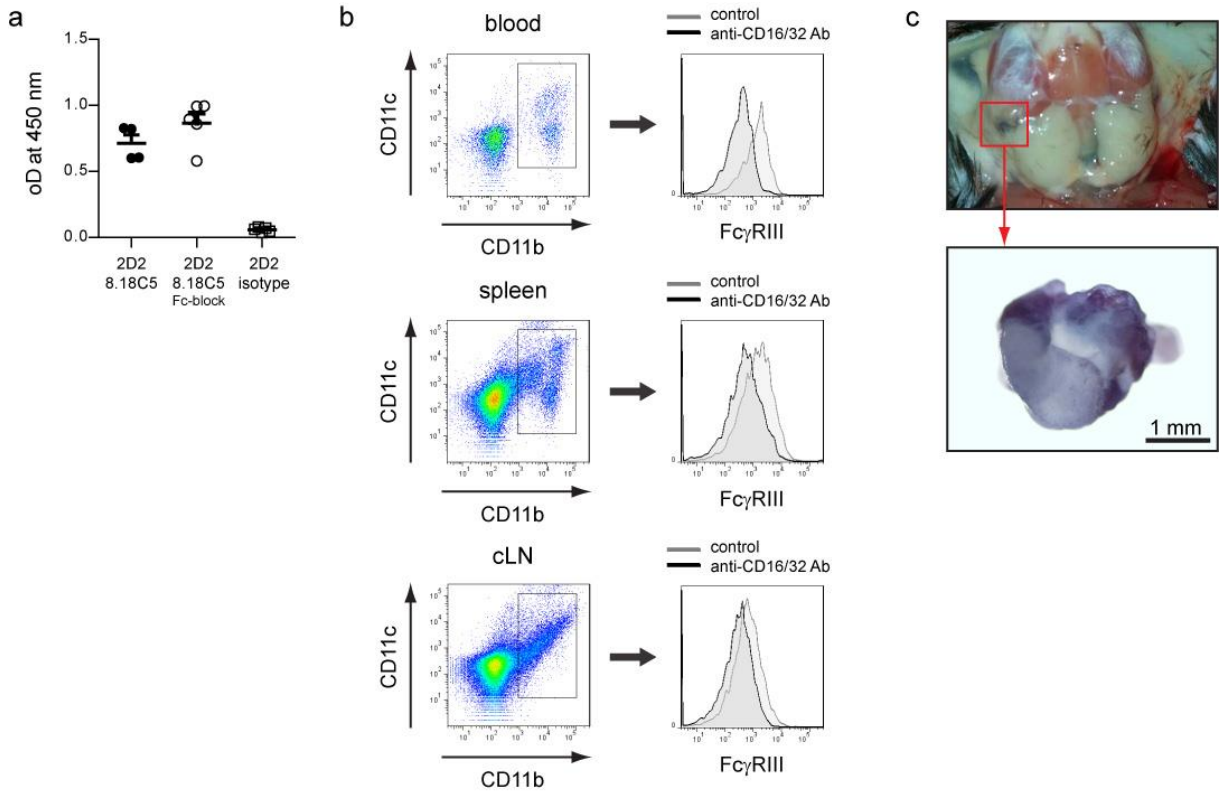

Suppl. Fig. 3 Drainage of intrathecally applied antigen and *in vivo* blockade of Fcγ receptor. **a** Naïve 2D2 mice were treated daily with Fc receptor blocking anti-CD16/CD32 or control Ab i.p. during the entire experiment. Starting at day (d)3, mice received three consecutive i.v. injections of 8.18C5 or control Ab. mMOG was injected intrathecally at d5. Anti-MOG Ab serum level was determined by ELISA (dilution 1:13,500) at the end of the experiment (d7). **b** Mice were treated three consecutive days with anti-CD16/CD32 Ab or control Ab. Representative FACS plots show the expression of Fcγ receptor III (right) on APC in blood, spleen and cervical lymph nodes (cLN). For analysis, cells were pre-gated on $CD11b^+/CD11c^+$ double positive cells (left); *n* = 3 mice/group. **c** Naïve WT mice were injected intrathecally with 10 µl of 10% Evans blue. Cervical lymph nodes were analyzed 1 hour after injection. The red square indicates the Evans blue-filled lymph node (upper picture); the lower picture shows the isolated lymph node in 40x magnification, scale bar =1 mm; *n* = 3.

Supplemental Figure 4

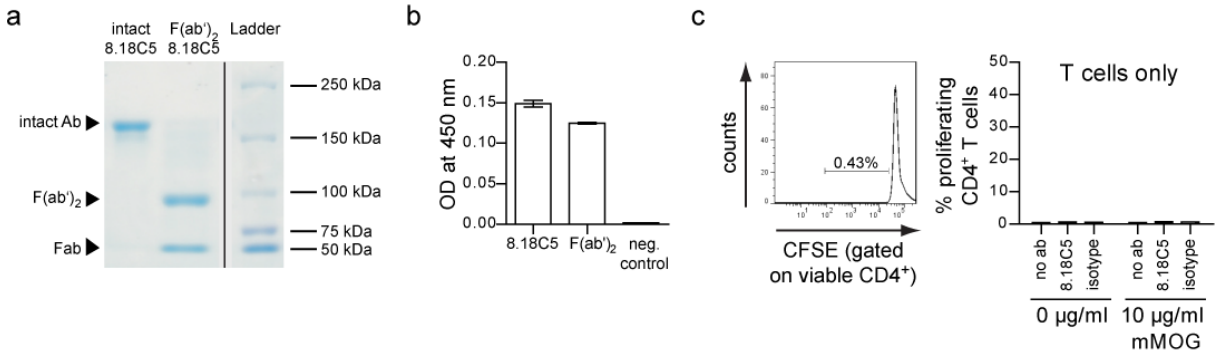

Suppl. Fig. 4 Functional analysis of 8.18C5 F(ab')$_2$ fragment and lack of a direct T cell stimulating effect of 8.18C5 Ab in the absence of APC. **a** 6% SDS-PAGE of intact 8.18C5 Ab (approx. 150 kDa) and its F(ab')$_2$ fragment (approx. 100 kDa) after digestion; an additional band at 50 kDa represents single Fab fragments. **b** mMOG ELISA of 8.18C5 F(ab')$_2$ fragments, intact 8.18C5 Ab and a negative control (unspecific Ab). Plate-bound Ab were detected with anti-mouse IgG Ab directed against the whole molecule. **c** CFSE-labeled MOG-specific 2D2 T cells cultured in the presence of mMOG and 8.18C5, or isotype control Ab. Proliferation of CD4$^+$ T cells determined by CFSE dilution (representative FACS plot, left; mean % of proliferating T cells in duplicates ± SEM, right).

Supplemental methods

Mice

MOG p35-55 TCR transgenic 2D2 mice were kindly provided by Dr. Kuchroo (Boston, USA). MOG Ig heavy chain knockin (Th) mice were kindly provided by Dr. Wekerle (Munich, Germany). WT C57BL/6 mice were purchased from Charles River (Sulzfeld, Germany). All murine experiments were carried out as approved by the government of Upper Bavaria (protocol number 55.2-1-54-2531-67-09) and the government of lower Saxony (protocol number 33.9-42502).

B cell depletion

B cell depletion was achieved by weekly i.p. injections of 200 µg of murine anti-CD20 or anti-ragweed isotype control Ab (both provided by Genentech, South San Francisco, USA) in 200 µl PBS.

Antigens and EAE induction regiments

Mouse MOG p35-55 (MEVGWYRSPFSRVVHLYRNGK) was synthesized by Auspep (Parkville, Australia). mMOG protein was kindly provided by C.C.A. Bernard and synthesized, purified and refolded as previously reported [4]. 8-10 week old female Th or WT mice were immunized subcutaneously with either a suboptimal dose of 35 µg/ml mMOG or an optimal dose of 50 µg/ml mMOG in CFA followed by 200 ng of pertussis toxin (Sigma-Aldrich, St. Louis, USA) i.p. at the day of immunization and 2 days thereafter. Alternatively, WT mice were immunized with 100 µg MOG p35-55 in CFA followed by two injections of 300 ng pertussis toxin. For spontaneous EAE experiments, Th mice were bred with 2D2 mice (Thx2D2). To induce EAE by transfer of MOG-specific Ab, a serum preperation containing anti-MOG Ab or mAb clone 8.18C5 were transferred into the tail vein of WT or 2D2 recipients. 150 µl Th serum

or control serum was injected twice a week up to a total of 5 injections; 150 µg 8.18C5 Ab or isotype control Ab (clone: MOPC-21, Bio X Cell, West Lebanon, USA) was injected twice a week up to a total of 10 injections. In recipients, no immunization or adjuvant treatment was added.

Evaluation of EAE

Mice were assessed for clinical signs of EAE as follows: 0 = no clinical disease, 1 = tail weakness, 2 = hind limb weakness, 3 = one paralyzed hind limb, 4 = two paralyzed hind limbs, 5 = moribund or dead. To evaluate balance and general motor function the elevated beam test was used. Therefore, mice were placed on a raised beam with a maximal height of 40 to 50 cm and a length of 100 cm. The time needed to traverse was measured. Mice were evaluated daily starting two weeks prior to the respective treatment.

Intrathecal injections

Mice were injected with 40 µg mMOG in 10 µl PBS or 10 µl of 10% Evans blue percutaneously into the cisterna magna with a 30-gauge needle in 45° anteflexion of the head.

Fc blocking in vivo

To block Fcγ receptors *in vivo*, mice were injected i.p. daily with 100 µg anti-CD16/CD32 Ab (Clone: 2.4G2, TONBO bioscience, San Diego, USA) in 100 µl 1xPBS starting two days prior to further treatments.

Generation of anti-MOG Ab containing serum

Serum containing high levels of pathogenic anti-MOG Ab or control serum was obtained from Th mice immunized with 100 µg mMOG (Th serum) or from WT mice immunized with 100 µg MOG p35-55 (control serum), respectively. 14 days after immunization, blood was obtained

by puncture of the left ventricle; serum was separated by centrifugation, pooled for further use and stored at -20°C.

Preparation and digestion of 8.18C5

Anti-MOG monoclonal Ab clone 8.18C5 was generated by hybridoma cells kindly provided by Dr. Christopher Linington. Hybridoma cells were cultured in complete medium (RPMI, 5-10% fetal calf serum, 50 U/ml penicillin, 50 µg/ml streptomycin, 2 mM L-glutamine, 1 mM sodium pyruvate, 0.05 mM β-mercaptoethanol) in large-scale flasks (Greiner bio-one, Kremsmuenster, Austria) and Ab was purified using rProtein A/Protein G Sepharose columns (rProtein A/Protein G GraviTrap, GE Healthcare, Little Chalfont, UK), according to manufacturer´s recommendations. 8.18C5 IgG was digested by ficin (Pierce Mouse IgG1 Fab and $F(ab')_2$ Preparation Kit, Thermo Scientific, Waltham, USA), according to manufacturer´s recommendations; integrity and binding capacity of 8.18C5 Ab and resulting 8.18C5 $F(ab')_2$ fragments was verified by 6% sodium dodecyl sulfate polyacrylamide gel electrophoresis (SDS-PAGE) under non-reducing conditions, followed by protein staining with Coomassie brilliant blue G250 (Biorad, Munich, Germany) and competitive anti-MOG enzyme linked immunosorbent assay (ELISA), respectively.

Assessment of T cell proliferation and differentiation in vitro

MACS-purified (Pan T cell Isolation Kit, Miltenyi, Bergisch Gladbach, Germany) CFSE-stained (CFSE Cell Division Tracker Kit, BioLegend, San Diego, USA) T cells from 2D2 mice were cultured with mMOG in the presence of 50 µg/ml 8.18C5 Ab, 8.18C5 $F(ab')_2$ fragment or isotype control Ab. 72 h thereafter, T cell proliferation and differentiation were evaluated by FACS.

Flow cytometric analysis

To obtain single cell suspensions of lymphoid tissues, respective spleens and lymph nodes were carefully dissected and passed through 70 µm strainer. Freshly obtained blood was mixed 1:2 with 1 mM EDTA and erythrocytes were lysed using BD Pharm Lyse Buffer, according to manufacturer's recommendation. B cells were stained for B220 (BioLegend) CD19 (BioLegend) and/or CD20 (BioLegend), T cells for CD3 and/or CD4 (all BD Bioscience). T cell differentiation was evaluated by intracellular cytokine staining for IFN-γ (eBioscience, San Diego, USA) and IL-17A (BD Bioscience) after 4-h incubation with PMA (50 ng/ml) and ionomycin (0.5 µg/ml) in the presence of monensin (1 µl Golgi-Stop per ml cell suspension, BD Bioscience). Dead cells were excluded using an Aqua Dead Cell Stain Kit (Invitrogen, Thermo Fisher Scientific, 405 nm excitation). CNS-infiltrating cells were isolated by discontinuous density gradient (Percoll) and stained in a similar manner [16] for CD3, CD4, IFN-γ and IL-17A. Myeloid APC were stained for CD11b and CD11c (both BioLegend). Expression of Fcγ receptor (FcγR) III was determined using anti-CD64 Ab (FcγRI, BioLegend).

ELISA for detection of MOG Ab

96-well plates were coated with 10 µg/ml conformational mMOG or conformational hMOG in 1xPBS overnight. Diluted samples were added for 2 h. After washing, plate-bound Ab of murine samples and 8.18C5 Ab were detected with HRP–conjugated anti-mouse IgG, directed against the Fc part of the bound Ab (1:6,000; Sigma-Aldrich) or against the whole molecule (1:5,000; Sigma-Aldrich).

Histology

Brain and spinal cord tissue was PBS-perfused and cryofixed or perfused and fixed with 4% paraformaldehyde and paraffin-embedded. To determine myelin loss and inflammatory infiltration, vertically- or horizontally-oriented sections were stained with Luxol Fast Blue and periodic acid Schiff (LFB/PAS) or hematoxylin and eosin (H&E), respectively.

Statistical analysis

EAE experiments were evaluated for significance using the Mann-Whitney test. The two-sided t test was used for all other statistical comparison. A value of $p < 0.05$ was considered significant. Data are presented as mean ± SEM.

5. Discussion

This thesis consists of three rather different projects with the common element only being focused on MS and its animal model of EAE. The first part focused on establishing inhibition of BTK as a novel therapeutic option. We analysed the effects on clinical disease severity and characterised the peripheral immune system. Additionally, we investigated the mechanism of action of the novel inhibitor evobrutinib. The second part investigated long-term high dose vitamin D supplementation. There we observed a clinical worsening which we traced back to a secondary hypercalcemia, exacerbating EAE by stimulating peripheral T cell function. The last part analysed the role of autoreactive antibodies in the initiation of disease. These antibodies were able to opsonize intrinsic antigens, activate myeloid cells via the Fc-receptor and thereby induce pro-inflammatory, antigen-specific T cells. The individual projects will be discussed separately on the following pages.

5.1. Inhibition of Bruton´s tyrosine kinase ameliorates CNS autoimmune disease by preventing B cell activation

Targeting B cells has proven to be a highly efficient way in reducing disease activity in MS patients (Greenfield and Hauser, 2018). However, current therapies mostly aim at long-term absence of activated B cells (Gelfand et al., 2017). One well studied approach is anti-CD20 pan-B cell depletion. CD20 is expressed on all B cells from the pre-B cell stage to the plasmablast stage. Therefore, the initial thought of using anti-CD20 to diminish antibody producing plasma cells proved to be incorrect (Häusler et al., 2018). Notwithstanding this, further investigations traced the tremendous success of anti-CD20 mediated pan B cell depletion to the abrogation of B cell APC function. However, since its broad expression, CD20 targeting depletion will also diminish regulatory functions of early B cells (Lehmann-Horn et al., 2013). Therefore, an alternative strategy of specifically targeting pathogenic B cell function while potentially maintaining their regulatory properties might prove equally efficient.

In this work we evaluated inhibition of BTK by the novel drug evobrutinib as a mono therapy in EAE and studied its mechanism of action. Evobrutinib was able to reduce clinical severity of B cell-mediated EAE as strongly as pan B cell depletion by anti-CD20. It diminished spinal cord demyelination and infiltration of immune cells into the CNS. While investigating the effects of evobrutinib on the peripheral immune system, we observed a change in the B cell phenotype. In the spleen, the cervical and inguinal lymph nodes as well as the blood, B cells were blocked from transitioning from a FO II to a FO I state. This particular differentiation is mediated by a strong BCR antigen and known to be a BTK-dependent step in the maturation (Cariappa et al., 2007). Additionally, we observed a reduction of activation markers on B cells and T cells. While the effect on B cells is presumably mediated by direct inhibition, our in vitro data points towards the reduction of T cell activation as a secondary event. Calcium mobilization is an early downstream event of both BCR and TCR signalling (Oh-hora and Rao, 2008). In B cells we described a strong inhibition of excitatory calcium influx by BCR stimulation after evobrutinib treatment equivalent to in vivo dosages. This inhibition had no effect on TCR-mediated calcium mobilization in T cells, pointing towards intact T cell capability in vivo. Most interestingly was the reduction of MHC class II expression on B cells, since this molecule mediates the presentation of antigen to T cells (Yuseff and Lennon-

Dumenil, 2013). Therefore, we investigated the APC function of B cells after evobrutinib treatment. In vitro we observed that evobrutinib diminished the ability of B cells to stimulate T cell proliferation and pro-inflammatory differentiation. Interestingly, evobrutinib increased the frequency of regulatory T cells. Since Th1 and Th17 cells mediate CNS disease (Domingues et al., 2010), the strong reduction in differentiation we observed in vitro could explain the clinical amelioration in vivo. Using quantitative PCR we showed that evobrutinib furthermore reduced the production of IFNγ after BCR stimulation. IFNγ is known to be a major driver of MHCII expression (Steimle et al., 1994). Reduced IFNγ would thereby lead to a reduction in MHCII expression and a diminished APC function of B cells. This would then translate into in indirect inhibition of T cell proliferation. Additionally, IFNγ expressing B cells have the ability to suppress the differentiation of naïve T cells to regulatory T cells (Olalekan et al., 2015). A reduction in B cell-derived IFNγ would thereby also mediate an increased Treg differentiation.

Lastly we investigated the expression and inducibility of BTK in B cells from healthy individuals and MS patients. We did not observe a difference in B cell frequencies or BTK expression. Interestingly, the inducibility of BTK phosphorylation increased with the maturation of B cells. However, we did not observe a difference between MS patients and healthy controls. The increased phosphorylation capacity of BTK in matured and class-switched B cells might hint that BTK inhibition would especially affect these cells. This potentially explains the observations of a recent phase II clinical study that reported clinical efficacy of evobrutinib as a mono therapy in MS, reducing new lesion formation and annual relapse rate (Montalban et al., 2019).

Additionally, evobrutinib has shown efficacy in other models of autoimmune disease. A near-complete inhibition of pre-clinical mouse models of rheumatoid arthritis (RA) and systemic lupus erythematodes (SLE) was reported, with reduced activation of B cells and auto-antibody production (Haselmayer et al., 2019). Additionally, Fc-receptor signalling was affected by BTK inhibition. In this thesis, we highlighted specific antibodies and Fc-receptor signalling as a novel way to induce CNS disease. Since BTK is centrally placed in BCR and FcR signalling, BTK inhibition would potentially block APC function on both B cells and myeloid cells (Weber et al., 2017).

Taken together we demonstrated that BTK inhibition is a promising new strategy of B cell targeting therapies in CNS autoimmunity. However, the question remains whether BTKi can rival pan B cell depletion in its effectiveness. Notwithstanding its tremendous success, there is currently no exit strategy for B cell depletion. Cessation of anti-CD20 therapy in EAE led to an increase in myelin-reactive, activated B cells (Häusler et al., 2018). Our results indicate, that BTKi might possess the potential to control the repopulation of B cells after an initial depletion. However, further investigations are needed to support that claim and position evobrutinib as a therapeutic option.

5.2. Continuous high dose vitamin D exacerbates central nervous system autoimmune disease by raising T cell excitatory calcium

Since a decreased concentration of vitamin D is often found in the serum of MS patients and MS incidence correlates with latitude and potentially thereby sun exposure, vitamin D is often supplemented in patients even without conclusive evidence of its benefit (Häusler and Weber, 2019). Although studies could show that addition of vitamin D to an ongoing interferon beta therapy reduced MRI activity, a sufficient vitamin D level is known to be necessary for the therapeutic benefit of IFN beta (Soilu-Hänninen et al., 2012; Waschbisch et al., 2014). This reduces the significance of these findings. In clinical practice, patients often receive a continuous supplementation without the necessary monitoring of serum vitamin D levels. The most extreme example might be the COIMBRA protocol, named after a Brazilian doctor who urges patients to unsupervised daily supplementation of up to 300.000 units of vitamin D (https://www.coimbraprotocol.com/the-protocol-1).

In this work we studied the effect of long term high-dose vitamin D supplementation as well as vitamin D deficiency and its effects on the clinical and histological outcome of EAE and the overall modulation of the peripheral immune system. We showed that not only vitamin D deficiency, but also elevated vitamin D serum levels led to increased clinical and histological EAE. In the periphery, myeloid cells and T cells showed an enhanced activation and T cell proliferation was accelerated. Previous studies investigating vitamin D supplementation reported a clinical benefit, even at higher doses (Cantorna et al., 1996; Lemire and Archer, 1991). However, these studies only investigated short term supplementation. Since it is

clinical practice to continuously supplement patients, we investigated the effect of long-term supplementation of high doses of vitamin D. We observed that long term high-dose vitamin D results in a secondary hypercalcemia in vivo, which was likely not the case in shorter therapy regiments. Investigating the effect on T cells in vitro, we observed that vitamin D and its metabolites inhibited T cell activation and proliferation. This confirms the long known activity of vitamin D as immune cell suppressing (Aranow, 2011). In addition, the effect strength was relatively increased on $CD8^+$ cells compared to $CD4^+$ cells, which differ in the expression of the vitamin D receptor (Veldman et al., 2000). However, raising calcium levels in vitro to the observed serum concentrations in vivo increased activation, proliferation and migration of T cells.

After elevating calcium independently of vitamin D in mice, we observed an upregulation of activation markers on T cells. These results indicate that in our setting, long-term high-dose vitamin D supplementation results in a secondary hypercalcemia which acts as a pro-inflammatory stimulus to T cells and overwrites the immune suppressing effect of vitamin D itself. This finding is supported by another study that injected the calcium-lowering hormone calcitonin and reported additive effects together with vitamin D therapy (Becklund et al., 2009). A T cell receptor stimulus promotes a calcium release from the endoplasmic reticulum and in a secondary step from the extracellular space (Oh-hora and Rao, 2008). Only the greater, secondary influx from the extracellular space is able to raise cellular and nuclear calcium levels over longer periods of time and promote activation and differentiation (Trebak and Kinet, 2019; Vig and Kinet, 2009). We showed that raising extracellular calcium levels resulted in an increase of calcium mobilization upon TCR stimulation. Increased calcium mobilization has been shown to be associated with increased activation, proliferation and pro-inflammatory differentiation of lymphocytes. We furthermore showed that raising calcium in vitro to the observed serum levels in vivo increased the production of pro-inflammatory cytokines and promoted T cell proliferation and migration over a BBB model. Dysfunctional calcium channels genetically introduced in T cells have been shown to be able to completely block EAE in mice (Ma et al., 2010). This is substantiated by the suppression of EAE by the therapeutic blockage of calcium channels by nimodipine (Schampel et al., 2017). Taken together with our findings, we can conclude that vitamin D

mediated immune-regulation can be overwritten by prolonged high-dose supplementation leading to secondary hypercalcemia and exacerbated T cell-mediated CNS pathogenicity.

Similarly to our observations, hypercalcemia can often occur in high-dose vitamin D supplemented MS patients, to a greater extent when combined with calcium intake, and has been associated with an increased MRI activity and relapse rate (Marcus et al., 2012). MS patients supplemented with 50.000 international unit (IU) of vitamin D every 3 days showed enhanced immune cell activation, whereas in contrast, a moderate supplementation led to reduced activity (Muris et al., 2016; Naghavi Gargari et al., 2015).

In conclusion, excessive vitamin D supplementation causing hypercalcemia might pose a novel risk factor in CNS disease. Therefore, patients and clinicians alike should be cautious when it comes to long term vitamin D supplementation.

5.3. Myelin-reactive antibodies initiate T cell-mediated CNS autoimmune disease by opsonisation of endogenous antigen.

In this work we showed that in the absence of antigen-specific APCs, myelin-targeting antibodies alone are sufficient to induce CNS autoimmune disease in MOG TCR transgenic mice. In the active immunization model of EAE using full length protein, antigen recognition by B cells via their BCR is essential (Weber et al., 2010). However, we here describe another mode of initiation of disease via the opsonisation of antigen by specific antibodies and the Fc-receptor mediated activation of myeloid cells. While these two distinct mechanisms seem rather different, the key element is specific recognition of small amounts of CNS antigen by APCs and subsequent promotion of T cell proliferation, differentiation and pro-inflammatory function.

Antibodies in demyelinating CNS disease have been extensively studied. In neuromyelitis optica (NMO), in which Aquaporin (AQP)-4 targeting antibodies lead to astrocyte loss, it has been described that AQP4 antibodies in individual patients were present even years before disease onset (Kinoshita and Nakatsuji, 2012). Furthermore, it was observed that MS patients and healthy individuals possess similar levels of anti-MOG antibodies in the serum (Lampasona et al., 2004). This lead to the conclusion, that those peripheral antibodies—

usually unable to cross the BBB—can only enhance ongoing demyelination but not initiate disease. At first sight, these findings seem to conflict with our results. They however, reflect two different mechanisms of initiation of disease. In double transgenic mice, containing MOG-specific B and T cells, a spontaneous onset of disease can be observed, even in the absence of MOG antibodies. This is mediated by the APC function of MOG-specific B cells, which recognize, process and present their respective antigen via the BCR to MOG-specific T cells. On the other side, injecting serum of Th mice or MOG-specific antibodies into 2D2 mice, the antibodies can opsonize and thereby "mark" the antigen for unspecific APCs, such as macrophages, which recognize the Fc part of the Ab.

However, both mechanisms depend on the presence of MOG-specific T cells, as Th mice alone or the injection MOG-specific antibodies in WT mice will not lead to CNS disease. It is questionable whether antibody titers in MS patients can reach levels comparable to immunized or transgenic mice. However, in light of B cell depleting therapies, this new notion of antibodies to completely bypass specific B cell APC function and thereby remaining immune to anti-CD20 needs to be recognized. One way to address this mode of disease mediation could be the interference with Fc receptor recognition of antibodies. As we successfully demonstrated, abrogating antibody-Fc receptor interaction either by blocking or deleting the receptor or by cleaving the antibody reduced antigen uptake in myeloid cells, activation of APCs and T cells as well as the proliferation of T cells. Since the CNS is an immune-privileged site, protected by the BBB which Abs cannot cross, the question remains where the initial recognition of CNS antigen occurs. The most plausible site is the cervical lymph node, which is the draining lymph node of the CNS, where traces of myelin were found in MS patients and EAE diseased mice (Aspelund et al., 2015; Fabriek et al., 2005). Surgical excision of these lymph nodes was able to reduce severity in chronic EAE (Phillips et al., 1997). Injecting mice peripherally with 8.18C5 and intrathecally with MOG protein, we observed an enhanced in vivo expansion of $CD4^+$ T cells in the lymph nodes and spleen of these healthy mice. This points towards peripheral lymphoid organs as the most likely site for initial recognition of CNS antigen by specific Abs. We used human IgG preparations to demonstrate that human Abs are generally able to opsonize antigen and promote phagocytosis by myeloid cells. It remains unclear whether this occurs in patients in a meaningful manner; however, serum from SLE patients specifically enhanced phagocytosis

of apoptotic cells by healthy donor macrophages in vitro (Sarmiento et al., 2007). In MS, the role of Abs has been restricted to the enhancement of ongoing CNS demyelination. Here, we report that CNS-reactive Abs are involved in initiation of disease by marking traces of otherwise unrecognized antigen. However, this mechanism ultimately depends on the presence of responding T cells, explaining why myelin-specific Abs found in healthy individuals do not cause detectable harm. Ultimately, this work highlights that independent of B cell targeting therapies, the humoral immune component may yield an up to date unrecognized therapeutic potential. This becomes of special interest in early disease stages or when B cell-oriented therapies fail in patients with high Ab titers.

6. Bibliography

Alberts, B., Johnson, A., Lewis, J., Raff, M., Roberts, K., and Walter, P. (2002). B Cells and Antibodies. Mol. Biol. Cell 4th Ed.

Aranow, C. (2011). Vitamin D and the Immune System. J. Investig. Med. Off. Publ. Am. Fed. Clin. Res. *59*, 881–886.

Aspelund, A., Antila, S., Proulx, S.T., Karlsen, T.V., Karaman, S., Detmar, M., Wiig, H., and Alitalo, K. (2015). A dural lymphatic vascular system that drains brain interstitial fluid and macromolecules. J. Exp. Med. *212*, 991–999.

Becklund, B.R., Hansen, D.W., and Deluca, H.F. (2009). Enhancement of 1,25-dihydroxyvitamin D3-mediated suppression of experimental autoimmune encephalomyelitis by calcitonin. Proc. Natl. Acad. Sci. U. S. A. *106*, 5276–5281.

Berkovich, R.R. (2016). Acute Multiple Sclerosis Relapse. Contin. Minneap. Minn *22*, 799–814.

Brandstadter, R., and Katz Sand, I. (2017). The use of natalizumab for multiple sclerosis. Neuropsychiatr. Dis. Treat. *13*, 1691–1702.

Cantorna, M.T., Hayes, C.E., and DeLuca, H.F. (1996). 1,25-Dihydroxyvitamin D3 reversibly blocks the progression of relapsing encephalomyelitis, a model of multiple sclerosis. Proc. Natl. Acad. Sci. U. S. A. *93*, 7861–7864.

Cariappa, A., Boboila, C., Moran, S.T., Liu, H., Shi, H.N., and Pillai, S. (2007). The recirculating B cell pool contains two functionally distinct, long-lived, posttransitional, follicular B cell populations. J. Immunol. Baltim. Md 1950 *179*, 2270–2281.

Chan, A., de Seze, J., and Comabella, M. (2016). Teriflunomide in Patients with Relapsing–Remitting Forms of Multiple Sclerosis. CNS Drugs *30*, 41–51.

Chaudhry, B.Z., Cohen, J.A., and Conway, D.S. (2017). Sphingosine 1-Phosphate Receptor Modulators for the Treatment of Multiple Sclerosis. Neurother. J. Am. Soc. Exp. Neurother. *14*, 859–873.

Coimbra, C. https://www.coimbraprotocol.com/

Compston, A. (1988). The 150th anniversary of the first depiction of the lesions of multiple sclerosis. J. Neurol. Neurosurg. Psychiatry *51*, 1249–1252.

Constantinescu, C.S., Farooqi, N., O'Brien, K., and Gran, B. (2011). Experimental autoimmune encephalomyelitis (EAE) as a model for multiple sclerosis (MS). Br. J. Pharmacol. *164*, 1079–1106.

Corneth, O.B.J., Klein Wolterink, R.G.J., and Hendriks, R.W. (2016). BTK Signaling in B Cell Differentiation and Autoimmunity. Curr. Top. Microbiol. Immunol. *393*, 67–105.

Diebold, M., Sievers, C., Bantug, G., Sanderson, N., Kappos, L., Kuhle, J., Lindberg, R.L.P., and Derfuss, T. (2018). Dimethyl fumarate influences innate and adaptive immunity in multiple sclerosis. J. Autoimmun. *86*, 39–50.

Domingues, H.S., Mues, M., Lassmann, H., Wekerle, H., and Krishnamoorthy, G. (2010). Functional and pathogenic differences of Th1 and Th17 cells in experimental autoimmune encephalomyelitis. PloS One *5*, e15531.

Fabriek, B.O., Zwemmer, J.N.P., Teunissen, C.E., Dijkstra, C.D., Polman, C.H., Laman, J.D., and Castelijns, J.A. (2005). In vivo detection of myelin proteins in cervical lymph nodes of MS patients using ultrasound-guided fine-needle aspiration cytology. J. Neuroimmunol. *161*, 190–194.

Gaetani, L., Prosperini, L., Mancini, A., Eusebi, P., Cerri, M.C., Pozzilli, C., Calabresi, P., Sarchielli, P., and Di Filippo, M. (2018). 2017 revisions of McDonald criteria shorten the time to diagnosis of multiple sclerosis in clinically isolated syndromes. J. Neurol. *265*, 2684–2687.

Gelfand, J.M., Cree, B.A.C., and Hauser, S.L. (2017). Ocrelizumab and Other CD20+ B-Cell-Depleting Therapies in Multiple Sclerosis. Neurotherapeutics *14*, 835–841.

Glatigny, S., and Bettelli, E. (2018). Experimental Autoimmune Encephalomyelitis (EAE) as Animal Models of Multiple Sclerosis (MS). Cold Spring Harb. Perspect. Med. *8*, a028977.

Goldenberg, M.M. (2012). Multiple Sclerosis Review. Pharm. Ther. *37*, 175–184.

Greenfield, A.L., and Hauser, S.L. (2018). B-cell Therapy for Multiple Sclerosis: Entering an era. Ann. Neurol. *83*, 13–26.

HART, S.P., SMITH, J.R., and DRANSFIELD, I. (2004). Phagocytosis of opsonized apoptotic cells: roles for “old-fashioned” receptors for antibody and complement. Clin. Exp. Immunol. *135*, 181–185.

Haselmayer, P., Camps, M., Liu-Bujalski, L., Nguyen, N., Morandi, F., Head, J., O’Mahony, A., Zimmerli, S.C., Bruns, L., Bender, A.T., et al. (2019). Efficacy and Pharmacodynamic Modeling of the BTK Inhibitor Evobrutinib in Autoimmune Disease Models. J. Immunol. Baltim. Md 1950 *202*, 2888–2906.

Häusler, D., and Weber, M.S. (2019). Vitamin D Supplementation in Central Nervous System Demyelinating Disease-Enough Is Enough. Int. J. Mol. Sci. *20*.

Häusler, D., Häusser-Kinzel, S., Feldmann, L., Torke, S., Lepennetier, G., Bernard, C.C.A., Zamvil, S.S., Brück, W., Lehmann-Horn, K., and Weber, M.S. (2018). Functional characterization of reappearing B cells after anti-CD20 treatment of CNS autoimmune disease. Proc. Natl. Acad. Sci. *115*, 9773–9778.

Kalron, A., Rosenblum, U., Frid, L., and Achiron, A. (2017). Pilates exercise training vs. physical therapy for improving walking and balance in people with multiple sclerosis: a randomized controlled trial. Clin. Rehabil. *31*, 319–328.

Kinoshita, M., and Nakatsuji, Y. (2012). Where Do AQP4 Antibodies Fit in the Pathogenesis of NMO? Mult. Scler. Int. *2012*.

Kuhlmann, T., Ludwin, S., Prat, A., Antel, J., Brück, W., and Lassmann, H. (2017). An updated histological classification system for multiple sclerosis lesions. Acta Neuropathol. (Berl.) *133*, 13–24.

La Mantia, L., Di Pietrantonj, C., Rovaris, M., Rigon, G., Frau, S., Berardo, F., Gandini, A., Longobardi, A., Weinstock-Guttman, B., and Vaona, A. (2016). Interferons-beta versus glatiramer acetate for relapsing-remitting multiple sclerosis. Cochrane Database Syst. Rev. *11*, CD009333.

Lampasona, V., Franciotta, D., Furlan, R., Zanaboni, S., Fazio, R., Bonifacio, E., Comi, G., and Martino, G. (2004). Similar low frequency of anti-MOG IgG and IgM in MS patients and healthy subjects. Neurology *62*, 2092–2094.

Larochelle, C., Alvarez, J.I., and Prat, A. (2011). How do immune cells overcome the blood-brain barrier in multiple sclerosis? FEBS Lett. *585*, 3770–3780.

Lassmann, H., and Bradl, M. (2017). Multiple sclerosis: experimental models and reality. Acta Neuropathol. (Berl.) *133*, 223–244.

Lassmann, H., Brück, W., Lucchinetti, C., and Rodriguez, M. (1997). Remyelination in multiple sclerosis. Mult. Scler. Houndmills Basingstoke Engl. *3*, 133–136.

Lassmann, H., Brück, W., and Lucchinetti, C. (2001). Heterogeneity of multiple sclerosis pathogenesis: implications for diagnosis and therapy. Trends Mol. Med. *7*, 115–121.

Lassmann, H., Brück, W., and Lucchinetti, C.F. (2007). The immunopathology of multiple sclerosis: an overview. Brain Pathol. Zurich Switz. *17*, 210–218.

Lehmann-Horn, K., Kronsbein, H.C., and Weber, M.S. (2013). Targeting B cells in the treatment of multiple sclerosis: recent advances and remaining challenges. Ther. Adv. Neurol. Disord. *6*, 161–173.

Lemire, J.M., and Archer, D.C. (1991). 1,25-dihydroxyvitamin D3 prevents the in vivo induction of murine experimental autoimmune encephalomyelitis. J. Clin. Invest. *87*, 1103–1107.

Litzenburger, T., Fässler, R., Bauer, J., Lassmann, H., Linington, C., Wekerle, H., and Iglesias, A. (1998). B Lymphocytes Producing Demyelinating Autoantibodies: Development and Function in Gene-targeted Transgenic Mice. J. Exp. Med. *188*, 169–180.

Lublin, F.D., Reingold, S.C., Cohen, J.A., Cutter, G.R., Sørensen, P.S., Thompson, A.J., Wolinsky, J.S., Balcer, L.J., Banwell, B., Barkhof, F., et al. (2014). Defining the clinical course of multiple sclerosis: the 2013 revisions. Neurology *83*, 278–286.

Ma, J., McCarl, C.-A., Khalil, S., Lüthy, K., and Feske, S. (2010). T-cell-specific deletion of STIM1 and STIM2 protects mice from EAE by impairing the effector functions of Th1 and Th17 cells. Eur. J. Immunol. *40*, 3028–3042.

Marcus, J.F., Shalev, S.M., Harris, C.A., Goodin, D.S., and Josephson, S.A. (2012). Severe hypercalcemia following vitamin d supplementation in a patient with multiple sclerosis: a note of caution. Arch. Neurol. *69*, 129–132.

Molnarfi, N., Schulze-Topphoff, U., Weber, M.S., Patarroyo, J.C., Prod'homme, T., Varrin-Doyer, M., Shetty, A., Linington, C., Slavin, A.J., Hidalgo, J., et al. (2013). MHC class II–dependent B cell APC function is required for induction of CNS autoimmunity independent of myelin-specific antibodies. J. Exp. Med. *210*, 2921–2937.

Montalban, X., Arnold, D.L., Weber, M.S., Staikov, I., Piasecka-Stryczynska, K., Willmer, J., Martin, E.C., Dangond, F., Syed, S., Wolinsky, J.S., et al. (2019). Placebo-Controlled Trial of an Oral BTK Inhibitor in Multiple Sclerosis. N. Engl. J. Med.

Moss, B.P., Rensel, M.R., and Hersh, C.M. (2017). Wellness and the Role of Comorbidities in Multiple Sclerosis. Neurother. J. Am. Soc. Exp. Neurother. *14*, 999–1017.

Muris, A.-H., Smolders, J., Rolf, L., Thewissen, M., Hupperts, R., Damoiseaux, J., and SOLARIUM study group (2016). Immune regulatory effects of high dose vitamin D3 supplementation in a randomized controlled trial in relapsing remitting multiple sclerosis patients receiving IFNβ; the SOLARIUM study. J. Neuroimmunol. *300*, 47–56.

Myers, C.D. (1991). Role of B cell antigen processing and presentation in the humoral immune response. FASEB J. Off. Publ. Fed. Am. Soc. Exp. Biol. *5*, 2547–2553.

Naghavi Gargari, B., Behmanesh, M., Shirvani Farsani, Z., Pahlevan Kakhki, M., and Azimi, A.R. (2015). Vitamin D supplementation up-regulates IL-6 and IL-17A gene expression in multiple sclerosis patients. Int. Immunopharmacol. *28*, 414–419.

Oh-hora, M., and Rao, A. (2008). Calcium signaling in lymphocytes. Curr. Opin. Immunol. *20*, 250–258.

Ohl, K., Tenbrock, K., and Kipp, M. (2016). Oxidative stress in multiple sclerosis: Central and peripheral mode of action. Exp. Neurol. *277*, 58–67.

Olalekan, S.A., Cao, Y., Hamel, K.M., and Finnegan, A. (2015). B cells expressing IFN-γ suppress Treg-cell differentiation and promote autoimmune experimental arthritis. Eur. J. Immunol. *45*, 988–998.

Ontaneda, D., Thompson, A.J., Fox, R.J., and Cohen, J.A. (2017). Progressive multiple sclerosis: prospects for disease therapy, repair, and restoration of function. Lancet Lond. Engl. *389*, 1357–1366.

Pan, Z., Lu, H., and Cheng, Q. (2013). Activities of daily living and lesion position among multiple sclerosis patients by Bayes network. Neural Regen. Res. *8*, 1327–1336.

Phillips, M.J., Needham, M., and Weller, R.O. (1997). Role of cervical lymph nodes in autoimmune encephalomyelitis in the Lewis rat. J. Pathol. *182*, 457–464.

Popescu, B.F., Frischer, J.M., Webb, S.M., Tham, M., Adiele, R.C., Robinson, C.A., Fitz-Gibbon, P.D., Weigand, S.D., Metz, I., Nehzati, S., et al. (2017). Pathogenic implications of distinct patterns of iron and zinc in chronic MS lesions. Acta Neuropathol. (Berl.) *134*, 45–64.

Rahmanzadeh, R., Weber, M.S., Brück, W., Navardi, S., and Sahraian, M.A. (2018). B cells in multiple sclerosis therapy-A comprehensive review. Acta Neurol. Scand. *137*, 544–556.

Ramkumar, B., Chadha, M.K., Barcos, M., Sait, S.N.J., Heyman, M.R., and Baer, M.R. (2008). Acute promyelocytic leukemia after mitoxantrone therapy for multiple sclerosis. Cancer Genet. Cytogenet. *182*, 126–129.

Sarmiento, L.F., Muñoz, L.E., Chirinos, P., Bianco, N.E., and Zabaleta-Lanz, M.E. (2007). Opsonization by anti-dsDNA antibodies of apoptotic cells in systemic lupus erythematosus. Autoimmunity *40*, 337–339.

Sartoris, S., Scupoli, M.T., Scarpellino, L., Paiola, F., Jotterand-Bellomo, M., Tridente, G., and Accolla, R.S. (1990). Inducible and constitutive MHC class II gene expression. Distinct tissue-specific genetic controls. J. Immunol. Baltim. Md 1950 *145*, 1960–1967.

Schampel, A., Volovitch, O., Koeniger, T., Scholz, C.-J., Jörg, S., Linker, R.A., Wischmeyer, E., Wunsch, M., Hell, J.W., Ergün, S., et al. (2017). Nimodipine fosters remyelination in a mouse model of multiple sclerosis and induces microglia-specific apoptosis. Proc. Natl. Acad. Sci. U. S. A. *114*, E3295–E3304.

Schwenkenbecher, P., Sarikidi, A., Bönig, L., Wurster, U., Bronzlik, P., Sühs, K.-W., Pul, R., Stangel, M., and Skripuletz, T. (2017). Clinically Isolated Syndrome According to McDonald 2010: Intrathecal IgG Synthesis Still Predictive for Conversion to Multiple Sclerosis. Int. J. Mol. Sci. *18*.

Simpson, S., der Mei, I. van, and Taylor, B. (2018). The Role of Vitamin D in Multiple Sclerosis: Biology and Biochemistry, Epidemiology and Potential Roles in Treatment. Med. Chem. Shariqah United Arab Emir. *14*, 129–143.

Sinha, S., Boyden, A.W., Itani, F.R., Crawford, M.P., and Karandikar, N.J. (2015). CD8+ T-Cells as Immune Regulators of Multiple Sclerosis. Front. Immunol. *6*.

Smith, K.J., and McDonald, W.I. (1999). The pathophysiology of multiple sclerosis: the mechanisms underlying the production of symptoms and the natural history of the disease. Philos. Trans. R. Soc. Lond. B. Biol. Sci. *354*, 1649–1673.

Soilu-Hänninen, M., Aivo, J., Lindström, B.-M., Elovaara, I., Sumelahti, M.-L., Färkkilä, M., Tienari, P., Atula, S., Sarasoja, T., Herrala, L., et al. (2012). A randomised, double blind, placebo controlled trial with vitamin D3 as an add on treatment to interferon β-1b in patients with multiple sclerosis. J. Neurol. Neurosurg. Psychiatry *83*, 565–571.

Steimle, V., Siegrist, C.A., Mottet, A., Lisowska-Grospierre, B., and Mach, B. (1994). Regulation of MHC class II expression by interferon-gamma mediated by the transactivator gene CIITA. Science *265*, 106–109.

Thompson, A.J., Banwell, B.L., Barkhof, F., Carroll, W.M., Coetzee, T., Comi, G., Correale, J., Fazekas, F., Filippi, M., Freedman, M.S., et al. (2018). Diagnosis of multiple sclerosis: 2017 revisions of the McDonald criteria. Lancet Neurol. *17*, 162–173.

Trebak, M., and Kinet, J.-P. (2019). Calcium signalling in T cells. Nat. Rev. Immunol. *19*, 154.

Trebst, C., Voss, E., Skripuletz, T., and Stangel, M. (2010). Specific immune intervention with monoclonal antibodies for the treatment of multiple sclerosis. Curr. Med. Chem. *17*, 640–650.

Varrin-Doyer, M., Pekarek, K.L., Spencer, C.M., Bernard, C.C.A., Sobel, R.A., Cree, B.A.C., Schulze-Topphoff, U., and Zamvil, S.S. (2016). Treatment of spontaneous EAE by laquinimod reduces Tfh, B cell aggregates, and disease progression. Neurol. Neuroimmunol. Neuroinflammation *3*, e272.

Veldman, C.M., Cantorna, M.T., and DeLuca, H.F. (2000). Expression of 1,25-dihydroxyvitamin D(3) receptor in the immune system. Arch. Biochem. Biophys. *374*, 334–338.

Vig, M., and Kinet, J.-P. (2009). Calcium signaling in immune cells. Nat. Immunol. *10*, 21–27.

Waschbisch, A., Sanderson, N., Krumbholz, M., Vlad, G., Theil, D., Schwab, S., Mäurer, M., and Derfuss, T. (2014). Interferon Beta and Vitamin D Synergize to Induce Immunoregulatory Receptors on Peripheral Blood Monocytes of Multiple Sclerosis Patients. PLoS ONE *9*.

Weber, A.N.R., Bittner, Z., Liu, X., Dang, T.-M., Radsak, M.P., and Brunner, C. (2017). Bruton's Tyrosine Kinase: An Emerging Key Player in Innate Immunity. Front. Immunol. *8*, 1454.

Weber, M.S., Prod'homme, T., Patarroyo, J.C., Molnarfi, N., Karnezis, T., Lehmann-Horn, K., Danilenko, D.M., Eastham-Anderson, J., Slavin, A.J., Linington, C., et al. (2010). B-cell activation influences T-cell polarization and outcome of anti-CD20 B-cell depletion in central nervous system autoimmunity. Ann. Neurol. *68*, 369–383.

Weinshenker, B.G. (1998). The natural history of multiple sclerosis: update 1998. Semin. Neurol. *18*, 301–307.

Wekerle, H. (2017). B cells in multiple sclerosis. Autoimmunity *50*, 57–60.

Yuseff, M.I., and Lennon-Dumenil, A.M. (2013). Studying MHC class II presentation of immobilized antigen by B lymphocytes. Methods Mol. Biol. Clifton NJ *960*, 529–543.

Zafranskaya, M., Oschmann, P., Engel, R., Weishaupt, A., van Noort, J.M., Jomaa, H., and Eberl, M. (2007). Interferon-β therapy reduces CD4+ and CD8+ T-cell reactivity in multiple sclerosis. Immunology *121*, 29–39.

7. Curriculum vitae

general information
Ludwig-Prandtl-Str. 52, 37077 Goettingen, Germany | 08.03.1990 | German
+49 178 4082183 | sebastian.torke@online.de

PROFESSIONAL EXPERIENCE

12/2015- PhD candidate, Weber Group, *Neuropathology, University Medical Centre Goettingen, Germany*
· Exploring the role of BTK inhibition in induced and spontaneous EAE models

EDUCATION

10/2013-07/2015 M.Sc. Molecular Medicine, Grade 1.74 *Georg-August-University of Goettingen, Germany*

10/2010-09/2013 B.Sc. Molecular Medicine, Grade 1.86 *Georg-August-University of Goettingen, Germany*

09/2006-07/2009 Abitur (University Entrance Qualification), Grade 1.6 *BSZ für Agrarwirtschaft "Justus von Liebig" Dresden, Germany*

PUBLICATION LIST

BRAIN in press:
High dose vitamin D exacerbates central nervous system autoimmunity by raising T cell-excitatory calcium
Häusler D*, Torke S*, Peelen E, Bertsch T, Djukic M, Nau R, Larochelle C, Zamvil SS, Brück W, Weber MS
*These authors contributed equally.

Proc Natl Acad Sci U S A. 2018 Sept:
Functional characterization of reappearing B cells after anti-CD20 treatment of CNS autoimmune disease.
Häusler D*, Häusser-Kinzel S*, Feldmann L, Torke S, Lepennetier G, Bernard CCA, Zamvil SS, Brück W, Lehmann-Horn K, Weber MS. *These authors contributed equally.

Acta Neuropathol. 2016 Jul:
Myelin-reactive antibodies initiate T cell-mediated CNS autoimmune disease by opsonization of endogenous antigen.
Kinzel S*, Lehmann-Horn K*, Torke S, Häusler D, Winkler A, Stadelmann C, Payne N, Feldmann L, Saiz A, Reindl M, Lalive PH, Bernard CC, Brück W, Weber MS. * These authors contributed equally.

CONFERENCE CONTRIBUTIONS

13th International Congress of Neuroimmunology 2016 Poster: *B cell-derived IL-10 regulates pro-inflammatory activity of myeloid cells in a clinically meaningful manner.* Torke, S; Kinzel, S; Lehmann-Horn, K; Brück, W; Weber, MS.

16th European School of Neuroimmunology 2017 Poster: *Exploring the role of BTK inhibition in induced and spontaneous EAE models.* Torke, S; Weber, MS.

33th Congress of the European Committee for Treatment and Research in Multiple Sclerosis 2017 Talk: *B cell-mediated experimental CNS autoimmunity is modulated by inhibition of Bruton's tyrosine kinase*. Torke, S; Grenningloh, R; Boschert, U; Weber, MS.

34th Congress of the European Committee for Treatment and Research in Multiple Sclerosis 2018 Poster: *Inhibition of Bruton's tyrosine kinase selectively prevents antigen-activation of B cells and ameliorates B cell-mediated experimental autoimmune encephalomyelitis*. Torke, S; Grenningloh, R; Boschert, U; Weber, MS.

71st Annual meeting of the American Academy of Neurology 2019 poster: *Inhibition of Bruton's Tyrosine Kinase Selectively Prevents Antigen-Activation of B cells and Ameliorates B-Cell-Mediated Experimental Autoimmune Encephalomyelitis.* Torke, S; Grenningloh, R; Boschert, U; Weber, MS.

LABORATORY EXPERIENCE

10/2014-04/2015 Hanisch Group, *Neuropathology, University Medical Centre Goettingen, Germany*
- Master thesis: Role of TLR4 in immunoglobulin challenges in microglia
- Intracranial operations in mice, histology, FACS, ELISA

08/2014-10/2014 Hanisch Group, *Neuropathology, University Medical Centre Goettingen, Germany*
- Modulation of TLR4 signalling in murine microglia by stimulation of β2 adrenergic-receptors with long lasting agonist salbutamol
- FACS, intracranial operations in mice, ELISA

03/2014-05/2014 Olson Group, *Beatson Institute of Cancer Research, Cancer Research UK Glasgow*
- Phosphorylation of ROCK1 under starved and unstarved conditions
- Mass Spectrometry, Western blotting, cell culture, immunostaining

11/2013–01/2014 Stahl-Henning Group, *Unit of infection models, German Primate Centre Goettingen, Germany*
- Diagnostics of Herpes B and SIV infections in rhesus macaques
- ELISA, next generation sequencing

07/2013-09/2013 Wienands Group, *Molecular and Cellular Immunology, University of Goettingen, Germany*
- Bachelor thesis: SLP65 recruitment to B-cell receptor
- FACS, calcium signalling

02/2013-03/2013 Morley Group, *Department of Cardiology, Langone Medical Centre, New York University*
- 3D modelling of mice hearts, optical mapping

09/2012 Kopka Group, *Laboratory of Radioisotopes, University of Goettingen, Germany*
- Instruction course: working with isotopes

09/2012 Schmidt Group, *Dept. of Biochemistry, University of Goettingen, Germany*
- Instruction course: MALDI-TOF mass spectroscopy

08/2012 Wulf Group, *Dept. of Haematology and Oncology, University Medical Centre Goettingen, Germany*
- Wnt signalling in lymphoma cells
- FACS analysis

07/2012-08/2012 Hahn Group, *Dept. of Human Genetics, University of Goettingen, Germany*
- basal cell carcinoma and hedgehog signalling cascade
- paraffin sectioning and HE-staining

03/2012-04/2012 Thelen Group, *Dept. of Urology, University Medical Centre Goettingen, Germany*
- castration resistant prostate carcinoma
- real-time PCR

02/2012-03/2012 Klopfenstein Group, *Dept. of Biophysics, Third Physical Institute, University of Goettingen, Germany*
- microtubule transport and motor proteins
- fluorescence microscopy

LANGUAGES AND OTHER QUALIFICATIONS

German – native English – fluent Spanish – advanced Latin – advanced
Animal handling course according to Federation of European Laboratory Animal Science Associations (FELASA B)
Advanced knowledge of Microsoft Office, GraphPad Prism, FlowJo, ImageJ, 4D "Tierbase", Adobe Illustrator
Experience with statistical programs MATLAB and R